

# **Supplementary wavelength calibration methods for SALT/RSS spectropolarimetric observations**

Justin Cooper

Submitted in fulfillment of the requirements for the degree

Magister Scientiæ

in the Faculty of Natural and Agricultural Sciences

Department of Physics

University of the Free State

South Africa

Date of submission: September 2024

Supervised by: Prof. B. van Soelen, Department of Physics

# Abstract

TODO:

- Done last
- Flow from use of SALT and pipeline and basics of its science implementations into why a more streamlined wavelength calibration is an improvement.
- Give summary of results.
- Aim for a paragraph ( $\sim 600$ ) without going too in-depth into anything specific.
- Brian's comment: Abstract should summarize paper. Include results, conclusions, etc.

**Keywords:** STOPS, POLSALT, IRAF, SALT, RSS, Development: Python, Pipeline, Calibration: wavelength, Polarization: optical, galaxies: AGN, Blazars, Spectropolarimetry, Astrophysics, Astronomy,

TODO:

- Add Keywords → look up the astronomy journal keywords
- Look up keywords for pipeline development and data reduction.

## Acknowledgements

I hereby acknowledge and express my sincere gratitude to the following parties for their valuable contributions:

- **TODO: Add acknowledgements!**



# Contents

|          |  |           |
|----------|--|-----------|
| <b>1</b> | <b>Introduction</b>  | <b>1</b>  |
| <b>2</b> | <b>Spectropolarimetry and the SALT RSS</b>                         | <b>3</b>  |
| 2.1      | Spectroscopy . . . . .   | 3         |
| 2.1.1    | Telescope Optics . . . . .   | 3         |
| 2.1.2    | Slit . . . . .   | 4         |
| 2.1.3    | Collimator . . . . .   | 4         |
| 2.1.4    | Dispersion Element . . . . .                                       | 4         |
| 2.1.5    | Camera Optics . . . . .  | 5         |
| 2.1.6    | Detector . . . . .   | 5         |
| 2.1.7    | Dispersion of Light . . . . .                                      | 5         |
| 2.1.8    | Detector and Spectroscopic Calibrations . . . . .                  | 9         |
| 2.2      | Polarimetry . . . . .  | 15        |
| 2.2.1    | Polarization . . . . .   | 16        |
| 2.2.2    | Polarization Measurement . . . . .                                 | 19        |
| 2.2.3    | Polarimetric Calibrations . . . . .                                | 22        |
| 2.3      | Spectropolarimetry . . . . .                                       | 23        |
| 2.3.1    | Spectropolarimetric Measurement . . . . .                          | 24        |
| 2.3.2    | Spectropolarimetric Calibrations . . . . .                         | 25        |
| 2.4      | The Southern African Large Telescope . . . . .                     | 26        |
| 2.4.1    | The Primary Mirror . . . . .                                       | 26        |
| 2.4.2    | Tracker and Tracking . . . . .                                     | 27        |
| 2.4.3    | SALT Instrumentation . . . . .                                     | 28        |
| <b>3</b> | <b>Existing and Developed Software</b>                             | <b>31</b> |
| 3.1      | POLSALT . . . . .  | 31        |
| 3.1.1    | Raw Image Reductions . . . . .                                     | 32        |
| 3.1.2    | Wavelength Calibrations . . . . .                                  | 32        |
| 3.1.3    | Spectral Extraction . . . . .                                      | 33        |
| 3.1.4    | Raw Stokes Calculations . . . . .                                  | 33        |
| 3.1.5    | Final Stokes Calculations . . . . .                                | 34        |
| 3.1.6    | Visualization . . . . .  | 34        |
| 3.1.7    | Post-Processing Analysis . . . . .                                 | 34        |
| 3.1.8    | POLSALT Limitations and the Need for Supplementary Tools . . . . . | 35        |
| 3.2      | IRAF . . . . .   | 36        |
| 3.2.1    | Identify . . . . .   | 37        |

|          |   |            |
|----------|---|------------|
| 3.2.2    | Reidentify . . . . .                          | 37         |
| 3.2.3    | Fitcoords . . . . .                           | 39         |
| 3.2.4    | Transform . . . . .                           | 40         |
| 3.3      | STOPS . . . . .                               | 41         |
| 3.3.1    | Splitting . . . . .                           | 41         |
| 3.3.2    | Joining . . . . .                             | 43         |
| 3.3.3    | Sky Line Checks . . . . .                     | 47         |
| 3.3.4    | Cross Correlation . . . . .                   | 47         |
| 3.4      | General Reduction Procedure . . . . .         | 50         |
| 3.4.1    | Initial Setup . . . . .                       | 50         |
| 3.4.2    | POLSLT Pre-Reductions . . . . .               | 51         |
| 3.4.3    | Wavelength Calibration . . . . .              | 52         |
| 3.4.4    | POLSLT Reduction Completion . . . . .         | 54         |
| <b>4</b> | <b>Testing and Application</b>                | <b>57</b>  |
| 4.1      | Testing STOPS . . . . .                       | 57         |
| 4.1.1    | Testing the split Method . . . . .            | 57         |
| 4.1.2    | Testing the join Method . . . . .             | 59         |
| 4.2      | Wavelength Solution Checks . . . . .          | 61         |
| 4.2.1    | Cross Correlation Checks . . . . .            | 61         |
| 4.2.2    | Sky Line Checks . . . . .                     | 63         |
| 4.3      | Application of STOPS . . . . .                | 63         |
| 4.3.1    | Spectropolarimetric Standards . . . . .       | 63         |
| 4.3.2    | Spectropolarimetric Science Targets . . . . . | 64         |
| <b>5</b> | <b>Conclusions</b>                            | <b>67</b>  |
| 5.1      | Future Work . . . . .                         | 67         |
| <b>A</b> | <b>The Modified Reduction Process</b>         | <b>69</b>  |
| <b>B</b> | <b>STOPS Source Code</b>                      | <b>77</b>  |
| <b>C</b> | <b>Proceedings</b>                            | <b>115</b> |
|          | <b>Bibliography</b>                           | <b>131</b> |

# List of Acronyms and Symbols

|          |   |
|----------|---|
| A-DC     | Analog-to-Digital Converter                               |
| ADC      | Atmospheric Dispersion Compensator                        |
| AGN      | Active Galactic Nucleus                                   |
| Ar       | Argon   |
| CCD      | Charged-Coupled Device                                    |
| CLI      | Command Line Interface                                    |
| CMOS     | Complementary Metal-Oxide-Semiconductor                   |
| CuAr     | Copper-Argon  |
| FITS     | Flexible Image Transport System                           |
| FWHM     | Full Width at Half Maximum                                |
| GUI      | Graphical User Interface                                  |
| HDU      | Header and Data Unit                                      |
| HEASA    | High Energy Astrophysics South Africa                     |
| HET      | Hobby-Eberly Telescope                                    |
| HgAr     | Mercury-Argon   |
| HRS      | High Resolution Spectrograph                              |
| IRAF     | <i>Image Reduction and Analysis Facility</i>              |
| L+45°    | Linear +45° Polarized                                     |
| L−45°    | Linear −45° Polarized                                     |
| LCP      | Left Circularly Polarized                                 |
| LHP      | Linear Horizontally Polarized                             |
| LVP      | Linear Vertically Polarized                               |
| Ne       | Neon-Argon  |
| NIR      | Near Infra-Red  |
| NIRWALS  | Near Infra-Red Washburn Labs Spectrograph                 |
| POLSALT  | <i>Polarimetric reductions for SALT</i>                   |
| RCP      | Right Circularly Polarized                                |
| RMS      | Root Mean Square  |
| RSS      | Robert Stobie Spectrograph                                |
| S/N      | Signal-to-Noise Ratio                                     |
| SAAO     | South African Astronomical Observatory                    |
| SAC      | Spherical Aberration Corrector                            |
| SALT     | Southern African Large Telescope                          |
| SALTICAM | SALT Imaging Camera                                       |
| STOPS    | <i>Supplementary Tools for POLSALT Spectropolarimetry</i> |
| ThAr     | Thorium-Argon   |

|     |                          |
|-----|--------------------------|
| UV  | Ultraviolet              |
| VPH | Volume Phase Holographic |
| Xe  | Xenon                    |

# Chapter 1

## Introduction

TODO: Very short intro to Spectroscopy, Polarization, and Spectropolarimetry and their importance in astronomy

TODO: Problem Statement, VERY IMPORTANT, roughly a sentence but problem thoroughly fleshed out.

TODO: Focus on AGN implications and implementations such as the types of objects and a short history for each type of object, Blazar focus with specification on BL Lacs and FSRQs, the Unified Model, ~~The Blazar sequence~~

TODO: Brian's comment: Highlight importance of polarimetry for understanding emission and how that plays a role in AGN.

TODO: Basics of modelling (Different energy/wavelength ranges used and what the models tell us about emission processes/structure) so that Hester's results can be noted for applications of the pipeline.

TODO: General layout of Dissertation



# Chapter 2

## Spectropolarimetry and the SALT RSS

This chapter gives an overview of the basics of spectropolarimetry (§ 2.3), and how it functions, following from the principles of both spectroscopy (§ 2.1) and polarimetry (§ 2.2). Further, it is discussed how these techniques are practically implemented for Southern African Large Telescope (SALT) (§ 2.4), using the Robert Stobie Spectrograph (RSS) (§ 2.4.3), and how the spectropolarimetric reduction process is completed (§ 2.4.3).

### 2.1 Spectroscopy

Spectroscopy originated in its most basic form with Newton's examinations of sunlight through a prism (Newton and Innys, 1730) but came to prominence as a field of scientific study with Wollaston's improvements to the optics elements (Wollaston, 1802), Fraunhofer's use of a diffraction grating instead of a prism (der Wissenschaften, 1824), and Bunsen and Kirchoff's classifications of spectral features to their respective chemical elements (Kirchhoff and Bunsen, 1861).

The simplest spectrometer schematic, as shown in Figure 2.1, consists of incident light collected from the telescope's optics, labelled A, being focused onto a slit, B, and passed through a collimator, C. The collimator collimates the light allowing a dispersion element, D, to disperse the light into its constituent wavelengths. The resultant spectrum is focused by camera optics, E, onto a focal plane, F. Viewing optics are situated at the focal plane in the case of a spectroscope and a detector is situated at the focal plane in the case of a spectrograph.

#### 2.1.1 Telescope Optics

The telescope optics refers simply to all the components of a telescope necessary to acquire a focal point at the spectrometer entrance, labelled B. The focal point in most traditional telescope designs is fixed relative to the telescope and so the spectrometer may be mounted at that point. In cases where the telescope is designed to have a moving focal point relative to the telescope (see Buckley et al., 2006; Cohen, 2009; Ramsey et al., 1998), the spectrometer, or a signal transfer method such as a fibre feed to the spectrometer, must also move along the telescope's focal path.

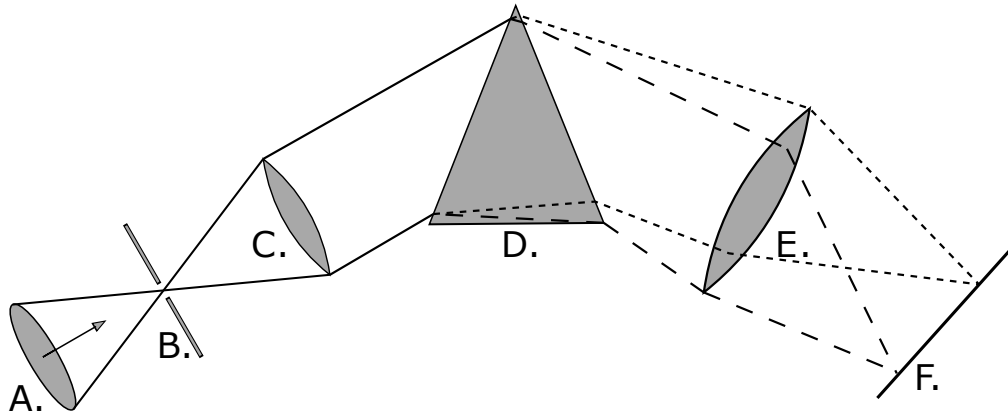


**Figure 2.1:** Layout depicting the light path through a spectrometer. Diagram adapted from Birney et al. (2006).

### 2.1.2 Slit

The slit's function is to control the amount of incident light entering a spectrometer and, along with the exposure time of the detector, prevents over-exposures of bright sources on highly sensitive detectors (Tonkin, 2013). If a source is spatially resolvable, or larger than the seeing conditions, the slit additionally acts to spatially limit the source to increase the spectral resolution, resulting in sharper features in the resultant spectrum. Without the slit the spectral resolution would be determined by the projected width of the source on the detector, or the seeing if the source was a star-like point source. Increasing the spectral resolution comes with the trade-off of decreasing the light collected from the source and thus acquiring a less intense resultant spectrum. Multiple spectra may be acquired simultaneously when the slit is positioned such that collinear sources lie along the slit.

The spectrometer is usually situated at the focal point. In cases where this is not feasible due to restrictions, for example restrictions of weight or size, a fibre feed may be situated behind the slit on the telescope. This allows the signal to be routed away from the telescope to a controlled environment with only minuscule losses.

### 2.1.3 Collimator

The collimators function is to collimate the focused light from the telescope, ensuring that all light rays run parallel before reaching the dispersion element. The focal ratio of the collimator ( $f_c/D_c$ , where  $f$  refers to the focal length and  $D$  refers to the diameter) should ideally match the focal ratio of the telescope ( $f_T/D_T$ ).

### 2.1.4 Dispersion Element

Including a dispersion element in the optical path is what defines a spectrometer. As the name suggests, a dispersion element disperses the light incident on it into its constituent wavelengths and produces a spectrum. There are two types of dispersion elements, namely the prism and the diffraction grating, which operate on different principles, as discussed in § 2.1.7.

### 2.1.5 Camera Optics

The lens functions similarly to that of the telescope's optics but in this case focuses the dispersed light onto a receiver situated at the focal plane. As mentioned previously, an eye piece is fixed to the focal point for a spectroscope while a spectrograph employs a detector.

### 2.1.6 Detector

The two most prevalent detector types in spectroscopy are the Charged-Coupled Device (CCD) and Complementary Metal-Oxide-Semiconductor (CMOS) detectors. In astronomical spectroscopy however, sources are fainter and exposure times are much longer and so the CCD detectors are by far the preferred detector as their output has a higher-quality and lower-noise when compared to CMOS cameras under the same conditions (Janesick et al., 2006).

The CCD is a detector composed of many thousands of pixels which can store a charge so long as a voltage is maintained across the pixels. Each pixel detects incoming photons using photo-sensitive capacitors through the photoelectric effect and converts the photons to a charge (Buil, 1991). There are also thermal agitation effects which introduce noise to the charge accumulated by a pixel, further discussed in § 2.1.8. Once the exposure is finished the accumulated charge is read column by column, row by row, through an Analog-to-Digital Converter (A-DC) which produces a two-dimensional array of ‘counts’.

### 2.1.7 Dispersion of Light

Light can be broken up into its constituent wavelengths through two different physical phenomena, namely dispersion and diffraction, which dispersive elements use to create spectra. Dispersive prisms and diffractive gratings each have their strengths and weaknesses and a wide spectrum of instruments exist which implement either, or both, concepts. Regardless of the specific element, dispersive elements all have a resolving power,  $R$ , and an angular dispersion. Generally, while the angular dispersion is a more involved process to determine, the resolving power of a spectrograph can be measured as:

$$R = \frac{\lambda}{FWHM}, \quad (2.1)$$

where  $\lambda$  is the wavelength of an incident monochromatic beam and Full Width at Half Maximum (FWHM) refers to the width of the feature on the detector at half of its maximum intensity.

#### Prism

The prism operates on the principle that the refractive index of light,  $n$ , varies as a function of its wavelength,  $\lambda$ . Prisms were the only dispersive elements available for early spectroscopic studies, but they were not without flaw. The angular dispersion of a prism is given by:

$$\frac{\partial\theta}{\partial\lambda} = \frac{B}{a} \frac{dn}{d\lambda}, \quad (2.2)$$

where  $\theta$  is the angle at which the refracted light differs from the incident light,  $\lambda$  is the wavelength of the incident light,  $B$  is the longest distance the beam would travel through



**Figure 2.2:** Geometry of a prism refracting an incident monochromatic beam at a minimum deviation angle. Diagram adapted from Birney et al. (2006).

the prism.  $a = L \sin(\alpha)$  is the maximal beam width that would fit onto a prism with a transmissive surface of length  $L$  for a given angle,  $\alpha$ , at which a beam would strike the transmissive surface, as shown in Figure 2.2.

The refractive index of a material as a function of its wavelength,  $n(\lambda)$ , can be approximated by Cauchy's equation:

$$n(\lambda) = A_C + \frac{B_C}{\lambda^2} + \frac{C_C}{\lambda^4} + \dots, \quad (2.3)$$

where  $A_C, B_C, C_C$  are the Cauchy coefficients and have known values for certain materials. Cauchy's equation is a much simpler approximation of the refractive index that remains very accurate at visible wavelengths (Jenkins and White, 1976). Taking only the first term of the derivative of the Cauchy equation allows us to approximate the angular dispersion of a prism,

$$\frac{\partial \theta}{\partial \lambda} = -\frac{B}{a} \frac{2B_C}{\lambda^3} \propto -\lambda^{-3}, \quad (2.4)$$

which shows that the angular dispersion of a prism is wavelength dependent and furthermore that longer wavelengths are dispersed less than shorter wavelengths (Birney et al., 2006; Hecht, 2017). The dependence of the angular dispersion,  $d\theta/d\lambda$ , on the wavelength,  $\lambda$ , is crucial for the formation of a spectrum but this cubic, non-linear, relation results in a non-linear spectrum. Since prisms rely on the refractive index of the material they are made of, they have low angular dispersions.

Multiple prisms can be used to increase the angular dispersion but as the dispersion is non-linear it becomes increasingly more difficult to calibrate. The more material and material boundaries the light must pass through, the more its intensity decreases due to attenuation effects and Fresnel losses. Even so, the transmittance of modern prisms for their selected wavelength range is generally very high due to improved manufacturing methods as well as improved transmitting materials.<sup>1</sup>

---

<sup>1</sup>See manufacturers technical specifications, THORLABS, or Edmund Optics for example.

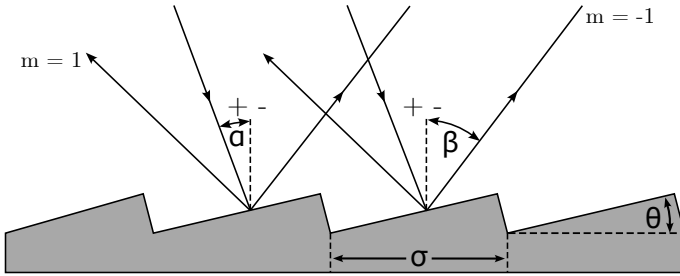


**Figure 2.3:** Geometry of a reflective blazed grating refracting an incident monochromatic beam. Diagram adapted from Birney et al. (2006).

## Diffraction Grating

The alternative dispersing element is a diffraction grating, which operates on the principle that as light interacts with a grating where the groove size is comparable to the light's wavelength, the light is dispersed through constructive and destructive interference. This interference results in multiple diffracted beams  $m$ , called orders, either side of a central reflected, or transmitted, beam such that  $m \in \mathbb{Z}$ , where  $m = 0$  is the non-dispersed, or reflected, beam.

An example of a reflective blazed grating is illustrated in Figure 2.3. Here a monochromatic beam is incident on the grating at an angle of  $\alpha$  from the grating normal. Due to the interference, a diffracted beam of wavelength  $\lambda$  is found at an angle of  $\beta$  from the grating normal. The relation between the incident and diffracted beams is given by the grating equation:

$$m\lambda = \sigma(\sin(\alpha) \pm \sin(\beta)), \quad (2.5)$$

where  $\sigma$  is the groove spacing of the grating and  $m$  is the order of the diffracted beam being considered. The grating equation also applies to transmission gratings, though care should be taken for the signs of  $\alpha$  and  $\beta$ .

Equation 2.5 also shows that different diffracted beams may share an angle of dispersion for beams not in the same order. The regions of an order that do not overlap with another order are called free spectral ranges. An order-blocking filter may be used to account for the overlaps and increase the free spectral range. A diffraction grating can also be blazed by an angle  $\theta$ , as illustrated in Figure 2.3. Blazing refers to the fact that the grooves on the surface of the grating are not symmetrical. The asymmetry of the grooves diffracts the incident beam such that most of the beam's intensity is found in a reflected, zeroth order, beam. The wavelength at which a blazed spectrograph is most effective is called the blaze wavelength,  $\lambda_b$ , which is determined by:

$$\begin{aligned} m\lambda_b &= 2\sigma \sin(\theta) \cos(\alpha - \theta), \text{ where} \\ 2\theta &= \alpha + \beta. \end{aligned} \quad (2.6)$$

Taking the derivative of Equation 2.5 with respect to  $\lambda$  while keeping  $\alpha$  constant, allows us to determine the angular dispersion of a diffraction grating,

$$\frac{\partial \beta}{\partial \lambda} = \frac{m}{\sigma \cos(\beta)}. \quad (2.7)$$



**Figure 2.4:** Diagram of a grism for an incident monochromatic beam of light and a diffracted beam of order  $m = 1$ . Diagram adapted from Birney et al. (2006).

Substituting  $m/\sigma$  with the grating equation results in

$$\frac{\partial \beta}{\partial \lambda} = \frac{\sin(\alpha) + \sin(\beta)}{\lambda \cos(\beta)} \propto \lambda^{-1}. \quad (2.8)$$

Similar to the dispersion of a prism, Equation 2.8 shows that the dispersion of a grating is wavelength dependent, but this dependence is only inversely proportional and thus more uniform across a wavelength range than that of a prism. Furthermore, shorter wavelengths are refracted less than longer wavelengths since there is no negative relation between the angular dispersion and the wavelength (Birney et al., 2006; Hecht, 2017).

### Alternate Diffraction Elements

As mentioned before, multiple subgroups exist for both dispersive prisms and diffractive gratings. For prisms, along with the single and multiple prism setups mentioned, there also exists grisms and immersed gratings. A grism (Grating Prism), as shown in Figure 2.4, refers to a transmissive grating etched onto one of the transmissive faces of a prism and allows a single camera to capture both spectroscopic and photometric images without needing to be moved, with and without the grism in the path of the beam of light, respectively. An immersed grating refers to a grism modified such that the transmissive grating is coated with reflective material. The primary source of dispersion for both grisms and immersive gratings is the grating and any aberration effects from the prism are negligible in comparison.

Other types of gratings include the Volume Phase Holographic (VPH) grating as well as the echelle grating. The VPH grating consists of a photoresist, which is a light-sensitive material, sandwiched between two glass substrates. Diffraction is possible since the photoresist's refractive index varies near-sinusoidally perpendicularly to the gratings lines, as seen in Figure 2.5. This allows for sharper diffraction orders and low stray light scattering as compared to more traditional gratings but since blazing is not possible the

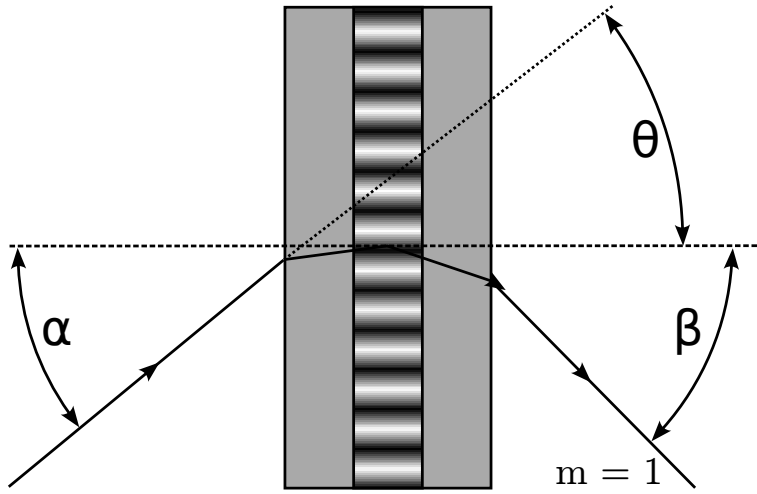


**Figure 2.5:** Diagram of a VPH grating for an incident monochromatic beam of light. Diagram adapted from Birney et al. (2006).

efficiency is decreased. An echelle grating refers to a diffraction grating with higher groove spacing which is optimized for use at high orders. The high order of the diffracted beam allows for greater angular dispersion which is most useful when combined with another dispersion element to cross-disperse a spectrum, resulting in a high resolution spectrum.

### 2.1.8 Detector and Spectroscopic Calibrations

Acquiring a spectrum from observations is more involved than simply reading out the data recorded on the CCD. A raw science image, which is the raw counts of the observed source read from the CCD with no calibrations applied, has on it a combination of useful science data as well as noise. The noise is a combination of random noise introduced through statistical processes and systematic noise introduced through the instrumentation and the observation conditions the source was observed under. This noise causes an uncertainty in the useful data and can be minimized, predominantly by calibrating for the systematic noise, but never fully removed (Howell, 2006).

The dominant source of noise in a raw image is detector noise. CCDs are manufactured to have a small base charge in each pixel, called the ‘bias’ current which allows the readout noise, a type of random noise, to better be sampled. There is also an unintentional additional charge which is linearly proportional to the exposure time and originates from thermal agitation of the CCD material, called the ‘dark’ current. The dark current can be minimized and possibly ignored if the CCD is adequately cooled. These types of noise add to the charge held by a pixel and are thus considered additive.

The CCD is not a perfect detector and the efficiency of it and the optics of the telescope also contribute noise to the image. The efficiency of a CCD is referred to as the Quantum Efficiency, and it is a measure of what percentage of light striking the detector is actually recorded and converted to a charge. The efficiency of the CCD and telescope optics is also wavelength dependent and so the noise that results from them is more complex than that of additive noise. This type of noise is referred to as multiplicative noise.



**Figure 2.6:** Diagram of the inner logic of a CCD. Figure adapted from Litwiller (2001).

Additive noise, such as bias and dark currents, is inherent to CCD images, and as such needs to be subtracted out first when performing calibrations. Bias currents can be found by taking a bias image or by adding an overscan region to each image. A bias image is an image where the charges on the CCD are reset and then immediately read off without exposing anything on the detector, effectively taking an image with zero exposure time. Alternatively, to save time during an observational run, overscan regions may be added to the images. An overscan region refers to adding a few cycles to the readout of each column of the CCD such that the base current is read out and appended to each image.

Dark currents can be found by taking an image with nothing exposed onto the detector for a certain exposure time. This resultant dark image can then be scaled to the science images exposure time since the dark current should be linearly proportional to exposure time. When the detector is capable of being held at precise temperatures, dark images may be taken over multiple hours during the day to produce a high quality master dark image that may then be scaled and subtracted from all subsequent images.

Next, multiplicative noise, such as a CCD's pixel-to-pixel response, should be accounted for. This pixel-to-pixel response should be uniform across the image and to achieve this an average response may be divided out. The average response is referred to as a 'flat' image or flat-field and may be acquired by observing a uniformly illuminated surface to determine the pixel-to-pixel response.

Dome flats are images taken of a relatively flat surface, usually the inside of a telescope's dome, and are used in both photometry and spectroscopy. The surface is uniformly and indirectly illuminated by a projector lamp, ideal for flat-field images. Alternate flat-fielding methods, such as night sky and twilight flats, are available but are suited solely for photometry.

Night sky flats are produced from science images containing mostly sky. The science images are combined using the 'mode' statistic which removes any celestial objects at the cost of a low Signal-to-Noise Ratio (S/N) flat-field.

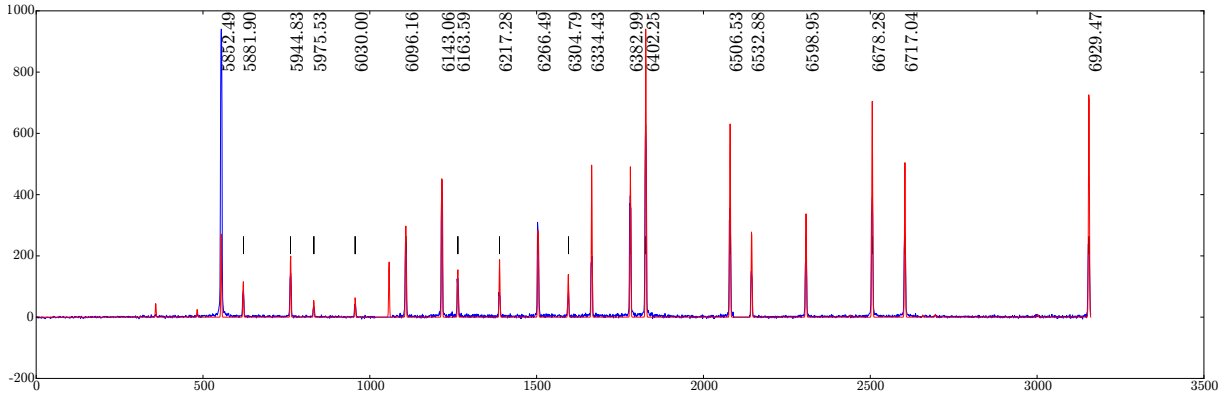


**Figure 2.7:** Example of an arc spectrum for NeAr taken with SALT’s RSS using the PG1800 grating at a grating angle of  $34.625^\circ$ , an articulation angle of  $69.258^\circ$ , and covering a wavelength range of  $\sim 5600 - 6900 \text{ \AA}$ . Plot adapted from SALT’s published Longslit Line Atlases, (2023).<sup>2</sup>

Twilight flats are produced from images of the twilight (or dawn) sky. They are taken when the Sun has just set, in the opposite direction, at  $\sim 20^\circ$  from zenith and provide a better S/N at the cost of careful timing of the images.

A flat-field must be normalized before being used to correct any science images since it only acts to account for the pixel-to-pixel response and not for the additive errors. A normalized spectroscopic flat image,  $F_\lambda^n(x, y)$ , can be calculated as:

$$F_\lambda^n(x, y) = \frac{F_\lambda(x, y) - B(x, y) - (\frac{t_S}{t_D})D(x, y)}{\text{med}_{lp}(F_\lambda(x, y) - B(x, y) - (\frac{t_S}{t_D})D(x, y))}, \quad (2.9)$$

where  $F_\lambda(x, y)$  is the non-corrected flat image,  $B(x, y)$  is the bias image,  $D(x, y)$  is the dark image which is scaled by the exposure time of the science image,  $t_S$ , and the dark image,  $t_D$ .  $\text{med}_{lp}$  is a low-pass median filter which smoothes out any rapid changes in the pixel-to-pixel response, removing the illumination contribution.

The calibrated science image,  $S_\lambda^*(x, y)$ , which accounts for the bias and dark currents as well as the flat fielding can then be calculated as:

$$S_\lambda^*(x, y) = \frac{S_\lambda(x, y) - B(x, y) - (\frac{t_S}{t_D})D(x, y)}{F_\lambda^n(x, y)}. \quad (2.10)$$

When multichannel CCDs are used, which consist of multiple CCDs or a CCD with multiple output amplifiers, additional calibrations, specifically cross-talk corrections and mosaicking, are required. Cross-talk noise refers to contamination that occurs during readout in one channel from another channel with a high signal and occurs because the signals can not be completely isolated from one another. Cross-talk corrections therefore account for this signal contamination between channels being read out at the same time (Freyhammer et al., 2001). Mosaicking is necessary for multichannel CCDs since the digitized signal read out from the detector has no reference of the physical location of the pixel it was detected at. Mosaicking, therefore, correctly orients the data acquired from a multichannel detector so that a single correctly oriented image is produced.

---

<sup>2</sup>NeAr plot sourced from <https://astronomers.salt.ac.za/data/salt-longslit-line-atlas/>



**Figure 2.8:** The first seven Chebyshev polynomials ( $T_0$  through  $T_6$ ) as defined by Equation 2.12 over the region  $[-1, 1]$  for which they are orthogonal. Plot adapted from (Press et al., 2007) (2023)<sup>3</sup>

## Wavelength Calibration

Finally, since the dispersion element breaks the incident light into its constituent wavelengths non-linearly (§ 2.1.7), the relation between the pixel on a detector and the wavelength of the light incident on it is unknown. Ideally, the spectrometer's optics would be modelled to produce a reliable pixel to wavelength calibration (see E.g. Liu and Hennelly, 2022), but this becomes increasingly more difficult for spectrometers with complex, non-sedentary, optical paths.

Alternatively, a source with well-defined spectral features, with said features evenly populating the wavelength region of interest, such as in Figure 2.7 may be observed. The observed frame is commonly referred to as an ‘arc’ frame, after the arc-lamps used to acquire the spectra, and should be observed alongside the science frames over the course of an observation run.

It is important that the arc frame is observed at the same observing conditions and parameters as the science frames since the optical path will vary over the course of an observing run and for different observing parameters, invalidating previously acquired arc frames. The wavelength calibrations then consist of defining a two-dimensional pixel-to-wavelength conversion function from the arc frame which may later be applied to calibrate the science frames. The two most common approximations for wavelength calibrations are the Chebyshev and Legendre polynomial approximations.

---

<sup>3</sup>Excellent resources on Chebyshev and Legendre polynomials are available digitally at [www.numerical.recipes/book](http://www.numerical.recipes/book).

**Chebyshev Polynomials** The Chebyshev polynomials are defined explicitly as:

$$T_n(x) = \cos(n \cos^{-1}(x)), \quad (2.11)$$

or recursively as:

$$\begin{aligned} T_0(x) &= 1, \\ T_1(x) &= x, \text{ and} \\ T_{n+1}(x) &= 2xT_n(x) - T_{n-1}(x), \text{ for } n \geq 1, \end{aligned} \quad (2.12)$$

where  $T$  is a Chebyshev polynomial of order  $n$ .<sup>4</sup> An important property of Chebyshev polynomials is that they are orthogonal polynomials. This means that the inner product of any two differing Chebyshev polynomials,  $T_i(x)$  and  $T_j(x)$ , over the range  $[-1, 1]$  is zero, as shown by:

$$\int_{-1}^1 T_i(x) T_j(x) \frac{1}{\sqrt{1-x^2}} dx = \begin{cases} 0, & i \neq j \\ \pi/2, & i = j \neq 0 \\ \pi, & i = j = 0 \end{cases}, \quad (2.13)$$

where  $1/\sqrt{1-x^2}$  is the weighting factor for Chebyshev polynomials. This property is important because it means that the coefficients in the Chebyshev polynomial expansion are independent of one another, allowing for a unique solution when approximating an unknown function (Arfken and Weber, 1999; Press et al., 2007). A Chebyshev approximation of an unknown wavelength calibration function is given by:

$$f(x) \approx \sum_{i=0}^N c_i T_i(u), \text{ or} \quad (2.14)$$

$$F(x, y) \approx \sum_{i=0}^N \sum_{j=0}^M c_{ij} T_i(u) T_j(v), \quad (2.15)$$

for a one- or a two-dimensional wavelength surface function, respectively. Here  $N$  and  $M$  are the desired  $x$  and  $y$  orders, and  $c_i$  and  $c_{ij}$  are the Chebyshev polynomial coefficients (Florinsky and Pankratov, 2015; Leng, 1997). Since the orthogonality property of the Chebyshev polynomials only holds true over the range  $[-1, 1]$ , the  $(x, y) \in ([0, a], [0, b])$  pixel coordinates must be remapped to  $u, v \in [-1, 1]$  following the relation:

$$(u, v) = \frac{2(x, y) - a - b}{b - a}. \quad (2.16)$$

The Chebyshev polynomials are more suited for wavelength calibrations than standard polynomials since they are orthogonal and have minima and maxima located at  $[-1, 1]$ , as seen in Figure 2.8. This means that the Chebyshev approximation is exact when  $x = x_n$ , where  $x_n$  are the positions of the  $n - 1$   $x$ -intercepts of  $T_N(x)$ . These properties greatly minimize the error in the Chebyshev approximation, even at lower orders (Arfken and Weber, 1999).

---

<sup>4</sup>Chebyshev polynomials are denoted  $T$  as a hold-over from the alternate spelling of ‘Tchebycheff’.



**Figure 2.9:** The first six Legendre polynomials ( $P_0$  through  $P_5$ ) as defined by Equation 2.20 over the region  $[-1, 1]$  for which they are orthogonal. Plot adapted from Geek3, CC BY-SA 3.0, via Wikimedia Commons (2023).

**Legendre Polynomials** Similar to the Chebyshev polynomials, the Legendre polynomials may be defined explicitly as:

$$P_n(x) = \frac{1}{2^n n!} \frac{d^n}{dx^n} (x^2 - 1)^n, \quad (2.17)$$

or recursively as:

$$\begin{aligned} P_0(x) &= 1, \\ P_1(x) &= x, \text{ and} \\ (n+1)P_{n+1}(x) &= (2n+1)xP_n(x) - nP_{n-1}(x), \text{ for } n \geq 1, \end{aligned} \quad (2.18)$$

where  $P$  is a Legendre polynomial of order  $n$ . Legendre polynomials also hold the property of orthogonality. This means that the inner product of any two differing Legendre polynomials,  $P_i(x)$  and  $P_j(x)$ , over the range  $[-1, 1]$  is zero, as shown by:

$$\int_{-1}^1 P_i(x) P_j(x) dx = \begin{cases} 0, & i \neq j \\ \frac{2}{2n+1}, & i = j \end{cases}, \quad (2.19)$$

where a weight of 1 is the weighting factor for Legendre polynomials (Dahlquist and Björck, 2003; Press et al., 2007). A Legendre approximation of an unknown wavelength calibration function is given by:

$$f(x) \approx \sum_{n=0}^N a_n P_n(u), \text{ or} \quad (2.20)$$

$$F(x, y) \approx \sum_{i=0}^N \sum_{j=0}^M a_{ij} P_i(u) P_j(v), \quad (2.21)$$

for a one-dimensional wavelength function or a two-dimensional surface function, respectively. Here  $N$  and  $M$  are the desired  $x$  and  $y$  orders,  $u$  and  $v$  are the same mapping variable as in Equation 2.16, and  $a_{ij}$  are the Legendre polynomial coefficients.

Legendre polynomials benefit from having the orthogonality condition with no weight necessary ( $w = 1$ ) which makes their coefficients computationally easier to compute but increases the error in a Legendre approximation when compared to that of the error in a Chebyshev approximation for functions of the same order,  $N$  (Ismail, 2005).

Regardless of which method of polynomial approximation is chosen, the polynomials are fit by varying the relevant coefficients using the least squares method. The resultant minimized function may then be used to convert the science frames from an ( $x$ -pixel,  $y$ -pixel) coordinate system to a ( $\lambda$ ,  $y$ -pixel) coordinate system.

## 2.2 Polarimetry

Both Huygens and Newton came to the conclusion that light demonstrates transversal properties (Huygens, 1690; Newton and Innys, 1730), which was later further investigated and coined as ‘polarization’ by Malus (Malus, 1809). Malus also investigated the polarization effects of multiple materials including some of which were birefringent, such as optical calcite, which he referred to as Iceland spar after Bartholinus’ investigations of the material (Bartholinus, 1670).

Fresnel built on Malus’ work showing that two beams of light, polarized at a right angle to one another, do not interfere, conclusively proving that light is transversal in nature, opposing the widely accepted longitudinal nature of light due to the prevalent belief in the ether. He later went on to correctly describe how polarized light is reflected and refracted at the surface of optical dielectric interfaces, without knowledge of the electromagnetic nature of light. Fresnel’s equations for the reflectance and transmittance,  $R$  and  $T$ , are defined as:

$$\begin{aligned} R_s &= \left| \frac{Z_2 \cos \theta_i - Z_1 \cos \theta_t}{Z_2 \cos \theta_i + Z_1 \cos \theta_t} \right|^2, \\ R_p &= \left| \frac{Z_2 \cos \theta_t - Z_1 \cos \theta_i}{Z_2 \cos \theta_t + Z_1 \cos \theta_i} \right|^2, \\ T_s &= 1 - R_s, \text{ and} \\ T_p &= 1 - R_p, \end{aligned} \tag{2.22}$$

where  $s$  and  $p$  are the two polarized components of light perpendicular to one another,  $Z_1$  and  $Z_2$  are the impedance of the two media, and  $\theta_i$ ,  $\theta_t$ , and  $\theta_r$  are the angles of incidence, transmission, and reflection, respectively (Fresnel, 1870).

Nicol was the first to create a polarizer, aptly named the Nicol prism, where the incident light is split into its two perpendicular polarization components, namely the ordinary and extraordinary beams. Faraday discovered the phenomenon where the polarization plane of light is rotated when under the influence of a magnetic field, known as the Faraday effect. Brewster calculated the angle of incidence,  $\theta_B = \arctan n_2/n_1$ , at which incident polarized light is perfectly transmitted through a transparent surface, with refractive indexes of  $n_1$  and  $n_2$ , while non-polarized incident light is perfectly polarized when reflected and partially polarized when refracted.

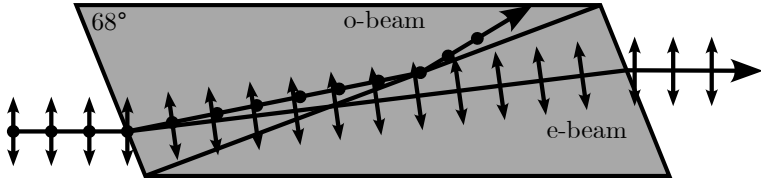


**Figure 2.10:** Diagram of a Nicol prism for incident non-polarized light. Diagram adapted from Fred the Oyster, CC BY-SA 4.0, via Wikimedia Commons (2023).

Stokes' work created the first consistent description of polarization and gave us the Stokes parameters which describe an operational approach to measuring polarization (discussed further in § 2.2.1) (Stokes, 1852). Hale was the first to apply polarization to astronomical observations, using a Fresnel rhomb and Nicol prism as a quarter-wave plate and polarizer, respectively (Hale, 1908, 1979). Wollaston also created a prism, similarly named the Wollaston prism, which allowed simultaneous observation of the ordinary and extraordinary beams due to the smaller deviation angle (Wollaston, 1802). Finally, Chandrasekhar's work furthered our understanding of astrophysical polarimetry by explaining the origin of polarization observed in starlight as well as mathematically modeling the polarization of rotating stars, which came to be named Chandrasekhar polarization (Chandrasekhar, 1950).

### 2.2.1 Polarization

Maxwell's equations for an electromagnetic field propagating through a vacuum are given as:

$$\begin{aligned} \nabla \cdot \mathbf{E} &= 0, \\ \nabla \cdot \mathbf{B} &= 0, \\ \nabla \times \mathbf{E} &= -\frac{1}{c} \frac{\partial \mathbf{B}}{\partial t}, \text{ and} \\ \nabla \times \mathbf{B} &= \frac{1}{c} \frac{\partial \mathbf{E}}{\partial t}, \end{aligned} \quad (2.23)$$

where  $\mathbf{E}$  and  $\mathbf{B}$  are the electric and magnetic field vectors, and  $c$  is the speed of light. In a right-handed  $(x, y, z)$  coordinate system, a non-trivial solution of an electromagnetic wave following Maxwell's Equations propagating along the  $z$ -axis, towards a hypothetical observer, is described by:

$$\begin{aligned} \mathbf{E} &= E_x \cos(kz - \omega t + \Phi_x) \hat{x} + E_y \cos(kz - \omega t + \Phi_y) \hat{y}, \text{ and} \\ \mathbf{B} &= \frac{1}{c} E_y \cos(kz - \omega t + \Phi_y) \hat{x} + \frac{1}{c} E_x \cos(kz - \omega t + \Phi_x) \hat{y}, \end{aligned} \quad (2.24)$$

where  $E_x$ ,  $E_y$ ,  $\Phi_x$ , and  $\Phi_y$  are all parameters describing the amplitude and phase of the electric field vector in the  $(x, y)$  plane, and with the magnetic field vector proportional and perpendicular to the electric field vector (Griffiths, 2005).

Considering only the electric field component and rewriting Equation 2.24 using complex values allows us to simplify the form of the solution to:

$$\mathbf{E} = \Re(\mathbf{E}_0 e^{-i\omega t}), \quad (2.25)$$

where we only consider the real part of the equation, and where  $\mathbf{E}_0$  is defined as:

$$\mathbf{E}_0 = E_x e^{i\Phi_x} \hat{x} + E_y e^{i\Phi_y} \hat{y}, \quad (2.26)$$

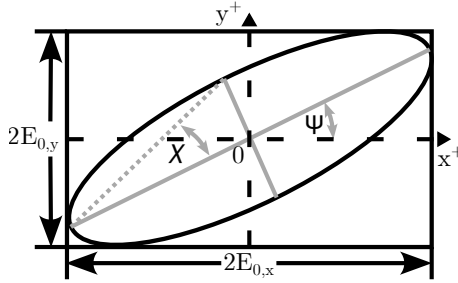


**Figure 2.11:** The polarization ellipse for an electric field vector propagating through free space. Diagram adapted from Inductiveload, PDM 1.0, via Wikimedia Commons (2023).

and is referred to as the polarization vector since it neatly contains the parameters responsible for the polarization properties (Degl’Innocenti, 2014).

For an electric field vector with oscillations in some combination of the  $x$  and  $y$  axes, the tip of the vector sweeps out an ellipse, as depicted in Figure 2.11. This ellipse is referred to as the polarization ellipse and has the form:

$$\left(\frac{\mathbf{E}_x}{\mathbf{E}_{0,x}}\right)^2 + \left(\frac{\mathbf{E}_y}{\mathbf{E}_{0,y}}\right)^2 - \frac{2\mathbf{E}_x\mathbf{E}_y}{\mathbf{E}_{0,x}\mathbf{E}_{0,y}} \cos \Phi = \sin^2 \Phi, \quad (2.27)$$

where  $\Phi = \Phi_x - \Phi_y$  is the phase difference between the  $x$  and  $y$  phase parameters. The degree of polarization for the polarization ellipse is related to the eccentricity of the ellipse and the angle at which it is rotated relates to the polarization angle. Since  $\mathbf{E}_{0,x}$ ,  $\mathbf{E}_{0,y}$ ,  $\Phi_x$ , and  $\Phi_y$  describe the wave, the polarization ellipse that results from these parameters is fixed as the wave continues to propagate.

Since observations consist of images taken over a desired exposure time, time averaging of Equation 2.27 over the exposure time is necessary. Given the periodical nature and high frequencies of the fields, the time averaging may be found over a single oscillation using:

$$\langle \mathbf{E}_i \mathbf{E}_j \rangle = \lim_{dt \rightarrow \infty} \frac{1}{T} \int_0^T \mathbf{E}_i \mathbf{E}_j dt, \quad \text{for } i, j \in (x, y), \quad (2.28)$$

where  $T$  is the total averaging time over the electric field vectors  $\mathbf{E}_i$  and  $\mathbf{E}_j$  (Collett, 2005). Applying the time averaging to Equation 2.27 and simplifying results in:

$$(E_{0x}^2 + E_{0y}^2)^2 - (E_{0x}^2 - E_{0y}^2)^2 - (2E_x E_y \cos \Phi)^2 = (2E_x E_y \sin \Phi)^2. \quad (2.29)$$

The expressions inside the parentheses can be found through observation and may also be represented as:

$$\mathbf{S} = \begin{pmatrix} S_0 \\ S_1 \\ S_2 \\ S_3 \end{pmatrix} = \begin{pmatrix} I \\ Q \\ U \\ V \end{pmatrix} = \begin{pmatrix} E_{0x}^2 + E_{0y}^2 \\ E_{0x}^2 - E_{0y}^2 \\ 2E_{0x}E_{0y} \cos \Phi \\ 2E_{0x}E_{0y} \sin \Phi \end{pmatrix}, \quad (2.30)$$

where  $S_0$  to  $S_3$  are referred to as the Stokes (polarization) parameters. The parameters describe the:  $S_0$ , total intensity (often normalized to 1);  $S_1$ , ratio of the Linear Horizontally Polarized (LHP) to Linear Vertically Polarized (LVP) light;  $S_2$ , ratio of the Linear  $+45^\circ$  Polarized ( $L+45^\circ$ ) to Linear  $-45^\circ$  Polarized ( $L-45^\circ$ ) light; and  $S_3$ , ratio of the Right Circularly Polarized (RCP) (clockwise) to Left Circularly Polarized (LCP)



**Figure 2.12:** The Poincaré sphere describing the polarization properties of a wave-packet propagating through free space. Diagram adapted from Inductiveload, PDM 1.0, via Wikimedia Commons (2023).

(counter-clockwise) light. When the intensity is normalized, the Stokes parameters range from 1 to  $-1$ , based on the dominating component of the parameter (Chandrasekhar, 1950; Stokes, 1852).

From Equation 2.29 and 2.30, the polarization parameters are related by:

$$I^2 = Q^2 + U^2 + V^2, \quad (2.31)$$

for entirely polarized light. Only beams of completely polarized light could be accounted for before Stokes' work on polarization. Using the Stokes parameters, we can now account for partially polarized light such that:

$$I^2 \geq Q^2 + U^2 + V^2, \quad (2.32)$$

where  $I$ ,  $Q$ ,  $U$ , and  $V$  are the normalized polarization parameters, often symbolized as

$$\bar{Q} = \frac{Q}{I}, \quad \bar{U} = \frac{U}{I}, \quad \text{and} \quad \bar{V} = \frac{V}{I}. \quad (2.33)$$

Similar to the polarization ellipse, the Stokes parameters may be depicted using the Poincaré sphere in spherical coordinates  $(IP, 2\Psi, 2\chi)$ , such that:

$$\begin{aligned} I &= S_0, \\ P &= \frac{\sqrt{S_1^2 + S_2^2 + S_3^2}}{S_0}, \text{ for } 0 \leq P \leq 1, \\ 2\Psi &= \arctan \frac{S_3}{\sqrt{S_1^2 + S_2^2}}, \text{ and} \\ 2\chi &= \arctan \frac{S_2}{S_1}, \end{aligned} \quad (2.34)$$

where  $I$  denotes the total intensity,  $P$  denotes the degree of polarization, or the ratio of polarized to non-polarized light in the wave-packet,  $\chi$  denotes the polarization angle, and  $\Psi$  denotes the ellipticity angle of the polarization ellipse.



**Figure 2.13:** A diagram of an ideal polarimeter. Diagram adapted from Degl'Innocenti and Landolfi (2004).

## 2.2.2 Polarization Measurement

Except for polarimetry in the radio-wavelength regime, the polarization of a beam can not be directly measured. The polarization properties may, however, be recovered from the beam through the manipulation of the four parameters given in Equation 2.24. This so-called manipulation is achieved by passing the beam through optical elements which vary the beam for differing amplitudes and phases. These matrix operations may be represented by their corresponding Mueller matrices.

For ideal components, the resultant beam  $\mathbf{S}'$  after passing through an optical element is given by  $\mathbf{S}' = \mathbf{MS}$ , where  $\mathbf{S}$  is the beam incident on the optical element and  $\mathbf{M}$  represents the  $4 \times 4$  Mueller matrix representing the optical element. Mueller matrices are especially useful when dealing with paths through optical elements as they observe the ‘train’ property (Priebe, 1969). This means that an incoming beam  $\mathbf{S}$  passing, in order, through elements with known Mueller matrices ( $\mathbf{M}_0, \dots, \mathbf{M}_N$ ) results in an outgoing beam  $\mathbf{S}'$  such that:

$$\mathbf{S}' = \mathbf{M}_N \dots \mathbf{M}_0 \mathbf{S}. \quad (2.35)$$

Some Mueller Matrices are given below with angles related to those in Figure 2.13, measured counter-clockwise in a right-handed coordinate system.

**General Rotation** The Mueller matrix for coordinate space rotations about the origin by an angle  $\theta$ ,

$$\mathbf{R}(\theta) = \begin{bmatrix} 1 & 0 & 0 & 0 \\ 0 & \cos 2\theta & \sin 2\theta & 0 \\ 0 & -\sin 2\theta & \cos 2\theta & 0 \\ 0 & 0 & 0 & 1 \end{bmatrix}. \quad (2.36)$$

**General Linear Retardance** The Mueller matrix for retardance where  $\alpha$  is the angle between the incoming vector and fast axis, and  $\delta$  is the retardance introduced by the retarder,

$$\mathbf{W}(\alpha, \delta) = \begin{bmatrix} 1 & 0 & 0 & 0 \\ 0 & \cos^2 2\alpha + \sin^2 2\alpha \cos \delta & \cos 2\alpha \sin 2\alpha(1 - \cos \delta) & \sin 2\alpha \sin \delta \\ 0 & \cos 2\alpha \sin 2\alpha(1 - \cos \delta) & \cos^2 2\alpha \cos \delta + \sin^2 2\alpha & -\cos 2\alpha \sin \delta \\ 0 & -\sin 2\alpha \sin \delta & \cos 2\alpha \sin \delta & \cos \delta \end{bmatrix}. \quad (2.37)$$

The retarder is often referred to by this retardance, e.g. if the retardance is  $\delta = \pi$  or  $\pi/2$ , the retarder is referred to as a half- or quarter-wave plate, respectively.

**General Linear Polarization** The Mueller matrix for linear polarization where  $\beta$  is the angle between the incoming vector and transmission axis,

$$\mathbf{P}(\beta) = \frac{1}{2} \begin{bmatrix} 1 & \cos 2\beta & \sin 2\beta & 0 \\ \cos 2\beta & \cos^2 2\beta & \cos 2\beta \sin 2\beta & 0 \\ \sin 2\beta & \sin 2\beta \cos 2\beta & \sin^2 2\beta & 0 \\ 0 & 0 & 0 & 0 \end{bmatrix}. \quad (2.38)$$

These matrices in combination with Equation 2.35 allow us to describe how the incoming Stokes parameters would change when passing through the various optical elements. For a setup similar to Figure 2.13, the detected Stokes parameters can be described by:

$$\begin{aligned} S'(\alpha, \beta, \gamma) \propto \frac{1}{2} \{ & I + [Q \cos 2\alpha + U \sin 2\alpha] \cos(2\beta - 2\alpha) \\ & - [Q \sin 2\alpha + U \cos 2\alpha] \sin(2\beta - 2\alpha) \cos \gamma \\ & + V \sin(2\beta - 2\alpha) \sin \gamma \}, \end{aligned} \quad (2.39)$$

where the retardance angle,  $\alpha$ , polarization angle,  $\beta$ , for a wave plate with a relative phase difference,  $\gamma$ , may be varied to acquire a system of equations that can be solved to retrieve the Stokes polarization parameters (Bagnulo et al., 2009).

Several or more frames taken under differing configurations may be used to reduce a system of equations to extract all four Stokes polarization parameters, but it is possible to extract the  $I$ ,  $Q$  and  $U$  polarization parameters using only four frames, or two dual-beam frames, for well-chosen configurations and assuming ideal components. This ideal configuration varies the retarder angle such that  $\Delta\alpha = \pi/8$  while keeping the polarizer stationary. More frames for additional retarder angles are advisable and often necessary, however, as they correct for any differences in sensitivity, such as may arise in a polarized flat field and which is further discussed in § 2.2.3 (Patat and Romaniello, 2006). From Equation 2.39 we see that the linear retarder element is the driving element of a polarizer as the first three Stokes parameters ( $S_{0-2}$ , or  $I$ ,  $Q$ , and  $U$ ) may be found by changing only the angle of retardance,  $\alpha$ .

**Wave Plates** Wave plates, also commonly referred to as retarders, are generally made from optically transparent birefringent crystals. A wave plate has a fast and slow axis, which are perpendicular to one another and both perpendicular to an incident beam. Due to the birefringence of the wave plate medium, the phase velocity of the beam polarized



**Figure 2.14:** Diagram of a Rochon prism. Included in the diagram are the optical axes of the differing sections of the birefringent material as well as polarizing directions of the incident beam, denoted using the  $\leftrightarrow$  and  $\odot$  symbols, for the  $O$ - and  $E$ -beams, respectively. Figure adapted from ChrisHodgesUK, CC BY-SA 3.0, via Wikimedia Commons (2023).

parallel to the fast axis, namely the extraordinary beam, slightly increases while that of the beam polarized parallel to the slow axis, namely the ordinary beam, remains unaffected. This difference in the perpendicular component's phase velocities introduces a relative phase difference between the two beams,  $\gamma$ , which is given by:

$$\gamma = \frac{2\pi\Delta n L}{\lambda_0} \quad (2.40)$$

where  $\Delta n$  and  $L$  refer to the birefringence and thickness of the wave plate medium, respectively, and  $\lambda_0$  refers to the vacuum wavelength of the beam (Hecht, 2017).

This relative phase difference determines the name of the wave plate, such that the  $\gamma = m(\pi/2)$  and  $\gamma = m(\pi/4)$  phase differences, for  $m \in \mathbb{Z}^+$ , refer to the half- and quarter-wave plates (which are the most common wave plate phases), respectively. Phase differences with an integer multiple of one another relate to the same phase difference and are referred to as multiple-order wave plates, while wave plates with a phase difference less than an integer multiple are referred to as zero-order wave plates. Several multiple-order wave plates can be combined by alternatively aligning the fast axis of one to the slow axis of another to create a compound zero-order wave plate (Hale and Day, 1988).

**Polarizers** Polarizers are typically made from two prisms, of a birefringent material, cemented together with an optically transparent adhesive. The actual effect of separating the perpendicular polarization components is achieved using varying effects, namely through:

- absorption of one of the polarized components, such as in Polaroid polarizing filters,
- total internal reflection of a single polarized component, such as in a Nicol prism (Figure 2.10),
- Refraction of a single polarized component, such as in a Rochon prism (Figure 2.14), or
- Refraction of both polarization components in differing directions, such as in a Wollaston prism (Figure 2.15).

**Wollaston Prisms** The Wollaston prism consists of two right-angle prisms consisting of a birefringent monoaxial material, cemented together with an optically transparent adhesive along their hypotenuses with their optical axes orthogonal, as seen in Figure 2.15. The Wollaston prism is a common optical polarizing element in astrophysical polarimetry which separates an incident beam into two linearly polarized  $O$ - and  $E$ -beams, orthogonal to one another, and deviated from their common axis equally. The deviation angle of the



**Figure 2.15:** Diagram of a Wollaston prism. Included in the diagram are the optical axes of the differing sections of the birefringent material as well as polarizing directions of the incident beam, denoted using the  $\leftrightarrow$  and  $\downarrow\uparrow$  symbols, for the  $O$ - and  $E$ -beams, respectively. Diagram adapted from fgalore, CC BY-SA 3.0, via Wikimedia Commons (2023).

polarized beams is determined by the wedge angle which is defined as the angle from the common hypotenuse to that of the outer transmission face of either prism.

Wollaston prisms benefit over simpler elements (such as those listed in the polarizer paragraph) since a single frame allows for the observation of both orthogonal polarization components. This halves the observational time required to collect enough data to calculate the Stokes parameters, at the cost of an increase in calibration and reduction difficulty (Simon, 1986).

### 2.2.3 Polarimetric Calibrations

The raw science images acquired during polarimetric observations contain a combination of useful science data as well as noise. Corrections and calibrations related to the detector remain unchanged from those described in § 2.1.8, while those related to correcting for the optical elements relate to corrections for spurious polarization effects.

#### Flat Fielding

Once the CCD calibrations have been completed, the polarization intrinsic to the optical elements needs to be accounted for such that the pixel-to-pixel response is made uniform. Flat-fielding is, once again, used to correct for this. The flats taken for polarimetry, however, introduce an additional challenge as the targets for conventional flats are polarized, such as twilight and dome flats which are polarized by light scattering in the atmosphere and the reflective surface of the dome, respectively.

If no unpolarized flat images can be taken for flat field calibrations then, when possible due to the polarimeter design, the wave plate may be constantly rotated to act as a depolarizing element; this is effective so long as the wave plate rotation period is much faster than the flat's exposure time. Alternatively, polarized flats may be taken at the same set of half-wave plate angles used for science observations and averaged together to achieve a similar depolarizing effect.

Observing additional ‘redundant’ exposures for the science and flat images increases the depolarizing effect up to the maximum of 16 half-wave plate positions, where exposures with a half-wave plate angle differing by  $\pi/4$  from another are considered redundant due to the  $O$ - and  $E$ -beams swapping between the related exposures.

Increasing the amount of redundant observations proportionally increases the time needed to observe all the exposures, which in turn introduces time-dependent effects such as fringing or intensity variations of the flat source. As such, a middle ground must be found for the amount of redundant frames observed. (Patat and Romanielo, 2006; Peinado et al., 2010).

### Dual-Beam Extraction and Alignment

After calibrations for the CCD and light path are accounted for, the *O*- and *E*-beams can be extracted and further reduced. The extraction depends heavily on the layout of the polarimeter but often a simple cropping of the differing sections is enough to separate the two images.

After extracting the *O*- and *E*-beams for a specific half-wave plate angle, the images need to be aligned such that the sources present in them overlap. The Wollaston prism needs to be corrected for as it introduces a beam deviation which differs across both images. The aligning of the *O*- and *E*-beams is crucial as the comparison of the dual images is what allows for the calculation of the polarization properties.

### Sky Subtraction

The polarization introduced by the sky introduces a difference in the intensity of the background sky and needs to be removed as it will influence the polarization results of the target source. Thankfully, the background polarization is an additive type of noise and may be subtracted out across the frames. This subtraction is done independently for both beams in a frame and for each frame since the background intensity of all observed polarimetric beams will differ based on the observational parameters.

## 2.3 Spectropolarimetry

As the name suggests, spectropolarimetry is the measurement of the polarization of light for a chosen spectral range and provides polarimetric results as a function of wavelength. As spectropolarimetry is so closely reliant on both spectroscopy and polarimetry, advancements in spectropolarimeters have always been gated by the advancements of spectrometers and polarimeters (as described in § 2.1 and § 2.2).

The most notable historical contributions of spectropolarimetry are those of spectropolarimetric studies instead of instrumental developments. Spectropolarimetry provides further insights into a materials physical structure, chemical composition, and magnetic field, allowing spectropolarimetry to be useful across multiple disciplines. In astronomy in particular, spectropolarimetry has been used to study the magnetic field, chemical composition, and underlying structure and emission processes of multiple types of celestial objects (see for example Antonucci and Miller, 1985; Donati et al., 1997; Wang and Wheeler, 2008).

Along with common points of consideration when developing any instrumentation for observational astronomy, such as resolution and sensitivity, spectropolarimeters need also consider the spectral response of the polarimetric components as well as the polarization



**Figure 2.16:** A spectropolarimetric target exposure as observed by the SALT RSS in spectropolarimetry mode.

response of the spectroscopic components as both are simultaneously in the light-path during observations and have noticeable affects on one another. Time is another constraint for spectropolarimetry as the incident light is separated both by wavelength and by polarization states. This division of the incident light results in increased exposure times for both target observations and observations necessary for calibrations.

Figure 2.16 illustrates a typical science image taken with a spectropolarimeter. The image contains the  $O$ - and  $E$ -beams which are both dispersed into their spectra. Spectropolarimetric results are acquired from measurements and calibrations of these images alongside any necessary calibration images.

### 2.3.1 Spectropolarimetric Measurement

The derived relations given in § 2.2.1, such as the Stokes parameters, describe polarization in general and are valid for both polarimetry and spectropolarimetry. Due to the time averaging of the observed light (Equation 2.28), any minor temporal variation, partial polarization, or monochromatic nature of the spectropolarimetric polarization parameters are accounted for.

For linear spectropolarimetry using a dual-beam polarizing element, an exposure measures the  $O$ - and  $E$ -beam wavelength dependent intensities,  $f_{O,i}(\lambda)$  and  $f_{E,i}(\lambda)$ , for a given wave plate angle  $\theta_i$  at angle  $i$ . These intensities thus relate to the wavelength dependent Stokes parameters as:

$$\begin{aligned} f_{O,i}(\lambda) &= \frac{1}{2}[I(\lambda) + Q(\lambda) \cos(4\theta_i) + U(\lambda) \sin(4\theta_i)], \text{ and} \\ f_{E,i}(\lambda) &= \frac{1}{2}[I(\lambda) - Q(\lambda) \cos(4\theta_i) - U(\lambda) \sin(4\theta_i)]. \end{aligned} \quad (2.41)$$

At least four linear equations are required to solve for three variables in a system of linear equations and thus at least two exposures must be taken to solve for the linear ( $I(\lambda)$ ,  $Q(\lambda)$ , and  $U(\lambda)$ ) polarization parameters (Degl'Innocenti et al., 2006; Keller, 2002).

The first Stokes parameter,  $I(\lambda)$ , may be recovered for each dual-beam exposure using

$$I_i(\lambda) = f_{O,i}(\lambda) + f_{E,i}(\lambda). \quad (2.42)$$

By calculating the  $I_i(\lambda)$  Stokes parameter for each wave plate position  $i$ , the variation of the target over the course of observation may be corrected for, resulting in the  $I(\lambda)$  Stokes parameter.

Next, the  $Q(\lambda)$  and  $U(\lambda)$  Stokes parameters are found by first defining the normalized difference in relative intensities,  $F_i(\lambda)$ , as:

$$F_i(\lambda) \equiv \frac{f_{O,i}(\lambda) - f_{E,i}(\lambda)}{f_{O,i}(\lambda) + f_{E,i}(\lambda)}, \quad (2.43)$$

which allows Equation 2.41 to be written, as

$$F_i(\lambda) = \bar{Q}(\lambda) \cos(4\theta_i) + \bar{U}(\lambda) \sin(4\theta_i) = P \cos(4\theta_i - 2\chi), \quad (2.44)$$

in terms of the normalized Stokes parameters, or, alternatively, the degree of polarization,  $P$ , and polarization angle,  $\chi$  (as described in Equation 2.33 and 2.34).

The optimal change in wave plate angle is  $\Delta\theta_i = \pi/8$  as it allows the normalized Stokes polarization parameters to be calculated as:

$$\begin{aligned} \bar{Q}(\lambda) &= \frac{2}{N} \sum_{i=0}^{N-1} F_i(\lambda) \cos\left(\frac{\pi}{2}i\right), \text{ and} \\ \bar{U}(\lambda) &= \frac{2}{N} \sum_{i=0}^{N-1} F_i(\lambda) \sin\left(\frac{\pi}{2}i\right), \end{aligned} \quad (2.45)$$

where  $N$  is the number of exposures taken, limited such that  $N \in [2, 16]$  (Patat and Romaniello, 2006).

### 2.3.2 Spectropolarimetric Calibrations

Just as the elements of a spectropolarimeter are an amalgamation of both a spectrometer and polarimeter, it naturally follows that the calibrations necessary to reduce spectropolarimetric data are a combination of the calibrations needed for spectroscopy and polarimetry, discussed further in § 2.1.8 and § 2.2.3. Even though the spectrometer and polarimeter components both have an effect on an incident beam following the light-path through the spectropolarimeter, the calibration procedures for both methods remain mostly independent of one another and as such need not be repeated here.

Spectropolarimetric calibrations are, however, more involved when compared to the same calibrations for either spectroscopy or polarimetry. Minor deviations in the calibrations across both the spectra and the polarized beam compound, especially when dealing with the wavelength calibration, resulting in poor Signal-to-Noise Ratio (S/N)'s. Generally, more exposures over longer timespans are required to acquire enough redundancy and signal for the calculation of the Stokes parameters on top of the time necessary for calibrations to be completed. It should therefore be noted just how important the calibrations are when dealing with spectropolarimetry.



**Figure 2.17:** The tracker, supporting structure, and primary mirror of SALT. Figure adapted from the SALT call for proposals (2022).<sup>5</sup>

## 2.4 The Southern African Large Telescope

Southern African Large Telescope (SALT) is a 10 m class optical/near-infrared telescope situated at the South African Astronomical Observatory (SAAO) field station near Sutherland, South Africa (Burgh et al., 2003). The operational design was based on the Hobby-Eberly Telescope (HET) situated at McDonald Observatory, Texas, which limits the pointing of the telescope’s primary mirror to a fixed elevation ( $37^\circ$  from zenith in the case of SALT) while still allowing for full azimuthal rotation (Ramsey et al., 1998). Both SALT and HET utilize a spherical primary mirror which is stationary during observations and a tracker housing most of the instrumentation that tracks the primary mirrors spherically shaped focal path. Figure 2.17 depicts SALT’s tracker (top left), supporting structure, and primary mirror (bottom right).

### 2.4.1 The Primary Mirror

The primary mirror is composed of 91 individual 1 m hexagonal mirrors which together form an 11 m segmented spherical mirror. Each mirror segment can be adjusted by actuators allowing the individual mirrors to approximate a single monolithic spherical mirror. The fixed elevation means that SALT’s primary mirror has a fixed gravity vector allowing for a lighter, cost-effective supporting structure when compared to those of a more traditional altitude-azimuthal mount but with the trade-off that the control mechanism and tracking have increased complexity (Buckley et al., 2006).

---

<sup>5</sup>[http://pysalt.salt.ac.za/proposal\\_calls/current/ProposalCall.html](http://pysalt.salt.ac.za/proposal_calls/current/ProposalCall.html)

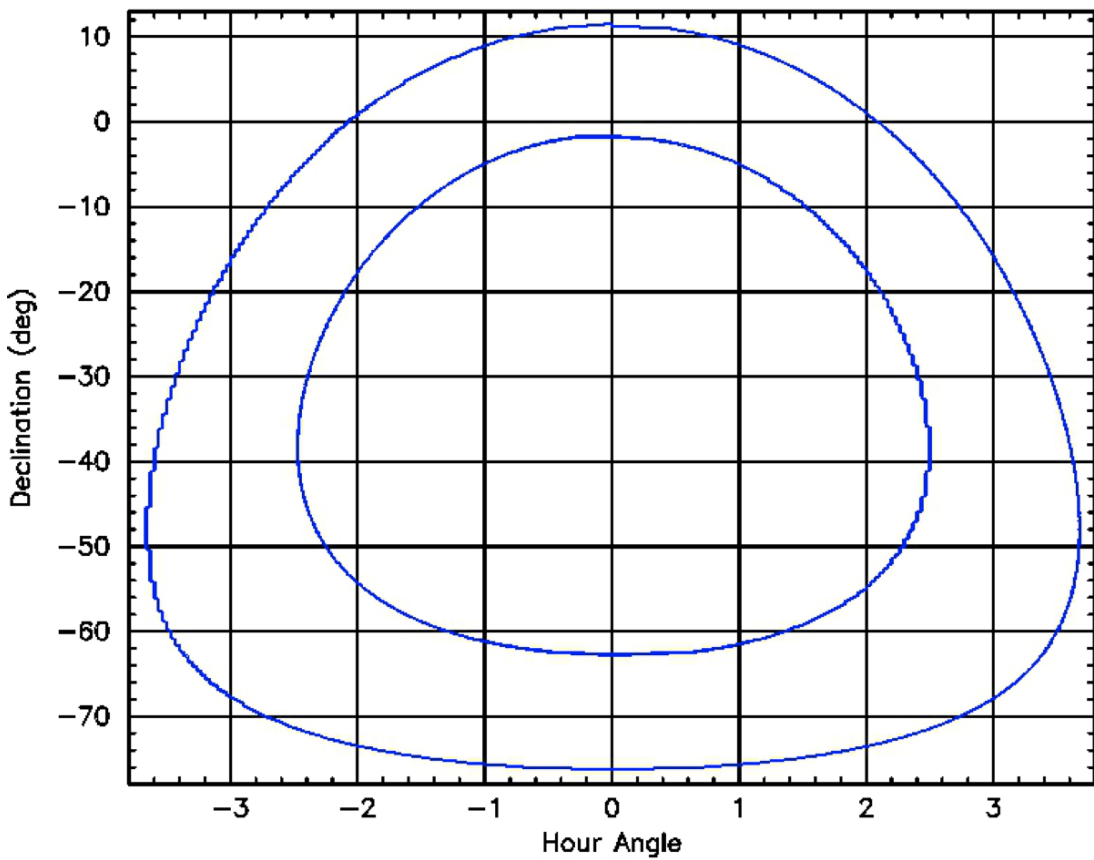


**Figure 2.18:** The visibility annulus of objects observable by SALT. Figure adapted from the SALT call for proposals (2013).<sup>6</sup>

### 2.4.2 Tracker and Tracking

During observations the primary mirror is stationary and the tracker tracks celestial objects across the sky by moving along the primary focus. The tracker is capable of 6 degrees of freedom with an accuracy of  $\sim 5 \mu\text{m}$  and is capable of tracking  $\pm 6^\circ$  from the optimal central track position. Targets at declinations from  $10.5^\circ$  to  $-75.3^\circ$ , as shown in Figure 2.18 are accessible during windows of opportunity. As the tracker moves along the track the effective collecting area varies and thus SALT has a varying effective diameter of  $\sim 7 \text{ m}$  to  $9 \text{ m}$  when the tracker is furthest and closest to the optimal central position, respectively.

The tracker is equipped with a Spherical Aberration Corrector (SAC) (O'Donoghue, 2000), and an Atmospheric Dispersion Compensator (ADC) (O'Donoghue, 2002), which corrects for the spherical aberration caused by the geometry of the primary mirror and allows access to wavelengths as short as  $3200 \text{ \AA}$ . These return a corrected flat focal plane with an  $8'$  diameter field of view at prime focus on to the science instruments, with a  $1'$  annulus around it used by the tracker in a closed-loop guidance system. The tracker also houses the calibration system which contains the Ar, CuAr, HgAr, Ne, ThAr, and Xe wavelength calibration lamps (Buckley et al., 2008).

---

<sup>6</sup>[https://pysalt.salt.ac.za/proposal\\_calls/2013-2/](https://pysalt.salt.ac.za/proposal_calls/2013-2/)



**Figure 2.19:** The optical path of the SALT RSS. Figure adapted from the SALT call for proposals (2023).<sup>7</sup>

### 2.4.3 SALT Instrumentation

SALT is equipped with the SALT Imaging Camera (SALTICAM) and the RSS science instruments onboard the tracker, and the High Resolution Spectrograph (HRS) and Near Infra-Red Washburn Labs Spectrograph (NIRWALS) science instruments which are fibre-fed from the tracker to their own climate controlled rooms. The RSS is currently the only instrument used for spectropolarimetry.

#### NIRWALS

The Near Infra-Red Washburn Labs Spectrograph (NIRWALS) is currently being commissioned and will have a wavelength coverage of 8000 to 17000 Å, providing medium resolution spectroscopy at  $R = 2000$  to 5000 over Near Infra-Red (NIR) wavelengths (Brink et al., 2022; Wolf et al., 2022). NIRWALS is fibre-fed from its integral field unit, containing 212 object fibers, along with a separate sky bundle, containing 36 fibers, housed in the SALT fibre instrument feed. It is ideally suited for studies of nearby galaxies.

#### HRS

The High Resolution Spectrograph (HRS) echelle spectrograph was designed for high resolution spectroscopy at  $R = 37000 - 67000$  covering a wavelength range of 3700 - 8900 Å and consists of a dichroic beam splitter and two VPH gratings (Nordsieck et al., 2003). This instrument is capable of stellar atmospheric and radial velocity analysis.

<sup>7</sup>[https://pysalt.salt.ac.za/proposal\\_calls/current/ProposalCall.html](https://pysalt.salt.ac.za/proposal_calls/current/ProposalCall.html)

| Grating Name        | Wavelength Coverage (Å) | Usable Angles (°) | Bandpass per tilt (Å) | Resolving Power (1.25'' slit) |
|---------------------|-------------------------|-------------------|-----------------------|-------------------------------|
| PG0300 <sup>8</sup> | 3700 – 9000             |                   | 3900/4400             | 250 – 600                     |
| PG0700 <sup>8</sup> | 3200 – 9000             | 3.0 – 7.5         | 4000 – 3200           | 400 – 1200                    |
| PG0900              | 3200 – 9000             | 12 – 20           | ~ 3000                | 600 – 2000                    |
| PG1300              | 3900 – 9000             | 19 – 32           | ~ 2000                | 1000 – 3200                   |
| PG1800              | 4500 – 9000             | 28.5 – 50         | 1500 – 1000           | 2000 – 5500                   |
| PG2300              | 3800 – 7000             | 30.5 – 50         | 1000 – 800            | 2200 – 5500                   |
| PG3000              | 3200 – 5400             | 32 – 50           | 800 – 600             | 2200 – 5500                   |

**Table 2.1:** Gratings available for use with the RSS. Table adapted from the SALT call for proposals (2023).

## SALTICAM

The SALT Imaging Camera (SALTICAM) functions as the acquisition camera and simple science imager with various imaging modes, such as full-mode and slot-mode imaging, and supports low exposure times, down to 50 ms (O'Donoghue et al., 2006). This enables photometry of faint objects, especially at fast exposure times.

## RSS

The Robert Stobie Spectrograph (RSS) functions as the primary spectrograph on SALT and can operate in long-slit spectroscopy and spectropolarimetry modes, a narrowband imaging mode, and multi-object and high resolution spectroscopy modes (for an in-depth discussion on operational modes see Kobulnicky et al., 2003, or the latest call for proposals).

**The Detector** The RSS detector consists of a mosaic of 3 CCD chips with a total pixel scale of 0.1267'' per unbinned pixel with varying readout times depending on the binning and readout mode. The mosaicking results in a characteristic double ‘gap’ in the frames and resultant spectra taken with the RSS, as seen in Figure 2.16.

**The Available Gratings** The RSS is equipped with a rotatable magazine of six VPH gratings, as listed in Table 2.1. Observations may be planned using simulator tools provided by SALT and are performed in the first order only. The RSS has a clear filter, as well as three Ultraviolet (UV) (with differing lower filtering ranges) and one blue order blocking filter available, used in conjunction with the various gratings to block out contamination from the second order.

**RSS Spectropolarimetry** Spectropolarimetry using the RSS is currently commissioned for long-slit linear spectropolarimetry, ( $I, Q, U$ ), where observations are taken following the waveplate pattern lists as in Table 2.2. Circular, ( $I, V$ ), and all-Stokes, ( $I, Q, U, V$ ), spectropolarimetry modes are in commissioning with observations including redundant half-wave plate pairs to be commissioned thereafter.<sup>9</sup>

<sup>8</sup>The PG0300 surface relief grating has been replaced with the PG0700 VPH grating as of November 2022 but has been included here as observations using the PG0300 are used in later sections.

<sup>9</sup>Commission status sourced from the latest ‘Polarimetry Observers Guide’ (2024).

| Linear ( $^{\circ}$ ) |               | Linear-Hi ( $^{\circ}$ ) |               | Circular ( $^{\circ}$ ) |               | Circular-Hi ( $^{\circ}$ ) |               | All Stokes ( $^{\circ}$ ) |               |
|-----------------------|---------------|--------------------------|---------------|-------------------------|---------------|----------------------------|---------------|---------------------------|---------------|
| $\frac{1}{2}$         | $\frac{1}{4}$ | $\frac{1}{2}$            | $\frac{1}{4}$ | $\frac{1}{2}$           | $\frac{1}{4}$ | $\frac{1}{2}$              | $\frac{1}{4}$ | $\frac{1}{2}$             | $\frac{1}{4}$ |
| 0                     | -             | 0                        | -             | 0                       | 45            | 0                          | 45            | 0                         | 0             |
| 45                    | -             | 45                       | -             | 0                       | -45           | 0                          | -45           | 45                        | 0             |
| 22.5                  | -             | 22.5                     | -             |                         |               | 22.5                       | -45           | 22.5                      | 0             |
| 67.5                  | -             | 67.5                     | -             |                         |               | 22.5                       | 45            | 67.5                      | 0             |
|                       | -             | 11.25                    | -             |                         |               | 45                         | 45            | 0                         | 45            |
|                       | -             | 56.25                    | -             |                         |               | 45                         | -45           | 0                         | -45           |
|                       | -             | 33.75                    | -             |                         |               | 67.5                       | -45           |                           |               |
|                       |               | 78.75                    | -             |                         |               | 67.5                       | 45            |                           |               |

**Table 2.2:** Spectropolarimetry waveplate patterns defined for the RSS. The stated angles refer to the angle of the half ( $\frac{1}{2}$ -) and quarter ( $\frac{1}{4}$ -) waveplate's optical axis from the perpendicular of the dispersion axis. Table adapted from the SALT call for proposals (2023).

# Chapter 3

## Existing and Developed Software: An Overview of POLSALT, IRAF, and STOPS

This chapter contains an overview of *Polarimetric reductions for SALT* (POLSALT) and the limitations faced during POLSALT wavelength calibrations (§ 3.1), a brief overview of the *Image Reduction and Analysis Facility* (IRAF) tasks relevant for spectropolarimetric wavelength calibrations (§ 3.2), and an overview of *Supplementary Tools for POLSALT Spectropolarimetry* (STOPS), the software developed to supplement the POLSALT reduction process (§ 3.3). Finally, a discussion of the updated reduction process, an example of which may be found in Appendix A, is included (§ 3.4).

### 3.1 POLSALT - *Polarimetric reductions for SALT*

The POLSALT (*Polarimetric reductions for SALT*) pipeline is the official reduction pipeline for spectropolarimetric data taken using the SALT RSS.<sup>1</sup> The newest version of the software, aptly named the ‘beta version’ (‘version’ 23 January 2020), was the version adapted in this study. It includes a GUI, depicted in Figure 3.1, which allows for limited interactivity during key steps in the reduction process.<sup>2</sup>

The steps that make up the POLSALT reduction pipeline include raw image reductions, wavelength calibrations, background subtraction and spectral extraction, raw Stokes calculations, final Stokes calculations, and visualization of the results. Accurate reductions at each step are crucial for accurate results and are thus briefly discussed below. Further details for the reduction process may be found at the POLSALT GitHub wiki.<sup>3</sup>

---

<sup>1</sup>POLSALT is made freely available via the POLSALT GitHub repository, available at <https://github.com/saltastro/polsalt>. It is strongly advised to follow the wiki for installation instructions.

<sup>2</sup>Installation files and instructions for the ‘beta version’ utilizing the GUI are available at <http://www.sao.ac.za/~ejk/polsalt/code/> in a TAR GZIP file.

<sup>3</sup>The GitHub wiki for POLSALT is available at <https://github.com/saltastro/polsalt/wiki>.



**Figure 3.1:** The layout of the `POLSALT` Graphical User Interface (GUI), including the contents of the reduction steps accessible via the dropdown menu. Note that there is no trailing forward slash after the ‘Top level data directory’. Figure created from a local instance of the `POLSALT` GUI.

### 3.1.1 Raw Image Reductions

Raw image reductions are run via `imred.py` and apply the necessary basic reductions to the raw data before any calibrations are applied. These reductions include overscan subtractions, gain corrections, crosstalk corrections, and mosaicking as well as attaching the bad pixel maps and pixel variance information. Files with raw image reductions performed have “`mxgbp`” prepended to their names. As of February 2022, raw image reductions are automatically run for all RSS spectropolarimetric observations as part of the default SALT basic reduction pipeline that is run daily.

### 3.1.2 Wavelength Calibrations

Wavelength calibration and cosmic-ray rejection is performed via `specpolwavmap.py` and separately calibrates the *O*- and *E*-beams, based on the arc frames, and applies a simple cosmic-ray rejection for all science frames. This step is interactive and allows the user to individually fit wavelength calibration maps to each beam. The importance of an accurate correlation between both beams has been touched on previously (§ 2.3.2) and will be further discussed in § 3.1.8. The wavelength calibrated results are saved as an additional ‘`WAV`’ wavelength extension to each science FITS file, which are prefixed with a “`w`”, and the *O*- and *E*-beams of the extensions are split into their own sub-extensions.



**Figure 3.2:** The layout of the interactive POLSALT spectra extraction GUI after selecting the ‘update tilt correction and windows’ button along the bottom border of the window. Figure created from a local instance of the POLSALT GUI.

### 3.1.3 Spectral Extraction

Background subtraction and spectral extraction is run via `specpoleextract_dev.py` which corrects for the beam-splitter distortion and tilt, performs sky subtraction, and extracts a one dimensional wavelength dependent spectrum for each beam sub-extension. This step is interactive with Figure 3.2 showing the interactive window used for spectral extraction. The user, using the brightest trace in the image as a reference, defines regions which span the wavelength axis which define the background and trace regions for the sky subtraction and spectral extraction. Files with background and geometric corrections applied are saved with “c” prepended to their names and files which contain the extracted one dimensional spectrum have “e” further prepended to their names.

### 3.1.4 Raw Stokes Calculations

The raw Stokes calculations are performed via `specpolrawstokes_dev.py` and identify waveplate pairs for which the intensity,  $I$ , and a ‘raw Stokes’ signal,  $S$ , are calculated as:

$$I = \frac{1}{2}(O_1 + O_2 + E_1 + E_2), \text{ and} \quad (3.1)$$

$$S = \frac{1}{2} \left[ \left( \frac{O_1 - O_2}{O_1 + O_2} \right) - \left( \frac{E_1 - E_2}{E_1 + E_2} \right) \right]. \quad (3.2)$$

The raw Stokes signal is calculated as the normalized difference of the  $O$ - and  $E$ -beams, for a waveplate pair, taken perpendicular to one another. The created files contain the raw Stokes information and use a very specific naming style; most notably the indexes of the related waveplate pairs, from Table 2.2, are included in the file names.



**Figure 3.3:** The layout of the interactive POLSALT visualization GUI after selecting the ‘Plot results’ button along the bottom border of the window. Figure created from a local instance of the POLSALT GUI.

### 3.1.5 Final Stokes Calculations

The Final Stokes calculations are performed via `specpolfinalstokes.py` and, using the waveplate pattern along with the raw Stokes signals, calibrates for the polarimetric zero-point and waveplate efficiency, and calculates the final Stokes parameters. Before the final Stokes calculations are performed, and if a sufficient number of redundant exposures were taken, the raw Stokes signals are culled to eliminate outlier signals which may arise from, for example, temporary atmospheric conditions affecting the signal. The culling is performed by comparing observation cycles against one another, comparing the deviation of the signal means which estimate the baseline systematic polarization fluctuations (due to imperfections in repeatability), and performing a  $\chi^2$  analysis to eliminate any statistical outliers.

### 3.1.6 Visualization

Plotting the results of the spectropolarimetric reduction process is done using `specpolview.py`, which generates a plot of the Intensity, Linear Polarization (%), and Equatorial Polarization Angle ( $^\circ$ ) against a shared wavelength axis, as seen in Figure 3.4. This step is interactive allowing the user control over various options, such as the wavelength range, binning, etc., with the GUI shown in Figure 3.3.

### 3.1.7 Post-Processing Analysis

Generally, the plot of the spectropolarimetric results is the stopping point for most reduction procedures as it contains or creates the desired results. However, additional tools exist which may be used after the polarization reductions, and which are not represented in the GUI, namely, flux calibration and synthetic filtering.

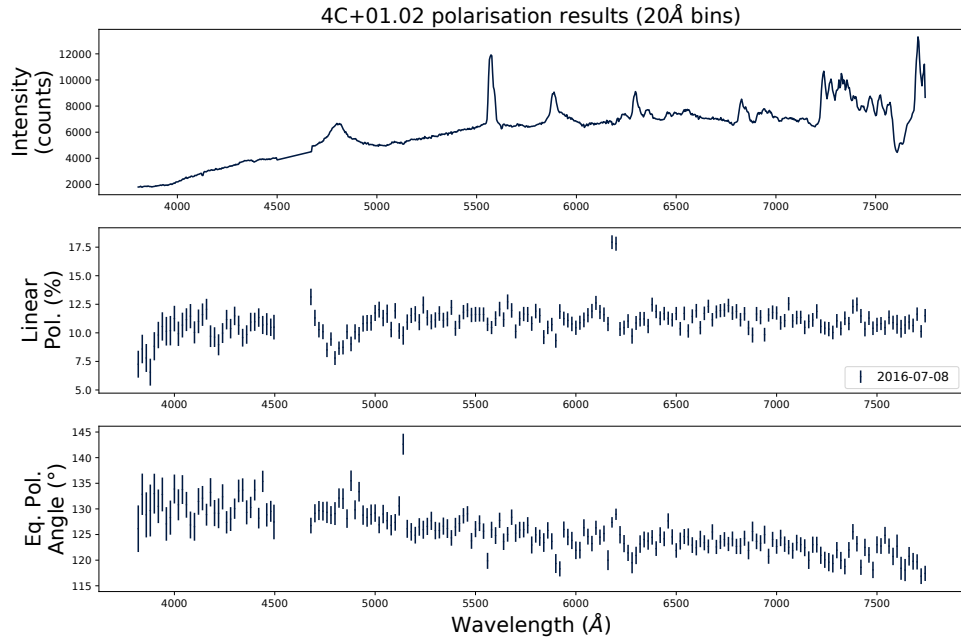


**Figure 3.4:** A typical plot resulting from the reduction process. Figure adapted from (Cooper et al., 2022).

Flux-calibrations are performed via `specpolflux.py` and are only intended for shape corrections of the spectrum. Additionally, a flux database file must exist for the observed standard and must be included in the working science directory.

Synthetic filtering is calculated via `specpolfilter.py` and computes the synthetically filtered polarization results. Any wavelength dependent throughput filter curve may be synthesized when defined by the user, but a few pre-defined filter curves are available, namely: the SALTICAMs *U*, *B*, *V*, *R*, and *I* Johnson-Cousins filter curves.

### 3.1.8 POLSALT Limitations and the Need for Supplementary Tools

The creation of supplementary tools for POLSALT spectropolarimetric reductions stemmed from the limitations of the wavelength calibration process and a need to compare wavelength solutions across the perpendicular *O* and *E* polarization beams. The process of calibrating wavelength solutions using the POLSALT pipeline is time-consuming for the average user, and often results in unexpected program crashes when receiving erroneous inputs or key presses. Due to the time-consuming process of recalibrating the wavelength solutions it is not feasible to perform the wavelength calibrations time and time again for anything larger than a handful of observations. This is particularly true for observations performed with the SALT PG0300 grating as the sparse spectral features of the Ar arc lamp are not handled well by the POLSALT pipeline.

Since PG0300 provided the widest wavelength range and highest throughput, it was almost exclusively used for observations of flaring blazars, resulting in a large backlog of unanalyzed data. The only arc available for the PG0300 grating with a close enough articulation and grating angle ( $\sim 10.68^\circ$  and  $\sim 5.38^\circ$ , respectively), was the Ar arc lamp which displays sparse spectral features with large gaps over the wavelength range at these grating and articulation angles (Figure 3.5). This often led the POLSALT pipeline to create inconsistent wavelength solutions, or to fail to create a wavelength solution altogether,



**Figure 3.5:** One of many Ar arc lamp spectra as provided by SALT for line identification. Plot adapted from SALT’s published Longslit Line Atlases (as of 2024), resized to fit within the document margins but otherwise unchanged.<sup>4</sup>

since minor deviations of identified spectral features resulted in large deviations in regions with no spectral features. To only further compound the difficulty of the wavelength calibrations, the spectrum of the Ar arc lamp contains a partial overlap of a higher order at longer wavelengths (§ 2.1.7, Equation 2.5).

The chosen solution to overcome the limitations of the wavelength calibration process was to use a well established wavelength calibration software which allowed for rapid recalibrations and provided a familiar interface. IRAF provides this familiar environment and reliability, in part thanks to its continued community development.

Unfortunately, IRAF is unable to natively parse the data structure implemented by POLSALT ‘as is’ and so the files must be restructured. This restructuring works both ways as once the IRAF reductions are complete the data structure must be restructured to match that of the POLSALT `wavelength calibration` output such that the reduction process may be completed in POLSALT.

## 3.2 IRAF - *Image Reduction and Analysis Facility*

The IRAF (*Image Reduction and Analysis Facility*) software is a collection of software designed specifically for the reduction and analysis of astronomical images and spectra (Tody, 1986, 1993). The software consists of many tasks which perform specific operations and which are grouped into relevant packages. Only a brief overview of the tasks will be provided here. Help documentation for any of the IRAF tasks may be found online or through the IRAF Command Line Interface (CLI) through the `?` or `:.help` ‘cursor commands’ when running interactive tasks, with more specific help documentation provided in the relevant section.<sup>5</sup>

Useful IRAF tasks that deserve a brief mention are: the `mkscript` task in the `system` package which allows a user to create and save a task along with the defined parameters

<sup>4</sup>The ‘low resolution’ Ar plot sourced from <https://astronomers.salt.ac.za/data/salt-longslit-line-atlas/>

<sup>5</sup>Online help for IRAF is available at <https://iraf.net/irafdocs/>

as a file which can later be called as a script,<sup>6</sup> the `implot` task in the `plot` package which allows the rows or columns of an image to be interactively displayed,<sup>7</sup> and the `eparam` task in the `language` package which allows the parameters of a task to be edited within the IRAF CLI.<sup>8</sup>

For the wavelength calibration of SALT spectropolarimetric data, the relevant tasks are the `identify` and `reidentify` tasks located in the `noao.onedspec` package, and the `fitcoords` and the (optional) `transform` tasks located under the `noao.twodspec.longslit` package. These tasks produce a two-dimensional wavelength solution which must be obtained separately for the *O*- and *E*-beam.

### 3.2.1 Identify

The `identify` task is used to interactively determine a one-dimensional wavelength function across a chosen row of an arc exposure by identifying features in the spectrum with known wavelengths.<sup>9</sup> The task creates the first approximation of the wavelength solution (see Figure 3.6) as well as a local database in which the solution is saved (see Listing 3.1). The initial solution is built on in subsequent tasks, and it is, therefore, imperative that the initial solution is well-fit to minimize errors further along the calibration process.

The execution of `identify` consists of identifying known features spanning the entire wavelength range and then removing any features which negatively impact the wavelength solution. A balance must be found between the number of identified features, the parameters of the fit, and the deviation of the fit from the known features.

### 3.2.2 Reidentify

The `reidentify` task is used to run the `identify` task autonomously and repeatedly across the entirety of the arc frame at defined (row) intervals.<sup>11</sup> The task uses the one-dimensional wavelength solution stored in the database created by the initial `identify` call and refits the positions of the relevant spectral features. The task may fail based on a number of conditions, most common of which is the loss of features as the task moves further from the row at which the user manually ran `identify`.

---

<sup>6</sup>Help documentation for the `mkscript` task may be found at [https://astro.uni-bonn.de/~sysstw/lfa\\_html/iraf/system.mkscript.html](https://astro.uni-bonn.de/~sysstw/lfa_html/iraf/system.mkscript.html).

<sup>7</sup>Help documentation for the `implot` task may be found at [https://astro.uni-bonn.de/~sysstw/lfa\\_html/iraf/plot.implot.html](https://astro.uni-bonn.de/~sysstw/lfa_html/iraf/plot.implot.html).

<sup>8</sup>Help documentation for the `eparam` task may be found at [https://astro.uni-bonn.de/~sysstw/lfa\\_html/iraf/language.eparam.html](https://astro.uni-bonn.de/~sysstw/lfa_html/iraf/language.eparam.html).

<sup>9</sup>Help documentation for the `identify` task may be found at [https://astro.uni-bonn.de/~sysstw/lfa\\_html/iraf/noao.onedspec.identify.html](https://astro.uni-bonn.de/~sysstw/lfa_html/iraf/noao.onedspec.identify.html).

<sup>10</sup>See also <https://iraf.net/irafdocs/formats/identify.php> for an explanation of the database contents.

<sup>11</sup>Help documentation for the `reidentify` task may be found at [https://astro.uni-bonn.de/~sysstw/lfa\\_html/iraf/noao.onedspec.reidentify.html](https://astro.uni-bonn.de/~sysstw/lfa_html/iraf/noao.onedspec.reidentify.html).

Listing 3.1: An example of the identify database contents.<sup>10</sup>

```
# Thu 15:19:16 13-May-2021
begin    identify arc00057[*,237]
  id arc00057
  task      identify
  image     arc00057[*,237]
  units    Angstroms
  features   35
      53.61 5944.74989  5944.834 13.0 1 1 15257
      140.19 6029.9793  6029.997 13.0 1 1 4652
      185.30 6074.34644  6074.338 13.0 1 1 13396
      207.49 6096.15873  6096.161 13.0 1 1 21700
      255.23 6143.0493  6143.063 13.0 1 1 33330
      276.13 6163.56995  6163.594 13.0 1 1 11344
      330.89 6217.29293  6217.281 13.0 1 1 13705
      381.10 6266.51524  6266.495 13.0 1 1 21747
      420.21 6304.8113  6304.789 13.0 1 1 10226
      450.49 6334.45415  6334.428 13.0 1 1 36235
      500.18 6383.04826  6382.991 13.0 1 1 35824
      519.85 6402.26802  6402.248 13.0 1 1 70163
      626.70 6506.56147  6506.528 13.0 1 1 46165
      653.73 6532.91083  6532.882 13.0 1 1 21413
      721.60 6598.98642  6598.953 13.0 1 1 26396
      803.21 6678.31069  6678.277 13.0 1 1 51338
      843.15 6717.0732  6717.043 13.0 1 1 36780
      1099.95 6965.36335  6965.431 13.0 1 1 5618.4 ar
      1169.57 7032.38598  7032.413 13.0 1 1 100000
      1317.05 7173.89814  7173.938 13.0 1 1 5000 decrease
      1391.52 7245.11148  7245.167 13.0 1 1 73545
      1537.20 7383.93022  7383.981 13.0 1 1 5557.5 ar
      1595.02 7438.83545  7438.898 13.0 1 1 15000 decrease
      1663.64 7503.86263  7503.869 13.0 1 1 30000 ar; increase
      1697.46 7535.84584  7535.774 13.0 1 1 8000 increase
      1802.64 7635.07335  7635.106 13.0 1 1 20000 ar; decrease
      2209.19 8014.79559  8014.786 13.0 1 1 3000 ar; decrease
      2604.58 8377.66137  8377.607 13.0 1 1 14543
      2734.54 8495.41423  8495.359 13.0 1 1 8765
      2763.48 8521.52355  8521.442 13.0 1 1 4537.5 ar
      2840.92 8591.20799  8591.258 13.0 1 1 2000 decrease
      2889.39 8634.67334  8634.647 13.0 1 1 3059
      2911.42 8654.39264  8654.383 13.0 1 1 3000 decrease
      2926.56 8667.93501  8667.944 13.0 1 1 702.5 ar
      3135.72 8853.77575  8853.867 13.0 1 1 1820

  function legendre
  order 4
  sample *
  naverage 1
  niterate 0
  low_reject 3.
  high_reject 3.
  grow 0.
  coefficients   8
      2.
      4.
      53.60757446289061
      3135.715576171875
      7425.420339270724
      1457.513831286474
      -26.15751926622308
      -3.000903509842187
```

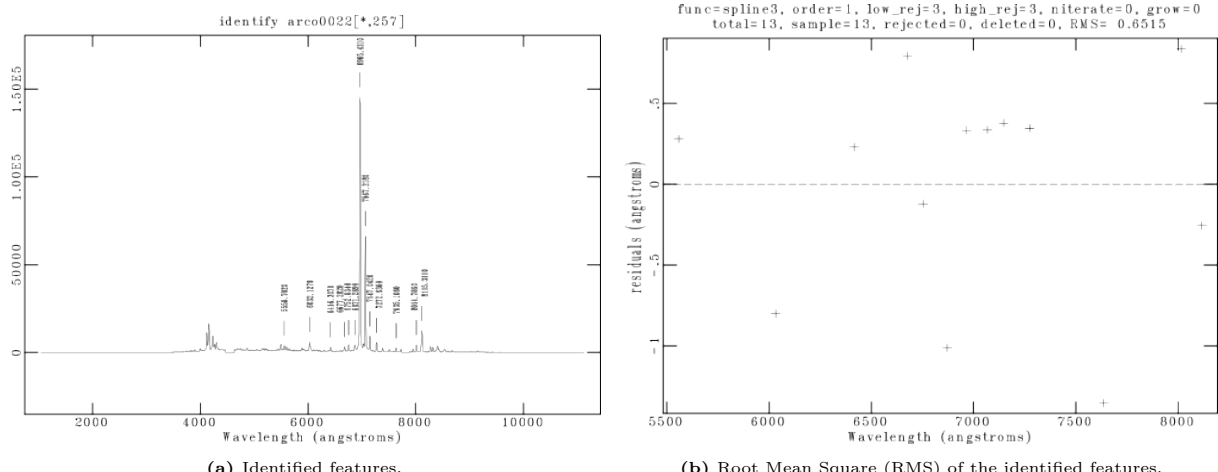


Figure 3.6: A plot and the RMS of the identified features found using the IRAF identify task. Figures created using the IRAF identify task.

**Listing 3.2:** An example of the `fitcoords` database contents.<sup>13</sup>

```
# Thu 15:26:55 13-May-2021
begin    arc00057
task      fitcoords
axis      1
units     angstroms
surface   33
      1.
      5.
      5.
      1.
      1.
      3199.
      1.
      474.
      7419.096745914063
      1510.03933621895
      -21.10886852752348
      -2.079553916887794
      0.06772631420528228
      0.7720164913117386
      -1.506773900054024
      0.1341878190232142
      -0.01659697703758917
      0.0251087019569153
      -3.318493303995171
      -0.3612632489821799
      0.003270665801371641
      -0.0157962041414068
      -0.003073690871589242
      0.007533453962924031
      0.02839687304474069
      -0.003233465769521899
      0.00174111456659807
      0.00645177595090841
      0.0105080093855621
      -0.01157827440314294
      -0.007789479002470706
      -0.006562085282926231
      -0.002321476801926803
```

When running `reidentify` non-interactively, it is recommended to set the `verbose` parameter to ‘yes’ as this will provide immediate confirmation if the task quit early. Regardless of whether the task quit successfully, the newly defined wavelength solutions are appended to the local database following the `identify` task database format, an example of which is given in Listing 3.1.

### 3.2.3 Fitcoords

The `fitcoords` task is used to find a two-dimensional surface function from the one-dimensional wavelength solutions found for specific rows in the previous steps.<sup>12</sup> The usage of `fitcoords` is similar to that of `identify` and consists of examining the distribution of identified points and eliminating any points that `reidentify` may have misidentified (see Figure 3.7).

By eliminating outliers with bad residuals and modifying the two-dimensional surface function’s type and degree, the overall error of the fit is decreased, aligning more closely to what the ‘true’ wavelength solution is. This surface function is the final two-dimensional wavelength solution for each two-dimensional spectrum. It is saved using the `fitcoords` database format, an example of which is given in Listing 3.2, as the list of parameters and function coefficients required to recreate the closest two-dimensional model. The IRAF wavelength solution is used by the `STOPS join` method to create the ‘WAV’ extension required by POLSALT, further described in § 3.3.2.

<sup>12</sup>Help documentation for the `fitcoords` task may be found at [https://astro.uni-bonn.de/~sysstw/lfa\\_html/iraf/noao.twodspec.longslit.fitcoords.html](https://astro.uni-bonn.de/~sysstw/lfa_html/iraf/noao.twodspec.longslit.fitcoords.html).

<sup>13</sup>See also <https://iraf.net/irafdocs/formats/fitcoords.php> for an explanation of the database contents.



**Figure 3.7:** A plot and the RMS of the features identified across the exposure using the IRAF `fitcoords` task. Figures created using the IRAF `fitcoords` task.

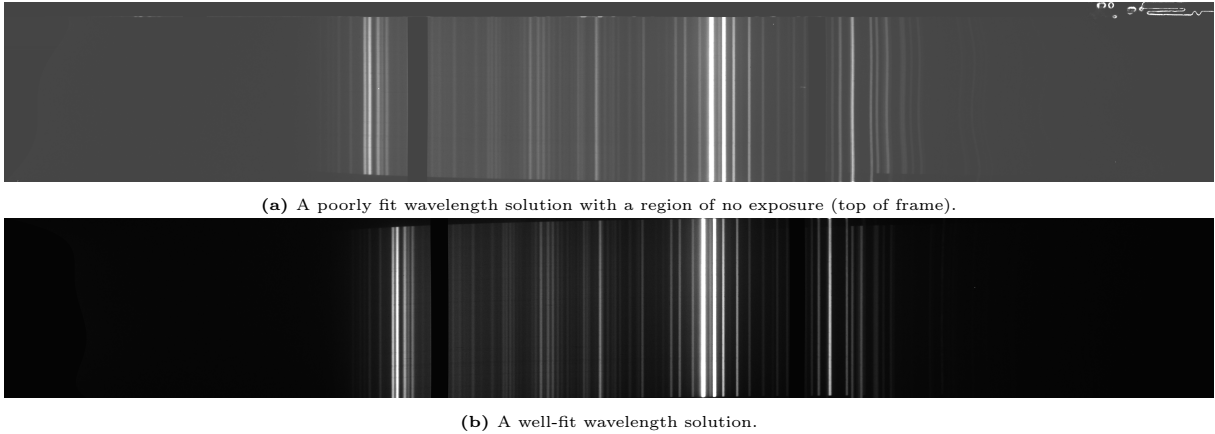


**Figure 3.8:** Examples of a poor fit (a) and well-fit (b) wavelength solution applied to the *O*- and *E*-beams of an arc image. The contrast of the figures were scaled to best capture any deviation of the arc lines. Figures created by the IRAF `transform` task.

### 3.2.4 Transform

The `transform` task is the optional final step in the IRAF wavelength calibration process.<sup>14</sup> Simply put, `transform` converts the  $(x_p, y_p)$  pixel units of an exposure to  $(\lambda, y_p)$  wavelength units which allows for an immediate check of whether the wavelength solution is consistent across the frame. Any general error in the wavelength solution may be spotted in the transformed images; ranging from minor errors, such as the arc lines or sky lines not being purely vertical across the frame, to more major errors, such as an incorrect wavelength solution skewing the exposure beyond recognition.

For example, Figure 3.8a shows a good fit to the wavelength solution, as after transformation all the sky lines run exactly vertical. Figure 3.8b, on the other hand, shows a seemingly good fit, but closer inspection reveals that the sky lines (especially towards the right of the frame) deviate from the vertical, indicating a poor fit to the wavelength solution.

<sup>14</sup>Help documentation for the `transform` task may be found at [https://astro.uni-bonn.de/~sysstw/lfa\\_html/iraf/noao.twodspec.longsit.transform.html](https://astro.uni-bonn.de/~sysstw/lfa_html/iraf/noao.twodspec.longsit.transform.html).

### 3.3 STOPS - *Supplementary Tools for POLSALT Spectropolarimetry*

*Supplementary Tools for POLSALT Spectropolarimetry* (STOPS) provides supplementary tools which convert the POLSALT and IRAF formats back and forth, allowing IRAF to be used for wavelength calibrations of SALT spectropolarimetric data. It also provides additional tools to check the accuracy of the wavelength calibration. STOPS is written in, and requires, Python 3 (3.11+) to run, as well as **Astropy** (6.0.0+) (Astropy Collaboration et al., 2013, 2018, 2022), **ccdproc** (2.4.1+) (Craig et al., 2017), **Matplotlib** (3.5.2+) (Hunter, 2007), **NumPy** (1.26.4+) (Harris et al., 2020), and **SciPy** (1.13.0+) (Virtanen et al., 2020).

The parsing of POLSALT data into an IRAF usable format and the reformatting of the IRAF wavelength calibrated data back into a POLSALT usable format, referred to as *splitting* and *joining*, is performed by the STOPS **split** and **join** methods, respectively.

Methods to verify the validity of the wavelength calibrations were also added to STOPS. The **skyline** method checks the sky line wavelength (*x*) positions across the frame as well as the variation of the sky lines across the positional (*y*) axis of the frame. The **correlate** method checks the correlation of the *O*- and *E*-beams either within a given Flexible Image Transport System (FITS) file or across multiple files (comparing only the *O*- and *E*-beams for each). With these two additional methods, a user is able to verify that the wavelength solutions do not conflict across the *O*- and *E*-beams and that no unexpected deviations are included in the wavelength solutions.

Help on the usage of STOPS in a CLI can be viewed by running:

---

```
$ python ~/STOPS --help
# OR
$ python ~/STOPS [split|join|correlate|skylines] --help
```

---

which retrieves and prints the help documentation to the CLI from Listing B.1 (in Appendix B), such as how to enable logging or increase the verbosity, or change default parameters of the various methods. Finally, help documentation for the specific STOPS methods may be found within this section (Listing 3.3 to 3.6) or in Appendix B.

#### 3.3.1 Splitting

As mentioned previously, the format of the FITS file created by POLSALT after basic CCD reductions and the format expected by IRAF to be used for the wavelength calibrations are incompatible. Basic POLSALT CCD reductions return FITS files which contain a primary header along with extensions for the science, variance, and ‘BPM’ images. These extensions carry the image of the trace (see Figure 3.9), the variance of the image, and a map of the pixels to be masked out, split into sub-extensions for both polarimetry beams, respectively.

While IRAF is capable of dealing with multiple traces in an extension or lists of input files, it is not as capable when dealing with multiple wavelength solutions contained in a single extension (as expected by the POLSALT **wavelength calibration**) or extensions containing sub-extensions (as expected by the POLSALT **spectral extraction**).

**Listing 3.3:** The ‘docstring’ for `split.py`


---

```

24 """
25 The `Split` class allows for the splitting of `polsalt` FITS files
26 based on the polarization beam. The FITS files must have basic
27 `polsalt` pre-reductions already applied (`mzgbp...` FITS files).
28
29 Parameters
30 -----
31 data_dir : str / Path
32     The path to the data to be split
33 fits_list : list[str], optional
34     A list of pre-reduced `polsalt` FITS files to be split within `data_dir`.
35     (The default is None, `Split` will search for `mzgbp*.fits` files)
36 split_row : int, optional
37     The row along which to split the data of each extension in the FITS file.
38     (The default is SPLIT_ROW (See Notes), the SALT RSS CCD's middle row)
39 no_arc : bool, optional
40     Decides whether the arc frames should be recombined.
41     (The default is False, `polsalt` has no use for the arc after wavelength calibrations)
42 save_prefix : dict[str, list[str]], optional
43     The prefix with which to save the O & E beams.
44     Setting `save_prefix` = ``None`` does not save the split O & E beams.
45     (The default is SAVE_PREFIX (See Notes))
46
47 Attributes
48 -----
49 arc : str
50     Name of arc FITS file within `data_dir`.
51     `arc` = `""` if `no_arc` or not detected in `data_dir`.
52 o_files, e_files : list[str]
53     A list of the `O`- and `E`-beam FITS file names.
54     The first entry is the arc file if `arc` defined.
55 data_dir
56 fits_list
57 split_row
58 save_prefix
59
60 Methods
61 -----
62 split_file(file: os.PathLike)
63     -> tuple[astropy.io.fits.HDUList]
64     Handles creation and saving the separated FITS files
65 split_ext(hdulist: astropy.io.fits.HDUList, ext: str = 'SCI')
66     -> astropy.io.fits.HDUList
67     Splits the data in the `ext` extension along the `split_row`
68 crop_file(hdulist: astropy.io.fits.HDUList, crop: int = CROP_DEFAULT (See Notes))
69     -> tuple[numpy.ndarray]
70     Crops the data along the edge of the frame, that is,
71     `O`-beam cropped as [crop:], and
72     `E`-beam cropped as [:crop].
73 update_beam_lists(o_name: str, e_name: str)
74     -> None
75     Updates `o_files` and `e_files`.
76 save_beam_lists(file_suffix: str = 'frames')
77     -> None
78     Creates (Overwrites if exists) and writes the `o_files` and `e_files` to files named
79     `o_{file_suffix}` and `e_{file_suffix}`, respectively.
80 process()
81     -> None
82     Calls `split_file` and `save_beam_lists` on each file in `fits_list` for automation.
83
84 Other Parameters
85 -----
86 **kwargs : dict
87     keyword arguments. Allows for passing unpacked dictionary to the class constructor.
88
89 Notes
90 -----
91 Constants Imported (See utils.Constants):
92     SAVE_PREFIX
93     CROP_DEFAULT
94     SPLIT_ROW
95
96
97 """

```

---

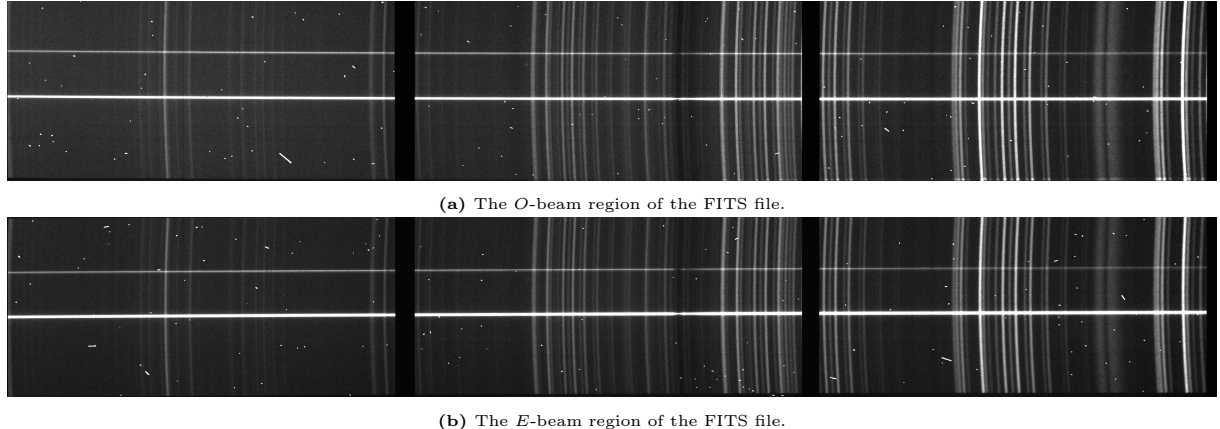


**Figure 3.9:** The split *O*- (a) and *E*-beams (b) as handed to **IRAF**. Figure created from the **STOPS** **split** method output.

To simplify the **IRAF** reduction procedure it was decided to separate the perpendicular polarization beams into their own files.

The files with POLSALT pre-reductions applied, namely FITS files with an ‘mxgbp’ prefix (§ 3.1), are used as the starting point for the supplementary tool’s **split** method. Running **split** finds all the FITS files for wavelength calibration within the working directory, creates two empty Header and Data Unit (HDU) structures for each FITS file (i.e. for both the *O*- and *E*-beam), and appends all header and science data necessary for wavelength calibration to the relevant HDU structure. Otherwise, defaults, such as which row to split the image along to separate the beams, were kept as close to the POLSALT pipeline as possible.

As the intent was always to parse the wavelength function back into POLSALT it was decided to keep these temporary FITS files as small as possible by only including the header and ‘SCI’ science extension. To aid the scripting of the **IRAF** wavelength calibration process, the **split** method also performs row cropping to exclude CCD regions which are not exposed to light, and creates files listing the split *O*- and *E*-beam FITS files which may be passed to the **IRAF** task inputs. Row cropping was decided on as **IRAF** does not handle rows with no exposure well, specifically when it comes to the autonomous **reidentify** task. The full **STOPS** **split** class docstring is given in Listing 3.3.

### 3.3.2 Joining

After the **IRAF** **fitcoords** task has been successfully run for both the *O*- and *E*-beams, the **STOPS** **join** method is used to extract and parse the wavelength solution from the **IRAF** database, and to create the wavelength calibrated FITS files required by the POLSALT pipeline. More specifically, the **join** method performs the following steps:

First, **join** parses the wavelength database file, described in § 3.2.3, for either a ‘Chebyshev’ or ‘Legendre’ solution, and calculates the wavelength at each  $(x_p, y_p)$  pixel position. This new image containing the corresponding wavelength values, seen in Figure 3.10, is appended to the wavelength calibrated FITS file as the ‘WAV’ extension.

Listing 3.4: The ‘docstring’ for join.py

```

32 """
33
34 The `Join` class allows for the joining of previously split files and the
35 appending of an external wavelength solution in the `polsalt` FITS file format.
36
37 Parameters
38 -----
39 data_dir : str / Path
40     The path to the data to be joined
41 database : str, optional
42     The name of the `IRAF` database folder.
43     (The default is "database")
44 fits_list : list[str], optional
45     A list of pre-reduced `polsalt` FITS files to be joined within `data_dir`.
46     (The default is ``None``, `Join` will search for `mxbgp*.fits` files)
47 solutions_list: list[str], optional
48     A list of solution filenames from which the wavelength solution is created.
49     (The default is ``None``, `Join` will search for `fc*` files within the `database` directory)
50 split_row : int, optional
51     The row along which the data of each extension in the FITS file was split.
52     Necessary when Joining cropped files.
53     (The default is 517, the SALT RSS CCD's middle row)
54 save_prefix : dict[str, list[str]], optional
55     The prefix with which the previously split `O`- & `E`-beams were saved.
56     Used for detecting if cropping was applied during the splitting procedure.
57     (The default is SAVE_PREFIX (See Notes))
58 verbose : int, optional
59     The level of verbosity to use for the Cosmic ray rejection
60     (The default is 30, I.E. logging.INFO)
61
62 Attributes
63 -----
64 fc_files : list[str]
65     Valid solutions found from `solutions_list`.
66 custom : bool
67     Internal flag for whether `solutions_list` uses the `IRAF` or a custom format.
68     See Notes for custom solution formatting.
69     (Default (inherited from `solutions_list`) is False)
70 arc : str
71     Deprecated. Name of arc FITS file within `data_dir`.
72 data_dir
73 database
74 fits_list
75 split_row
76 save_prefix
77
78 Methods
79 -----
80 get_solutions(wavlist: list / None, prefix: str = "fc") -> (fc_files, custom): tuple[list[str], bool]
81     Parse `solutions_list` and return valid solution files and if they are non-`IRAF` solutions.
82 parse_solution(fc_file: str, x_shape: int, y_shape: int) -> tuple[dict[str, int], np.ndarray]
83     Loads the wavelength solution file and parses keywords necessary for creating the wavelength extension.
84 join_file(file: os.PathLike) -> None
85     Joins the files,
86     attaches the wavelength solutions,
87     performs cosmic ray cleaning,
88     masks the extension,
89     and checks cropping performed in `Split`.
90     Writes the FITS file in a `polsalt` valid format.
91 check_crop(hdu: pyfits.HDUList, o_file: str, e_file: str) -> int
92     Opens the split `O`- and `E`-beam FITS files and returns the amount of cropping that was performed.
93 process() -> None
94     Calls `join_file` on each file in `fits_list` for automation.
95
96
97 Other Parameters
98 -----
99 no_arc : bool, optional
100     Deprecated. Decides whether the arc frames should be processed.
101     (The default is False, `polsalt` has no use for the arc after wavelength calibrations)
102 **kwargs : dict
103     keyword arguments. Allows for passing unpacked dictionary to the class constructor.
104
105 Notes
106 -----
107 Constants Imported (See utils.Constants):
108     DATADIR, SAVE_PREFIX, SPLIT_ROW, CR_PARAMS
109
110 Custom wavelength solutions must be formatted containing:
111     `x`, `y`, *coefficients...
112 where a solution are of order (x by y) and must contain x*y coefficients,
113 all separated by newlines. The name of the custom wavelength solution file
114 must contain either "cheb" or "leg" for Chebyshev or Legendre
115 wavelength solutions, respectively.
116
117 Cosmic ray rejection is performed using lacosmic [1]_ implemented in ccdproc via astroscreappy [2]_.
118
119 References
120 -----
121 .. [1] van Dokkum 2001, PASP, 113, 789, 1420 (article : https://adsabs.harvard.edu/abs/2001PASP..113.1420V)
122 .. [2] https://zenodo.org/records/1482019
123
124 """

```

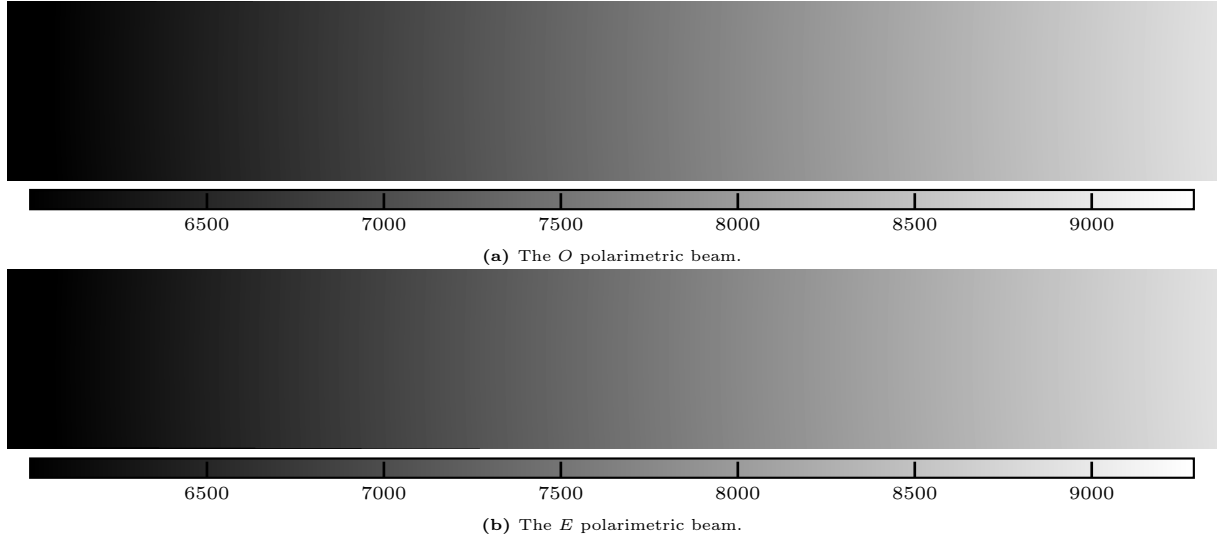


**Figure 3.10:** A representative ‘WAV’ extension of a FITS file, for the *O*- (a) and *E*-beam (b), ready to be processed by the POLSALT pipeline. The color bars show the wavelength in Å. Note that regions which fall outside the exposed region are masked by setting the corresponding pixel values of the wavelength and ‘BPM’ extensions to 0. Figure created from the `STOPS join` method output.

Second, cosmic-ray cleaning is performed on the ‘SCI’ extension using the `ccdproc` implementation of the `lacosmic` Python package which implements the L.A. Cosmic algorithm, based on Laplacian edge detection. The read noise and gain parameters used for cosmic ray cleaning were chosen based on the properties of the RSS, while the rest of the parameters were left as the default, following the publication and suggestions<sup>15</sup> by the algorithm’s creator, as well as the implementation of the algorithm in the python `ccdproc` package (McCully et al., 2018; van Dokkum, 2001). The chosen parameters work well for most cosmic rays, as can be seen when comparing Figure 3.9 to Figure 3.11, but may be modified as needed.

Next, `join` updates the headers to be near-identical to those created by the POLSALT `wavelength calibration`, most notably updating the data shape, ‘CTYPE3’, and data type, ‘BITPIX’, keywords. The only difference in the header is the ‘NAXIS2’ keyword, due to the cropping performed by `split`. The cropped region could be reintroduced but would be masked out and further discarded in the following POLSALT `spectra extraction` process, making it redundant.

Finally, the ‘WAV’ extension is masked to remove any uncalibrated wavelength regions as well as masked for the skewing of the trace introduced by the wollaston element. The masking of the wollaston skewing is necessary since POLSALT introduces a wollaston correction in the `spectra extraction` process. The ‘BPM’ extension is masked to reflect the valid wavelength calibrated region, and the files are saved with the POLSALT wavelength calibrated ‘wmxgbp’ prefix. The full STOPS `join` class docstring is given in Listing 3.4.

**Listing 3.5:** The ‘docstring’ for `skylines.py`


---

```

39
40 """
41 Class representing the Skylines object.
42
43 Parameters
44 -----
45 data_dir : Path
46     The directory containing the data files.
47 filenames : list[str]
48     The list of filenames to be processed.
49 beam : str, optional
50     The beam mode, by default "OE".
51 plot : bool, optional
52     Flag indicating whether to plot the continuum, by default False.
53 save_prefix : Path / None, optional
54     The prefix for saving the data, by default None.
55 **kwargs
56     Additional keyword arguments.
57
58 Attributes
59 -----
60 data_dir : Path
61     The directory containing the data files.
62 fits_list : list[str]
63     The list of fits file paths.
64 beams : str
65     The beam mode.
66 can_plot : bool
67     Flag indicating whether to plot the continuum.
68 save_prefix : Path / None
69     The prefix for saving the data.
70 wav_unit : str
71     The unit of wavelength.
72
73 Methods
74 -----
75 checkLoad(self, path1: str) -> np.ndarray:
76     Checks and loads the data from the given path.
77 transform(self, wav_sol: np.ndarray, spec: np.ndarray) -> np.ndarray:
78     Transforms the input wavelength and spectral data based on
79     the given wavelength solution.
80 rmvCont(self) -> np.ndarray:
81     Removes the continuum from the spectrum.
82 process(self) -> None:
83     Placeholder method for processing the data.
84 """

```

---



**Figure 3.11:** A representative ‘SCI’ extension of a FITS file, for the *O*- (a) and *E*-beam (b), ready to be processed by the POLSALT pipeline. The observed intensity is displayed via the grayscale value at each pixel. Figure created from the `STOPSjoin` method output.

### 3.3.3 Sky Line Checks

The `skyline` method has been implemented to compare the position of the sky lines on the ‘SCI’ extension, or arc lines in the arc exposure, to the known positions of the sky lines, or arc lines, as measured by SALT, respectively.<sup>16</sup> This provides an additional check of the accuracy of the wavelength solution across the frame. This method accepts both the IRAF `transform` FITS file or the ‘wmxgbp’ FITS files created by the `join` method as the input.

The `skyline` method loads the wavelength calibrated files, masks the traces present in the frames, transforms the frames from  $(x_p, y_p)$  pixel to  $(\text{\AA}, y_p)$  wavelength units if the frame was not transformed by `transform`,<sup>17</sup> and compares the peak wavelength position of the sky lines to the reference sky lines as measured by SALT. Finally, a figure is created containing a plot of the background spectra (offset by the respective legend entries superscript) with the known sky lines marked with a vertical line, and a plot of the closest identified peaks of said spectra.

Minor variations in the comparison of the sky lines are expected, such as those seen in Figure 3.12, but any uniform trends, such as those in Figure 3.13 (bottom left), indicate an underlying poor fit across the horizontal axis of the wavelength solution. The full STOPS `skyline` class docstring is given in Listing 3.5.

### 3.3.4 Cross Correlation

The `skyline` method allows for confirmation of a single wavelength solution, but has no means for comparing how the wavelength solutions of two polarization beams differ from each other. As the Stokes results, and thus final polarization results, are determined by the difference between the *O*- and *E*-beams, a direct comparison is not appropriate.

<sup>15</sup>Suggested parameters for the `lacosmic` algorithm may be found at <http://www.astro.yale.edu/dokkum/lacosmic/pars.html>.

<sup>16</sup>Both sky and arc lines are available at <https://astronomers.salt.ac.za/data/salt-longslit-line-atlas/>.

<sup>17</sup>The transformation applied by the `skyline` method uses linear interpolation and is thus less accurate at flux conservation than the transformation applied by the `transform` method.

**Listing 3.6:** The ‘docstring’ for `cross_correlate.py`


---

```

33 """
34 Cross correlate allows for comparing the extensions of multiple
35 FITS files, or comparing the O and E beams of a single FITS file.
36
37 Parameters
38 -----
39 data_dir : str / Path
40     The path to the data to be cross correlated
41 filenames : list[str]
42     The ecwmazbp*.fits files to be cross correlated.
43     If only one filename is defined, correlation is done against the two polarization beams.
44 split_ccd : bool, optional
45     Decides whether the CCD regions should each be individually cross correlated.
46     (The default is True, which splits the spectrum up into its separate CCD regions)
47 cont_ord : int, optional
48     The degree of a chebyshev to fit to the continuum.
49     (The default is 11)
50 plot : bool, optional
51     Decides whether the continuum fitting should be plotted
52     (The default is False, so no continua plots are displayed)
53 save_prefix : str, optional
54     The name or directory to save the figure produced to.
55     "" saves a default name to the current working. A default name is also used when save_prefix is a directory.
56     (The default is None, I.E. The figure is not saved, only displayed)
57
58 Attributes
59 -----
60 data_dir
61 fits_list
62 beams : str
63     The mode of correlation.
64     'OE' for same file, and 'O' or 'E' for different files but same extension.
65 ccds : int
66     The number of CCD's in the data. Used to split the CCD's if split_ccd is True.
67 cont_ord : int
68     The degree of the chebyshev to fit to the continuum.
69 can_plot : bool
70     Decides whether the continuum fitting should be plotted
71 offset : int
72     The amount the spectrum is shifted, mainly to test the effect of the cross correlation
73     (The default is 0, I.E. no offset introduced)
74 save_prefix
75 wav_unit : str
76     The units of the wavelength axis.
77     (The default is Angstroms)
78 wav_cdel : int
79     The wavelength increment.
80     (The default is 1)
81 alt : Callable
82     An alternate method of cross correlating the data.
83     (The default is None)
84
85 Methods
86 -----
87 load_file(filename: Path) -> tuple[np.ndarray, np.ndarray, np.ndarray]
88     Loads the data from a FITS file.
89 get_bounds(bpm: np.ndarray) -> np.ndarray
90     Finds the bounds for the CCD regions.
91 remove_cont(spec: list, wav: list, bpm: list, plot_cont: bool) -> None
92     Removes the continuum from the data.
93 correlate(filename1: Path, filename2: Path / None = None) -> None
94     Cross correlates the data.
95 ftcs(filename1: Path, filename2: Path / None = None) -> None
96     Cross correlates the data using the Fourier Transform.
97 plot(spec, wav, bpm, corrdb, lagsdb) -> None
98     Plots the data.
99 process() -> None
100    Processes the data.
101
102 Other Parameters
103 -----
104 offset : int, optional
105     The amount the spectrum is shifted, mainly to test the effect of the cross correlation
106     (The default is 0, I.E. no offset introduced)
107 **kwargs : dict
108     keyword arguments. Allows for passing unpacked dictionary to the class constructor.
109     ftcs : bool, optional
110         Decides whether the Fourier Transform should be used for cross correlation.
111
112 See Also
113 -----
114 scipy
115     https://docs.scipy.org/doc/scipy/reference/generated/scipy.signal.correlate.html
116
117 Notes
118 -----
119 Constants Imported (See utils.Constants):
120     SAVE_CORR
121
122 """

```

---



**Figure 3.12:** An example of a well calibrated wavelength solution, specifically shown for science images. Figure created via the `STOPS skyline` method.

Any observed unpolarized light, however, will reflect equally in both polarization beams and so the general trend of the two spectra may reasonably be expected to follow one another. The `correlate` method was created to allow for comparisons between the wavelength solutions of the *O*- and *E*-beams of a single exposure or the *O*- or *E*-beams of differing exposures by cross correlating the spectra.

The `correlate` method loads the `POLSALT spectra extraction` FITS files, removes the continuum and separates the CCD regions. The relevant CCD regions are cross correlated and the correlation peak is plotted and specified in the plot legend, as seen in Figure 3.14.

Sources under spectropolarimetric observation are generally expected to vary over time and, as such, the ratio of polarized to unpolarized light is also expected to vary. The accuracy of correlation may decrease as features with differences in the polarized component of the polarization beams change, and it is up to the user to determine the validity of the correlation result taking into consideration the two spectra being correlated. The differences in the features of the different spectra are often negligible when compared to the overall continuum of the spectra and are generally only reflected in a change in the intensity of said features when the continuum is removed. The full `STOPS split` class docstring is given in Listing 3.6.

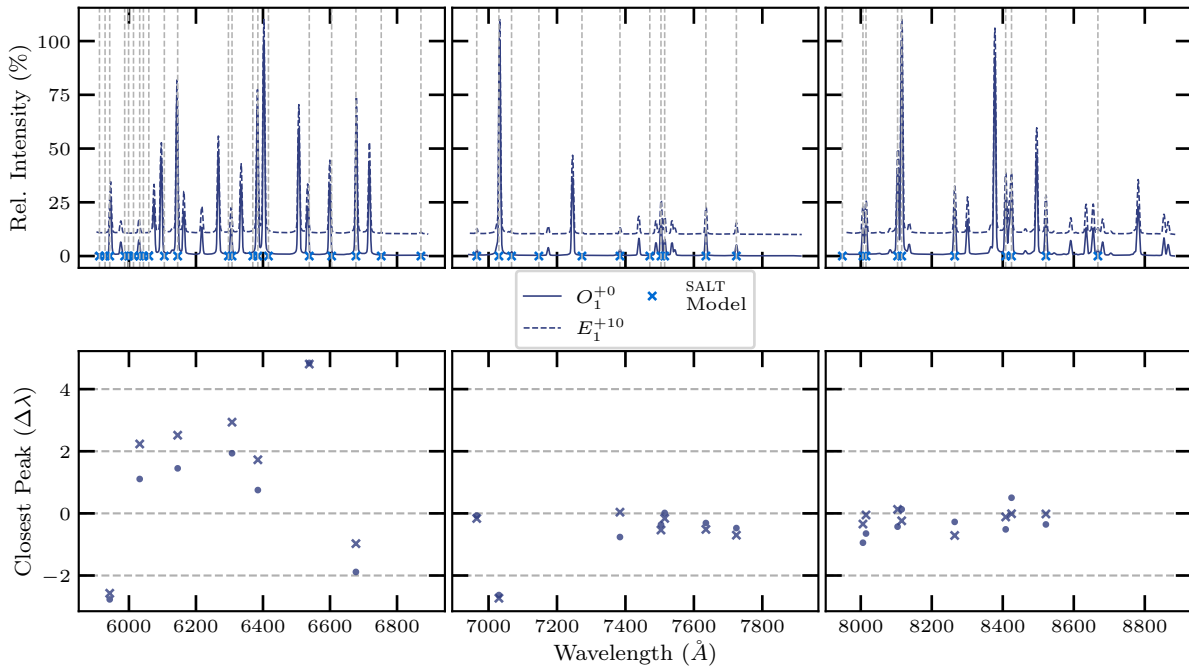


**Figure 3.13:** An example of a wavelength solution with a poor fit at shorter wavelengths (bottom left), specifically shown for an arc image. Arc lines are Figure created via the STOPS skyline method.

## 3.4 General Reduction Procedure

This section aims to provide a comprehensive discussion of the modified reduction procedure, an example of which is provided in Appendix A. As users all employ a variety of operating systems, language environments, and software setups, not much emphasis will be placed on how to get the software running or the managing of files; instead, the general order, seen in Figure 3.15, and commands necessary to complete each step of the reduction process are discussed, assuming that the software is running as intended.

### 3.4.1 Initial Setup

It is important to note that while POLSALT was developed in Python 2 (2.7), the STOPS supplementary tools were developed in, and require, Python 3 (3.11+), as well as the other requirements mentioned in § 3.3. While managing multiple versions of Python introduces some extra complication, it would not have been reasonable to develop STOPS in Python 2, as it has been deprecated, nor would it have been reasonable to update POLSALT to Python 3.

It is therefore recommended that the different versions of Python are managed using separate virtual environments. While the `anaconda` package manager was used in this study and is recommended, any package manager may be used. The `anaconda` environments are aliased ‘`salt`’ for Python 2.7 and ‘`stops`’ for Python 3.11. When Listings are provided (see for example Listing A.1 or the Listings in § 3.4.2 below), the `anaconda` environment is activated at the start of the Listing, otherwise it is assumed the previously specified environment is still active.



**Figure 3.14:** The resultant output plot of the STOPS `correlate` method. Figure created via the STOPS `correlate` method.

It is recommended to use POLSALT through the GUI as it provides a user-friendly environment while also sequentially listing each step of the reduction process in a dropdown menu, as seen in Figure 3.1. Reductions are possible, however, purely through the CLI using the POLSALT ‘beta’ scripts.

### 3.4.2 POLSALT Pre-Reductions

The POLSALT reduction process requires a file structure such that the raw data received from SALT is located in a folder named using the observing date with a sub-folder named `raw`, following the format `YYYYMMDD/raw/`. This directory structure allows POLSALT to create a ‘working’ directory following the format `YYYYMMDD/sci/` which contains all the files modified during the reduction process. Multiple reduction procedures using the same data may therefore be separated by simply renaming the `sci/` sub-folder.

The POLSALT GUI may be launched by opening a CLI and running the commands given in Listing A.1. Once the window, depicted in Figure 3.1, has launched, ensure that the first two paths at the top of the window point to the POLSALT and working directories, as seen in Figure 3.1. The ‘raw image reduction’ entry may then be selected from the dropdown menu and the pre-reductions run.

Alternatively, if the data already includes ‘mxgbp’ FITS files in the `YYYYMMDD/sci/` working directory, a CLI may be used to complete the initial pre-reductions using

---

```
$ cd <OBSDATE>/sci
$ conda activate salt
$ python ~/polsalt/scripts/reducepoldata_sc.py <OBSDATE>
```

---

which will start the full POLSALT reduction process. This process is quit once the POLSALT `wavelength calibration` GUI opens, and the alternate wavelength calibration procedure is followed.



**Figure 3.15:** A general workflow for data reductions using a combination of POLSALT, IRAF, and STOPS. Diagram adapted from Cooper et al. (2022).

### 3.4.3 Wavelength Calibration

The wavelength calibrations may now be completed in IRAF. This section concerns the procedure for parsing the FITS files to and from both IRAF and POLSALT, as well as the relevant task names and methods to be run to complete the calibrations. A base working case of each of the tasks and methods are presented in Listing A.2 to A.8, but it should be noted that the art of wavelength calibration consists of modifying the parameters to achieve a well-fit calibration function.

#### Preparing the Data for IRAF

Splitting the data is presented in Listing A.2. The STOPS `split` method may take multiple parameters, as seen in § 3.3, but default parameters should be used wherever possible. The most notable parameters are the directory, which defaults to the current working directory of the CLI, the split row, which defaults to POLSALT’s default center row, and the save prefix, which defaults to ‘`obeam`’ and ‘`ebeam`’.

#### IRAF Wavelength Calibrations

The IRAF wavelength calibrations are performed using the tasks described in § 3.2, namely the `identify`, `reidentify`, `fitcoords`, and optionally `transform` tasks.

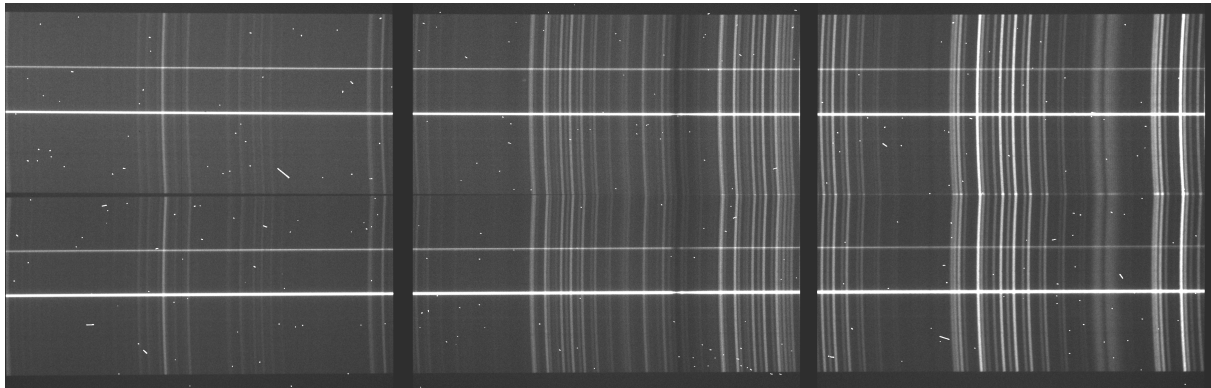


**Figure 3.16:** The ‘SCI’ extension of a typical spectropolarimetric FITS file taken with the SALT RSS, after basic POLSALT CCD reductions have been completed. Figure created from the `STOPS split` output.

In general, these tasks are run directly in the IRAF terminal using:<sup>18</sup>

---

```
cl> identify arc_files
cl> reidentify arc_ref arc_files
cl> fitcoords arc_files fit_2d
cl> transform files tr_file fit_2d
```

---

where ‘arc\_files’ refers to a list or file containing the FITS files relevant to the task, ‘arc\_ref’ refers to the FITS file previously identified, ‘fit\_2d’ refers to the name to be used for the final two-dimensional wavelength solution, and ‘tr\_file’ refers to the new name for the transformed input ‘files’.

The interactive tasks take up the bulk of the reduction time as this is where the fine-tuning of the reduction is done, through the use of cursor (or colon) commands, which allow modification of the parameters mid-reduction. Task parameters may, however, be edited beforehand within the IRAF terminal using the `eparam` task, and optionally saved, and quit or run using a combination of `:w`, and `:q` or `:go` cursor commands, respectively.

The reduction process in Appendix A, namely Listing A.4 to A.7, describes how the tasks may be scripted and saved for posterity. It is recommended to create an IRAF Command Language (cl) script for each task to keep track of which parameters were used and for simple recalibrations. The scripts are created using the `mkscript` task which interactively asks for a task to script and parameters to use. Multiple tasks may be appended to an IRAF script, allowing for the parameters of both beams to be tracked.

Running an IRAF script may be done by running:

---

```
cl> cl < script_name.cl
```

---

but is not suggested for interactive scripts, which run best when simply copied from the `<...>/sci/script_name.cl` file to the IRAF terminal.

<sup>18</sup>Please see the IRAF help docs, available at [https://astro.uni-bonn.de/~sysstw/lfa\\_html/iraf/iraf.html](https://astro.uni-bonn.de/~sysstw/lfa_html/iraf/iraf.html), on the relevant tasks for a comprehensive discussion of the parameters available.

### Preparing the Data for POLSALT

After the wavelength calibrations have been completed, the wavelength solution is parsed back into the format expected by POLSALT. Joining the separate beams with their respective wavelength solutions is performed in the CLI following Listing A.8.

Similar to the `split` procedure, the `join` procedure has the same defaults defined. The onus of keeping track of any previously changed default parameters falls to the user, but logging is implemented in STOPS (see the discussion on help documentation in § 3.3) which allows for later reference of any changed parameters.

### Sky Line Checks

The optional IRAF `transform` task and STOPS `skylines` method are used to confirm the wavelength solution across the frame (see § 3.3.3) by transforming and comparing known and observed sky line wavelength positions, respectively.

The `skyline` method is run in the CLI following Listing A.9. As with the rest of STOPS, default parameters describe the overplotting behavior for the *O*- and *E*-beams, the skylines provided by SALT, and the calculated variation of the wavelength axis of a frame.

### Cross Correlation Checks

The `correlate` method is run in the CLI following Listing A.11. The input of the `correlate` method takes the output of the POLSALT `spectra extraction` and is thus only run thereafter, but is mentioned here as the completion of the POLSALT reductions is not discussed in much depth. If the user wishes to compare the *O*- and *E*-beams of a single file then only that image name is to be provided, otherwise it is assumed that the user wishes to compare the same polarization beam across each file provided.

### Cleaning Up the IRAF and STOPS Output

Before the final POLSALT reductions, it is recommended that the user ‘clean up’ the `sci/` directory of all IRAF and STOPS files since the ‘wmxgbp’ FITS files are all that is expected by POLSALT. The POLSALT methods use wildcard file collection and as such any errant detections of files added by the user will result in unexpected crashes. It is suggested to move any additional files to a new subfolder following Listing A.10, but they may also be removed using:

```
$ rm beam*.fits arc*.fits frame* <any user created files>
```

### 3.4.4 POLSALT Reduction Completion

Reductions may now be completed using POLSALT. The reduction process consists of correcting for the wollaston tilt, extracting the spectra, creating the Stokes files, and displaying the results. The ‘beta’ version of POLSALT provides access to a GUI but may also be handled entirely through a CLI as scripts.

**Listing 3.7:** The modified `reducepoldata_sc.py` script file.

```

import os, sys, glob, shutil
poldir = '/home/justin/polsalt-beta/'                                     # Will differ according to user
reddir=poldir+'polsalt/'
scrdir=poldir+'scripts/'
sys.path.extend((reddir,scrdir,poldir))

datadir = reddir+'data/'
import numpy as np
from astropy.io import fits as pyfits
from specpolview import printstokes
from imred import imred
from specpolwavmap import specpolwavmap
from specpolextract_sc import specpolextract_sc
from specpolrawstokes import specpolrawstokes
from specpolfinalstokes import specpolfinalstokes

print sys.argv
obsdate = sys.argv[1]
print obsdate
os.chdir(obsdate)
if not os.path.isdir('sci'): os.mkdir('sci')
shutil.copy(scrdir+'script.py','sci')
os.chdir('sci')

# basic image reductions
infilelist = sorted(glob.glob('../raw/P*fits'))
imred(infilelist, '.', datadir+'bpm_rss_11.fits', crthresh=False, cleanup=True)

# basic polarimetric reductions
logfile='specpol'+obsdate+'.log'                                         # The following lines may be removed or commented out as below

# wavelength map
# infilelist = sorted(glob.glob('m*fits'))
# linelistlib=""
# specpolwavmap(infilelist, linelistlib=linelistlib, logfile=logfile)

# background subtraction and extraction
infilelist = sorted(glob.glob('wm*fits'))
extract = 10.      # star +/-5, bkg= +/- (25-35) arcsec: 2nd order is 9-20 arcsec away
locate = (-120.,120.)    # science target is brightest target in whole slit
#locate = (-20.,20.)

specpolextract_sc(infilelist,logfile=logfile,locate=locate,extract=extract)
#specpolextract_sc(infilelist,logfile=logfile,locate=locate,extract=extract, docomp=True, useoldc=True)

# raw stokes
infilelist = sorted(glob.glob('e*fits'))
specpolrawstokes(infilelist, logfile=logfile)

# final stokes
infilelist = sorted(glob.glob('*_h*.fits'))
specpolfinalstokes(infilelist, logfile=logfile)

```

## POLSALT Beta in the GUI

The reduction process using the POLSALT GUI is completed by selecting and, when applicable, interactively modifying the reduction step through the interactive windows, one-by-one, from the GUI's dropdown menu, as explained in Appendix A (p. 74 onwards).<sup>19</sup>

## POLSALT Beta through a CLI

Both GUI and CLI implementations of the POLSALT beta pipeline access the same script files. Although the GUI is more user-friendly, the CLI offers a more streamlined approach to the reduction process, allowing the reduction process to be automated once the IRAF wavelength solution is known and parsed into the 'wmxgbp' FITS file format. A modified version of the POLSALT beta `reducepoldata_sc.py` script (see Listing 3.7) is used to run the entire reduction process without needing to select which process to run next, using:

---

```
$ python reducepoldata_sc.py YYYYMMDD
```

---

where the only modification made to the `reducepoldata_sc.py` script file is the removal of a call to the `specpolwavmap` method.

---

<sup>19</sup>See the official POLSALT wiki or alternative online resources such as the SALT workshop slides.

The POLSALT beta `reducepoldata_sc.py` copies a `script.py` file into the science working directory, ‘YYYYMMDD/sci/’, which provides analysis scripts for analysis and modification of the POLSALT beta results. These tools consist of data culling for the final Stokes calculations, text and plot output, relative flux calibration corrections, and synthetic filtering of polarization results.

The POLSALT analysis scripts may be run using:

```
$ python script.py
```

followed by `specpolfinalstokes.py`, `specpolview.py`, `specpolflux.py`, or `specpolfilter.py`, for the different analysis modes, respectively.<sup>20</sup>

---

<sup>20</sup>Please see <https://github.com/saltastro/polsalt/wiki/Linear-Polarization-Reduction---Beta-version> for a comprehensive discussion of the POLSALT beta analysis scripts.

# Chapter 4

## Testing and Application

This chapter contains an overview of the testing performed for the development of STOPS (§ 4.1) and the checking of the replaced wavelength solutions (§ 4.2), as well as the application of STOPS on observations of both spectropolarimetric standards (§ 4.3.1) and science targets (§ 4.3.2).

### 4.1 Testing STOPS

The main challenge faced when developing STOPS was ensuring that the software was compatible with both the POLSALT and IRAF file structures. As development is an iterative process, STOPS was continually checked to ensure compatibility such that the varying STOPS method inputs were correctly parsed, and that their outputs were parsable by the relevant IRAF tasks or POLSALT methods.

To this end, observations which were verified to have been accurately reduced were duplicated for testing purposes, allowing for continual checks of the STOPS pipeline to be made during the development process. As the STOPS `split` and `join` methods are designed to convert between the POLSALT and IRAF file structures, greater emphasis was made to ensure that the output of both methods provided accurate and consistent results.

#### 4.1.1 Testing the split Method

The STOPS `split` method requires any POLSALT pre-reduced ('mxgbp'- prefixed) FITS files as input and outputs IRAF compatible ('(arc|beam)(O|E)'- prefixed) FITS file structures. As no 'split' FITS files are created during pure POLSALT reductions, the STOPS `split` method was tested by comparing the pre-reduced POLSALT files to the `split` method's output files, ensuring the correct structure and data integrity of the files handed off to IRAF.

Table 4.1 shows the FITS file information for the files before and after splitting. The split FITS files contain the split 'SCI' extension data and the 'Primary' header from the pre-reduced files, with any Header or Data differences mentioned below.

| Filename        | No. | Name      | Type       | Cards | Dimensions   | Format  |
|-----------------|-----|-----------|------------|-------|--------------|---------|
| POLSLT          | 0   | ‘Primary’ | PrimaryHDU | 161   | ()           |         |
|                 | 1   | ‘SCI’     | ImageHDU   | 19    | (3199, 1028) | float32 |
|                 | 2   | ‘VAR’     | ImageHDU   | 8     | (3199, 1028) | float32 |
|                 | 3   | ‘BPM’     | ImageHDU   | 8     | (3199, 1028) | uint8   |
| STOPS split ‘O’ | 0   | ‘Primary’ | PrimaryHDU | 162   | (3199, 474)  | float32 |
| STOPS split ‘E’ | 0   | ‘Primary’ | PrimaryHDU | 162   | (3199, 474)  | float32 |

**Table 4.1:** A comparison of the contents of a POLSLT pre-reduced FITS file to the STOPS split *O*- and *E*-beam FITS files. Table created using the `Astropy fitsinfo` CLI tool.



(a) The difference in the ‘SCI’ extensions, for the ‘O’ polarization beam.



(b) The difference in the ‘SCI’ extensions, for the ‘E’ polarization beam.

**Figure 4.1:** The difference between the POLSLT pre-reduced (‘mxgbp’- prefixed) FITS files and the STOPS ‘split’ (‘arc|beam)(O|E’- prefixed) files. Figures created using both the `POLSLT Raw image reduction` and `STOPS split` method outputs.

The header is left mostly untouched, and is only updated to represent the new data type and shape: the ‘BITPIX’ value is updated, from 8 to –32, and the ‘NAXIS’ value is updated, from 0 to 2; the ‘NAXIS1’ and ‘NAXIS2’ keywords are added, and their values are set to the new split ‘SCI’ data shape; and the ‘EXTEND’ keyword is removed.<sup>1</sup> This accounts for the discrepancy in the ‘Cards’ between the POLSLT and STOPS file header entries in Table 4.1.

Figure 4.1 shows that the POLSLT ‘SCI’ data is unmodified when copying the data to the STOPS FITS file, but only includes half of the data, for the relevant *O*- or *E*-polarization beam, Figure 4.1a and Figure 4.1b, respectively, with a cropping which defaults to 40 pixels (see § 3.3.1), introduced to the top- and bottom-most rows of the POLSLT data. This accounts for the discrepancy in the ‘Dimensions’ between the POLSLT and STOPS files in Table 4.1.

This output file structure was chosen for IRAF compatibility, and was tested over multiple grating and articulation angles, as well as with various data sets to ensure that the `split` method was robust and reliable.

<sup>1</sup>The ‘EXTEND’ keyword indicates that the FITS file contains multiple extensions while the ‘NAXIS1’ and ‘NAXIS2’ keywords indicate the shape and size of the data stored in the relevant extension.

| Filename   | No. | Name      | Type       | Cards | Dimensions     | Format  |
|------------|-----|-----------|------------|-------|----------------|---------|
| POLSLT     | 0   | 'Primary' | PrimaryHDU | 161   | ()             |         |
|            | 1   | 'SCI'     | ImageHDU   | 21    | (3199, 514, 2) | float32 |
|            | 2   | 'VAR'     | ImageHDU   | 10    | (3199, 514, 2) | float32 |
|            | 3   | 'BPM'     | ImageHDU   | 10    | (3199, 514, 2) | uint8   |
|            | 4   | 'WAV'     | ImageHDU   | 21    | (3199, 514, 2) | float32 |
| STOPs join | 0   | 'Primary' | PrimaryHDU | 161   | ()             |         |
|            | 1   | 'SCI'     | ImageHDU   | 21    | (3199, 474, 2) | float32 |
|            | 2   | 'VAR'     | ImageHDU   | 10    | (3199, 474, 2) | float32 |
|            | 3   | 'BPM'     | ImageHDU   | 10    | (3199, 474, 2) | uint8   |
|            | 4   | 'WAV'     | ImageHDU   | 21    | (3199, 474, 2) | float32 |

**Table 4.2:** A comparison of the POLSLT wavelength calibrated FITS file to the (IRAF wavelength calibrated) STOPs join FITS file. Table created using the Astropy `fitsinfo` CLI tool.

### 4.1.2 Testing the join Method

The `join` method requires both an IRAF database with wavelength solutions (or a custom wavelength solution) for both polarimetric beams and the POLSLT pre-reduced files as input and outputs POLSLT spectra extraction compatible ('wmxgbp'- prefixed) FITS file structures. Ensuring that the output format was correct was paramount as the POLSLT spectra extraction method is unable to process the files otherwise, thus halting the reduction process. Thankfully, the `join` method output could be compared to the POLSLT wavelength calibration method output files, ensuring that any changes introduced by the STOPs pipeline were well characterized.

Table 4.2 shows the FITS file information for both the POLSLT and STOPs wavelength calibrated files. Other than the 'Dimensions' of each 'ImageHDU' extension,<sup>2</sup> the FITS files are identical in structure.

Although the 'Cards' count is the same, minor differences across the headers are present. The 'HISTORY' keyword, which contains the POLSLT 'CRCLEAN' parameters and which default to 'upper= 4.0, lower= 1.5, sigmaveto= 2.0', is left as 'None' in the STOPs file.<sup>3</sup> Although STOPs performs cosmic ray cleaning (see § 3.3.2), the parameters are not stored in the header as POLSLT and STOPs implement different methods for cosmic ray cleaning. Other minor differences such as the date-times stored in the 'SALTLM' and 'SMOSAIC' keywords may also differ as they contain the date-times relating to the completion of the POLSLT pre-reductions. This accounts for the differences in the 'Cards' between the POLSLT and STOPs file header entries in Table 4.2.

Figure 4.2 shows the differences in the data between the POLSLT and STOPs wavelength calibrated files. It can be seen that the 'VAR' extensions (Figure 4.2b) are identical. The 'SCI' extensions (Figure 4.2a) differ only in that the cosmic ray cleaning has been applied to the STOPs data, whereas the POLSLT data applies a mask to the cosmic rays using the 'BPM' extension (Figure 4.2c). The 'BPM' and 'WAV' extensions (Figure 4.2d)

<sup>2</sup>The 'Dimensions' differ due to the before mentioned cropping of the top- and bottom-most rows of the data.

<sup>3</sup>The POLSLT pipeline performs cosmic ray cleaning using a  $10\sigma$  spike to cull cosmic rays. See the POLSLT source code for more information.

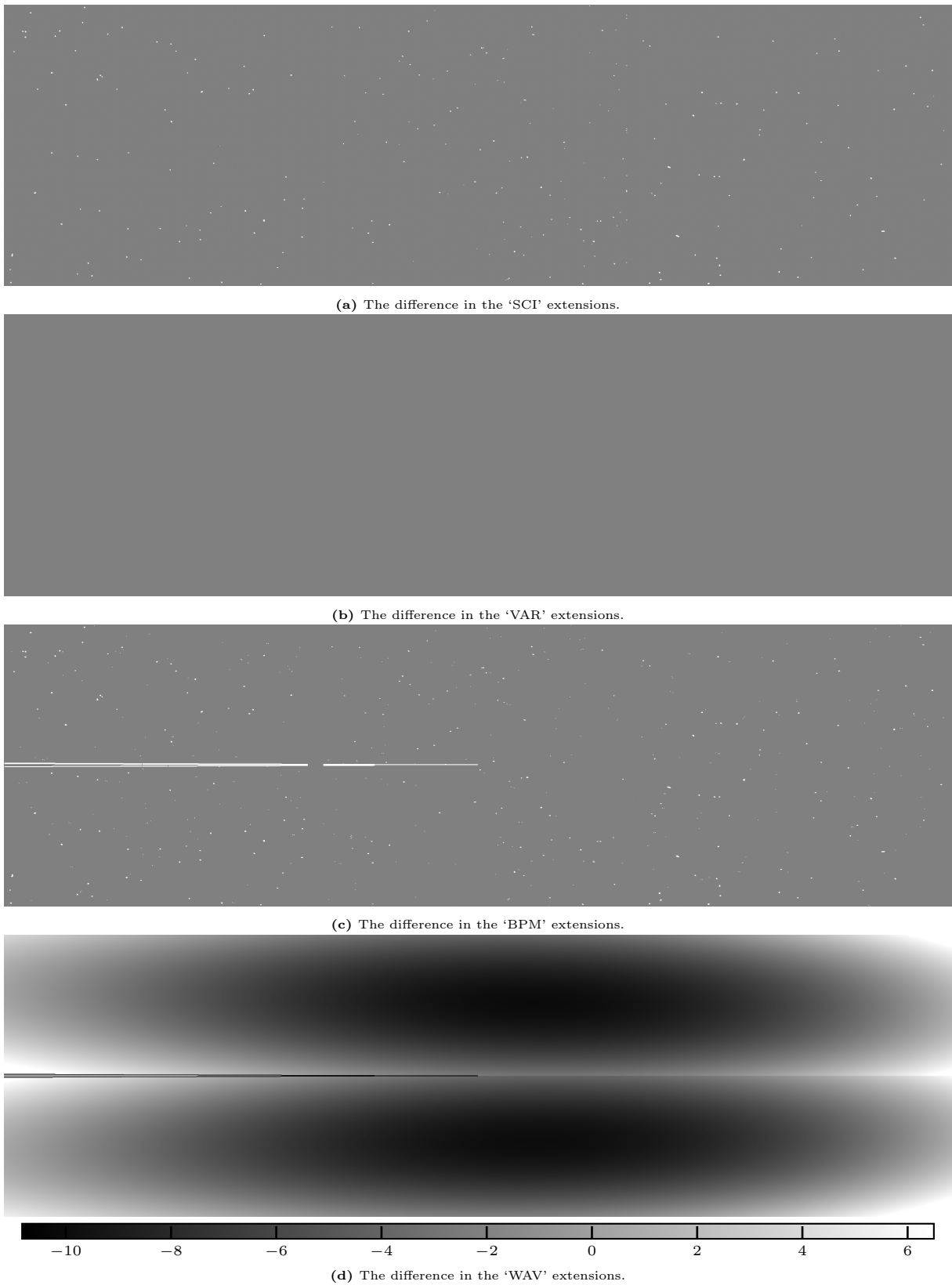


**Figure 4.2:** The difference of the FITS file extensions between the `POLSALT` and `STOPS` ('wmxgbp'- prefixed) wavelength calibrated files. Figures created using both the `POLSALT` and `STOPS` versions of the `POLSALT spectral extraction` input.

are also masked to account for the valid wavelength calibrated region. The ‘WAV’ extensions contain the differing wavelength solutions and as such naturally differ. This accounts for the differences in the data between the POLSALT and STOPS files.

Finally, the STOPS `join` method was tested to ensure compatibility and correctness of the output data in comparison to POLSALT. This involved testing the `join` method with various data sets to ensure that the output files were accurate and consistent.

## 4.2 Wavelength Solution Checks

The secondary challenge encountered when developing STOPS was ensuring that the wavelength solutions parsed by STOPS were unaffected by the pipeline and that they were similar to those created by POLSALT. This was achieved through the `correlate` and `skylines` methods, which were designed to validate the wavelength solutions produced by IRAF, but were later modified to parse both the IRAF and POLSALT wavelength solutions, allowing for further inspection of the two-dimensional wavelength solution.

Before the POLSALT wavelength calibrations were replaced with the IRAF wavelength calibrations, the accuracy of the new wavelength solutions needed to be validated. This was done both through the IRAF tasks, ensuring an accurate wavelength solution, and through the STOPS `correlate` and `skylines` methods, allowing the integration of the wavelength solutions to be validated.

**TODO: Add RMS results (Table / Figures / Both?) from wavelength solution checks (IRAF RMS, POLSALT RMS) to quantify differences.**

**TODO: Plot IRAF vs POLSALT RMS for sources?**

### 4.2.1 Cross Correlation Checks

The `correlate` method returns plots validating the wavelength solutions and so only has to accept the POLSALT `spectra extraction` ('ecwmxgbp'- prefixed) method output files as input.

The STOPS `correlate` method was tested by cross correlating generated *O*- and *E*-beam spectra with known offsets, with the aim of reacquiring said offsets, as shown in Figure 4.3. The spectra were generated with a feature in each CCD region, randomly offset in both the wavelength and intensity axes, Figure 4.3a.

Through cross correlation, Figure 4.3b, the introduced offsets, or ‘max lag’, were reacquired. For spectral regions with few features or features not much more significant than the continuum noise (such as the left most CCD region of Figure 4.3b), correlation may fail to determine the correct offset. It is clear that the returned ‘max lag’ is incorrect when the ‘max lag’ peak is not significantly larger than any noise of the continuum in the correlation plot.

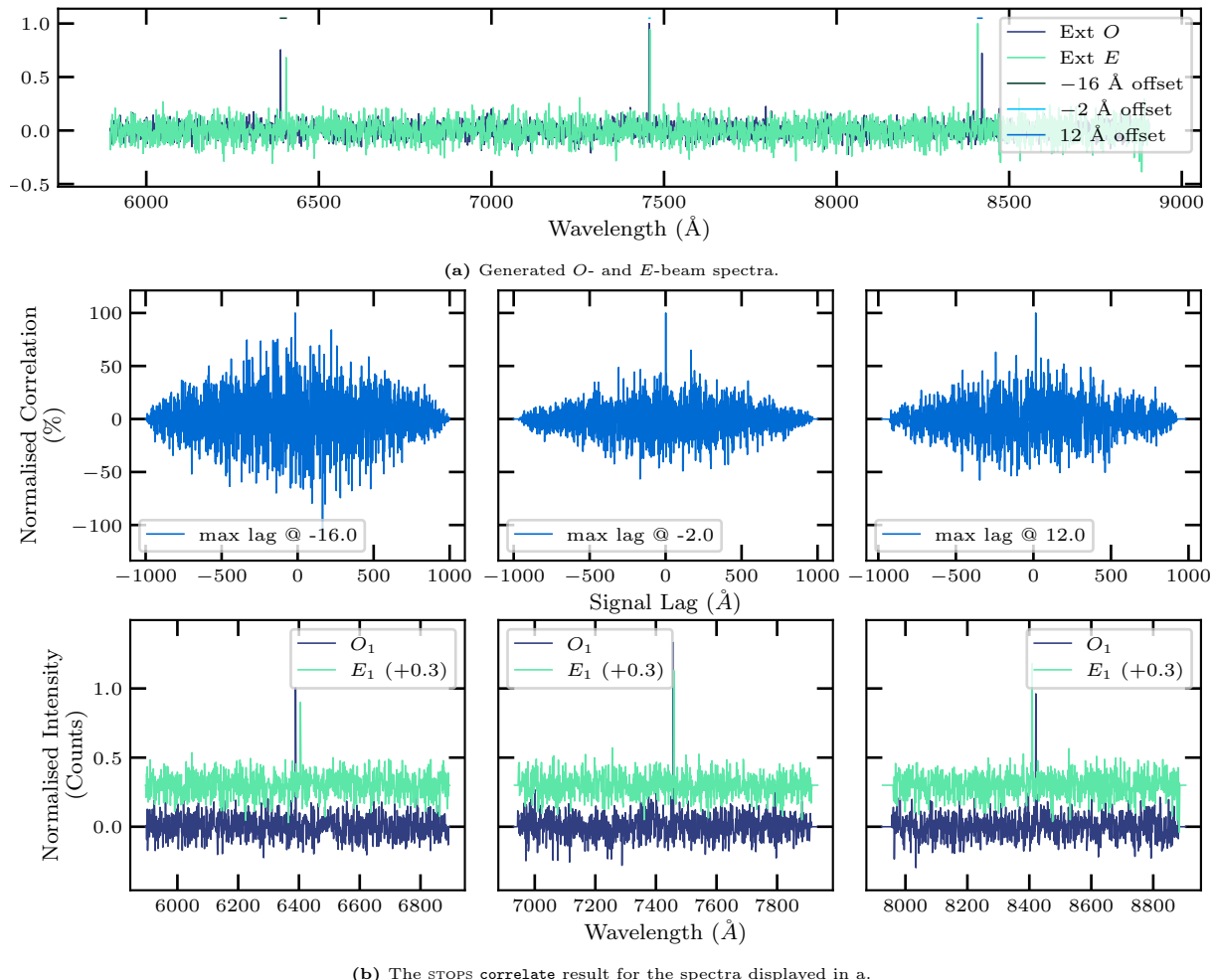


**Figure 4.3:** Reacquisition of synthetic offsets introduced to the  $O$ - and  $E$ -beam spectra (a) by cross-correlation (b, bottom row).

| Source | RA | DEC | Observation Date | Grating | Grating Angle | Articulation Angle | Exposure T |
|--------|----|-----|------------------|---------|---------------|--------------------|------------|
|--------|----|-----|------------------|---------|---------------|--------------------|------------|

**Table 4.3:** Spectropolarimetric standards discussed within this section.**TODO: Complete table of spectropolarimetric standards.**

### 4.2.2 Sky Line Checks

The `skylines` method returns plots validating the wavelength solutions and so only has to accept either the IRAF `transform` task or STOPS `join` method output files as input.

**TODO: Compare skylines from STOPS to ‘poor’ POLSALT spectral extraction (I.E. spectral extraction with no trace in the ‘target’ window and the ‘background’ window on region with no skylines).**

**TODO: Test ‘skylines’ using known spectral sky lines / telluric lines.**

**TODO: Insert figure illustrating skyline identification accuracy.**

## 4.3 Application of STOPS

The STOPS pipeline has been utilized in the reduction of a number of sources, both for calibration tests using spectropolarimetric standards, § 4.3.1, and for science observations of mostly flaring blazars, § 4.3.2.

### 4.3.1 Spectropolarimetric Standards

Spectropolarimetric standards must show little to no variability in both their spectroscopic and polarimetric properties. It is thus clear that blazars are not recommended as spectropolarimetric standards due to their high degree of variability.

**Source**

**TODO: For each standard:**

**TODO: Mention basic background information and a general discussion for source (A little more detail than included in paper).**

**TODO: General reduction steps performed (not necessary to constantly repeat self). Highlight any differences in reduction steps compared to science targets.**

**TODO: Insert figure(s) showing comparison plots of spectrum/polarization parameters from POLSALT and STOPS(or leave out POLSALT and just show comparison to (FORS1/2) published results). Also short discussion (what the results can tell us and why it is useful). Focus on polarization results.**

**TODO: Add a ‘see reference’ to final paragraph.**

| Source | RA                | DEC               | Observation Date | Grating | Grating Angle | Article |
|--------|-------------------|-------------------|------------------|---------|---------------|---------|
| 3C 279 | 12 56 11.16657958 | -05 47 21.5251510 |                  |         |               |         |

**Table 4.4:** Sources discussed from proceedings and publications within this section.**TODO: Complete table of science targets.**

### 4.3.2 Spectropolarimetric Science Targets

**TODO: Move to Introduction?**

The STOPS pipeline has been utilized in the reduction of a number of science targets, specifically focused on blazars. Blazars are a subset of Active Galactic Nucleus (AGN) with relativistic jets closely aligned to our line of sight, and are known for their rapid and high degree of variability across the electromagnetic spectrum.

Observations of these sources were performed using SALT, specifically using the RSS in spectropolarimetry mode (§ 2.4.3). SALT, and more specifically the RSS grating used (Table 2.1), limits the wavelength range to the optical and NIR regions. This allows for the study of the polarization properties of blazars within these wavelength regimes, which are often dominated by a polarized, non-thermal emission component arising in the jets, with an underlying non-polarized, thermal emission component arising from the host galaxy, dusty torus, and accretion disk components.

#### Development of Tools for the SALT/RSS Spectropolarimetry Reductions: Application to the Blazar 3C 279 (HEASA 2021)

As discussed in (Cooper et al., 2022, see also Appendix C), the STOPS pipeline was used during the reduction of the blazar 3C 279. It was shown that alternative wavelength solutions, such as those created using IRAF, are capable of being applied to SALT spectropolarimetric data.

The blazar 3C 279 was observed in linear spectropolarimetry mode, on 2017 May 17, using the PG0900 grating with two different grating angles ( $12.5^\circ$  and  $19.5^\circ$ ).

**TODO: Brief/unique reduction steps performed.**

**TODO: Insert figure(s) showing comparison plots of spectrum/polarization parameters from POLSALT and STOPS (or leave out POLSALT and just show published results). Also short discussion (what the results can tell us and why it is useful). Focus on polarization results.**

#### SALT Spectropolarimetric Pipeline Comparisons (HEASA 2022)

As discussed in (Cooper and van Soelen, 2023, see also Appendix C), **TODO: ...**

**TODO: Mention basic background information and a general discussion for source (summary of paper + necessary extra).**

**TODO: Brief/unique reduction steps performed.**

**TODO:** Insert figure(s) showing comparison plots of spectrum/polarization parameters from POLSALT and STOPS(or leave out POLSALT and just show published results). Also short discussion (what the results can tell us and why it is useful). Focus on polarization results.



# Chapter 5

## Conclusions

**TODO:** A summary of the dissertation, main focus on the results and that the supplementary pipeline is a success since it allows an alternate method using IRAF to wavelength calibrate the polsalt data.

### 5.1 Future Work

**TODO:** Edit paragraph below to mention python wavelength solutions implemented to ‘future-proof’ the pipeline.

Another option to perform the wavelength calibration is Python which allows for a more modern and flexible approach, but is not discussed here. What will be discussed, however, is the structure of the wavelength solutions created through Python to be later reintroduced to the POLSALT pipeline. The solutions must be stored such that the ‘ $x$ ’ and ‘ $y$ ’ orders of the solution, as well as all the coefficients ( $C_{00}$  to  $C_{xy}$ ) making up the solution, separated by new lines, are included. The only limitations to the names of the solution files is that they must make mention of the specific  $O$ - or  $E$ -beam as well as the wavelength solution type (e.g. ‘Chebyshev’, ‘Legendre’, etc.).



# Appendix A

## The Modified Reduction Process

This section of the Appendix aims to provide a minimum working example of the commands necessary to reduce POLSALT data using STOPS and IRAF. It contains the commands necessary to activate all software and run through the reduction process but makes no attempt at discussion.

Both POLSALT and IRAF are launched from the default CLI but use independent interfaces during the reduction process. To distinguish which window is in focus, the ‘\$’ token is used for default CLI commands while the ‘c1>’ and ‘>>>’ tokens are used for IRAF’s ‘xgterm’ single- and multi-line commands, respectively.

General instructions for the reduction process which might not necessarily be line-fed commands passed to a CLI may either be discussed outside a ‘Listing’ environment or included as part of the ‘Listing’ environment with a preceding ‘#’ token. Finally, POLSALT implements a GUI and thus takes no line-fed commands. As such, the instructions when using the POLSALT GUI follow those of the general instructions with the added exception that they relate to the GUI.

As a final note, some parameters are distinguished using an ‘<angle brackets>’ notation. They signify necessary parameters that may vary from reduction to reduction. Notable uses of this notation include the date of observation,  $\langle OBSDATE \rangle$  (formatted ‘YYYYMMDD’), the split science FITS files,  $\langle O\text{-beam FILES} \rangle$  or  $\langle E\text{-beam FILES} \rangle$ , the split arc FITS files,  $\langle O\text{-beam ARC} \rangle$  or  $\langle E\text{-beam ARC} \rangle$ , and a wildcard symbol,  $\langle * \rangle$ .

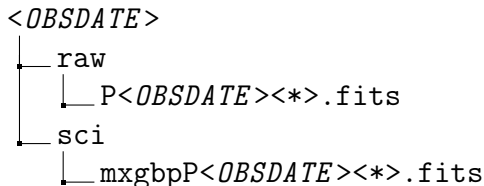


**Figure A.1:** The typical minimal file structure of data provided by SALT.

Ensure the data is formatted in a file structure similar to that in Figure A.1. Data located in the ‘sci’ folder is often provided by SALT but is not strictly necessary to begin the reduction process. If ‘mxgbp’ prefixed data is available, the reductions may be begun starting at Listing A.2. The POLSALT GUI is launched from the default CLI running the commands in Listing A.1.

**Listing A.1:** Launching the POLSALT GUI

---

```
$ cd ~/polsalt
$ conda activate salt
$ python -W ignore reducepoldataGUI.py &
```

---

Refer to Figure 3.1 for a depiction of the POLSALT GUI. To complete the POLSALT pre-calibrations, and with the GUI in focus:

- Ensure that the ‘POLSALT code directory’ is correct.
- Set the ‘Top level data directory’ to  $\langle OBSDATE \rangle$ .
- Ensure ‘Raw data directory’ is correct.
- Ensure ‘Science data directory’ is correct.
- Select ‘Raw image reduction’ from the ‘Data reduction step’ drop down menu.
- Check the tick boxes of all raw images to be processed (include the arc) in the display box covering the lower half of the GUI.
- Proceed with the reductions by clicking the ‘OK’ button.

The pre-calibrated ‘mxgbp’ FITS files are now available in the ‘sci’ folder. The files may be split using STOPS by running the commands in Listing A.2.

**Listing A.2:** Splitting data using STOPS

---

```
$ cd <OBSDATE>/sci
$ conda activate stops
$ python ~/STOPS . split
```

---

The split *O*- and *E*-beam FITS files are now available. The IRAF wavelength calibrations are now run. The IRAF xgterm CLI is launched using Listing A.3.

**Listing A.3:** Launching IRAF in xgterm

---

```
$ cd ~/iraf
$ xgterm -sb &
cl> conda activate salt
cl> cl
cl> noao
cl> twodspec
cl> longslit
cl> unlearn longslit
cl> longslit.dispaxis=1
```

---

The IRAF `identify` task requires an average feature width, ‘fwidth’, as a parameter. The width of a feature may be found in IRAF using the `implot` task<sup>1</sup> along with cursor commands, but may also be found using FITS viewing software, such as `ds9`.<sup>2</sup> The `identify` task may be run using the commands in Listing A.4.

**Listing A.4:** Running the IRAF `identify` task

---

```
cl> mkscript 01_identify.cl
cl> # Add identify to 01_identify.cl twice, for both beams
cl> # Edit the parameters of 01_identify.cl in a text editor
cl> # Paste an identify script into the CLI, resulting in:
cl>
cl> identify ("<O-beam ARC>",
>>> "", "", section="middle line", database="database",
>>> coordlist="linelists$idheneare.dat", units="", nsum="10", match=-3.,
>>> maxfeatures=50, zwidth=100., ftype="emission", fwidth=8.,
>>> cradius=5., threshold=0., minsep=2., function="spline3", order=2,
>>> sample="*", niterate=0, low_reject=3., high_reject=3., grow=0.,
>>> autowrite=no, graphics="stdgraph", cursor="", aidpars="")
```

---

The `identify` task will launch an interactive window. Cursor commands refer to keys that provide unique functionality to the interactive IRAF tasks. The cursor commands for `identify` allow the arc lines to be identified using ‘m’ (and typing the relevant wavelength), while ‘d’ and ‘i’ will delete a single and all identified arc lines, respectively. The ‘f’ cursor command will perform a preliminary fit which can be quit using the ‘q’ cursor command. The ‘l’ cursor command will attempt to identify any unidentified arc lines. Once complete, a figure of the identified lines may be saved using ‘:labels coord’ and ‘:.snap eps’, and the task safely quit with the ‘q’ cursor command.<sup>3</sup> The `identify` procedure is repeated, replacing  $<O\text{-beam } ARC>$  with  $<E\text{-beam } ARC>$ .

The `reidentify` task may be run using the commands in Listing A.5.

**Listing A.5:** Running the IRAF `reidentify` task

---

```
cl> mkscript 02_reidentify.cl
cl> # Add reidentify to 02_reidentify.cl twice, for both beams
cl> # Edit the parameters of 02_reidentify.cl in a text editor
cl> # Paste a reidentify script into the CLI, resulting in:
cl>
cl> reidentify ("<O-beam ARC>",
>>> "<O-beam ARC>", "yes", "", "", interactive="no", section="middle
>>> line", newaps=yes, override=no, refit=yes, trace=yes, step="10",
>>> nsum="10", shift="0.", search=0., nlost=0, cradius=5.,
>>> threshold=0., addfeatures=no, coordlist="linelists$idheneare.dat",
>>> match=-3., maxfeatures=50, minsep=2., database="database",
>>> logfiles="logfile", plotfile="", verbose=yes, graphics="stdgraph",
>>> cursor="", aidpars="")
```

---

<sup>1</sup>See [https://astro.uni-bonn.de/~sysstw/lfa\\_html/iraf/plot.implot.html](https://astro.uni-bonn.de/~sysstw/lfa_html/iraf/plot.implot.html) for documentation on the `implot` task.

<sup>2</sup>See <https://sites.google.com/cfa.harvard.edu/saoimageds9> for documentation on the `ds9` software.

<sup>3</sup>See [https://astro.uni-bonn.de/~sysstw/lfa\\_html/iraf/noao.onedspec.identify.html](https://astro.uni-bonn.de/~sysstw/lfa_html/iraf/noao.onedspec.identify.html) for documentation on the `identify` task.

The `reidentify` task will run autonomously so long as the `interactive` parameter is set to “no”.<sup>4</sup> Repeat the `reidentify` procedure, replacing  $\langle O\text{-beam } ARC \rangle$  with  $\langle E\text{-beam } ARC \rangle$  at both the ‘reference’ and ‘image’ parameter locations.

The `fitcoords` task may be run using the commands in Listing A.6.

**Listing A.6:** Running the `IRAF fitcoords` task

---

```
cl> mkscript 03_fitcoords.cl
cl> # Add fitcoords to 03_fitcoords.cl twice, for both beams
cl> # Edit the parameters of 03_fitcoords.cl in a text editor
cl> # Paste a fitcoords script into the CLI, resulting in:
cl>
cl> fitcoords ("<O-beam ARC> (exclude the file extension)" ,
>>> fitname="", interactive=yes, combine=no, database="database",
>>> deletions="deletions.db", function="chebyshev", xorder=6, yorder=6,
>>> logfiles="STDOUT,logfile", plotfile="plotfile",
>>> graphics="stdgraph", cursor="")
```

---

The `fitcoords` task will launch an interactive window. The x- and y-axis being plotted may be changed using the ‘x’ or ‘y’ cursor commands followed by the desired data axis (‘x’ for the x-axis, ‘y’ for the y-axis, or ‘r’ for the residuals).<sup>5</sup> Repeat the `fitcoords` procedure, replacing  $\langle O\text{-beam } ARC \rangle$  with  $\langle E\text{-beam } ARC \rangle$ .

The `transform` task may be run using the commands in Listing A.7.

**Listing A.7:** Running the `IRAF transform` task

---

```
cl> mkscript 04_transform.cl
cl> # Add transform to 04_transform.cl twice, for both beams
cl> # Edit the parameters of 04_transform.cl in a text editor
cl> # Paste a transform script into the CLI, resulting in:
cl>
cl> transform ("@<O-beam FILES>" ,
>>> "t/@<O-beam FILES>", "<O-beam ARC> (exclude the file extension)" ,
>>> minput="", moutput="", database="database", interptype="linear",
>>> x1="INDEF", x2="INDEF", dx="INDEF", nx="INDEF", xlog="no",
>>> y1="INDEF", y2="INDEF", dy="INDEF", ny="INDEF", ylog="no",
>>> flux="yes", blank="INDEF", logfiles="STDOUT,logfile")
```

---

The `transform` task will run autonomously.<sup>6</sup> Repeat the `transform` procedure, replacing the  $\langle O\text{-beam } FILES \rangle$  and  $\langle O\text{-beam } ARC \rangle$  with  $\langle E\text{-beam } FILES \rangle$  and  $\langle E\text{-beam } ARC \rangle$  at both parameter locations. Inspect the transformed images, most notably the arc images, using any FITS viewer as a cursory check that the wavelength calibrations were completed without error.

The ‘gain’ and ‘read noise’ are now needed as the cosmic-ray rejection of the STOPS `join` method accepts them as parameters. These parameters may be found using the ‘`GAINSET`’ and ‘`ROSPEED`’ keywords in the FITS headers. The cosmic ray rejection

<sup>4</sup>See [https://astro.uni-bonn.de/~sysstw/lfa\\_html/iraf/noao.onedspec.reidentify.html](https://astro.uni-bonn.de/~sysstw/lfa_html/iraf/noao.onedspec.reidentify.html) for documentation on the `reidentify` task.

<sup>5</sup>See [https://astro.uni-bonn.de/~sysstw/lfa\\_html/iraf/noao.twodspec.longslit.fitcoords.html](https://astro.uni-bonn.de/~sysstw/lfa_html/iraf/noao.twodspec.longslit.fitcoords.html) for documentation on the `fitcoords` task.

<sup>6</sup>See [https://astro.uni-bonn.de/~sysstw/lfa\\_html/iraf/noao.twodspec.longslit.transform.html](https://astro.uni-bonn.de/~sysstw/lfa_html/iraf/noao.twodspec.longslit.transform.html) for documentation on the `transform` task.

defaults to *GAINSET*=‘FAINT’, and *ROSPEED*=‘SLOW’. If the gain and read noise values differ from the defaults, the parameters should be updated when running `join`.<sup>7</sup>

The STOPS `join` method may be run using the commands in Listing A.8.

**Listing A.8:** Joining the data using STOPS

---

```
$ cd <OBSDATE>/sci
$ conda activate stops
$ python ~/STOPS . join
```

---

The STOPS `skylines` method may be run on any ‘joined’ or transformed FITS files, *<FILE(S)>*, using the commands in Listing A.9.

**Listing A.9:** Running the STOPS `skylines` method

---

```
$ cd <OBSDATE>/sci
$ conda activate stops
$ python ~/STOPS . skylines <FILE(S)>
```

---

The ‘sci/’ directory may now be slightly organized by running the commands in Listing A.10, moving all the files relevant to the wavelength calibrations into either the ‘database’ or ‘split\_files’ directories.

**Listing A.10:** Directory cleanup for POLSALT

---

```
$ cd <OBSDATE>/sci
$ mkdir split_files
$ mv *beam0* *beamE* *arc0* *arcE* split_files/
$ mv *.eps *.cl *.db database/
```

---

The POLSALT `spectra extraction` is now run. If the POLSALT GUI was closed it should now be reopened using Listing A.1. With the GUI in focus:

- Ensure all directories are still correct.
- Select ‘Spectra extraction’ from the ‘Data reduction step’ drop down menu.
- Check the tick boxes of all wavelength calibrated images to be processed (exclude the arc) in the display box covering the lower half of the GUI.
- Proceed with the reductions by clicking ‘OK’.

The POLSALT `spectra extraction` is interactive and will launch a separate GUI for the background subtraction and spectral extraction (see Figure 3.2). The background and spectral regions to be extracted may be adjusted, noting that adjustments affect both *O*- and *E*-beams. Once both background regions contain no trace and the spectral region fully contains only the science trace, the reduction may be completed by clicking ‘OK’.

---

<sup>7</sup>The read noise and gain may be determined from [http://pysalt.salt.ac.za/proposal\\_calls/current/ProposalCall.html](http://pysalt.salt.ac.za/proposal_calls/current/ProposalCall.html), specifically Table 6.1 and Table 6.2.

The STOPS `correlate` method may now be run on any ‘joined’ FITS files by running the commands in Listing A.11.

**Listing A.11:** Running the STOPS `correlate` method

---

```
$ cd <OBSDATE>/sci
$ conda activate stops
$ python ~/STOPS . correlate <FILE(S)>
```

---

The POLSALT `raw Stokes calculation`, `final Stokes calculation`, and `results visualisation` may now be completed. For the last time, if the POLSALT GUI was closed it should now be reopened using Listing A.1. With the GUI in focus:

- Ensure all directories are still correct.
- Select ‘Raw Stokes calculation’ from the ‘Data reduction step’ drop down menu.
- Check the tick boxes of all the extracted spectra images to be processed in the display box covering the lower half of the GUI.
- Proceed with the `raw Stokes calculation` by clicking ‘OK’.
- Select ‘Final Stokes calculation’ from the ‘Data reduction step’ drop down menu.
- Check the tick boxes of all the “raw Stokes” images to be processed in the display box covering the lower half of the GUI.
- Proceed with the `Final Stokes calculation` by clicking ‘OK’.
- Select ‘Results visualisation - interactive’ from the ‘Data reduction step’ drop down menu.
- Check the tick boxes of the “final Stokes” image to be visualized in the display box covering the lower half of the GUI.
- Proceed with the `visualisation` by clicking ‘OK’.

The POLSALT `visualisation` is interactive and will launch a separate GUI (See Figure 3.3). The GUI may be used to change the binning and parameters of the plot before saving the plot to a PDF file.

This concludes the minimum working example of the POLSALT reduction process when substituting the POLSALT `wavelength calibrations` with those done in IRAF. Aside from the final results, the file structure after reductions should resemble something akin to that provided in Figure A.2.

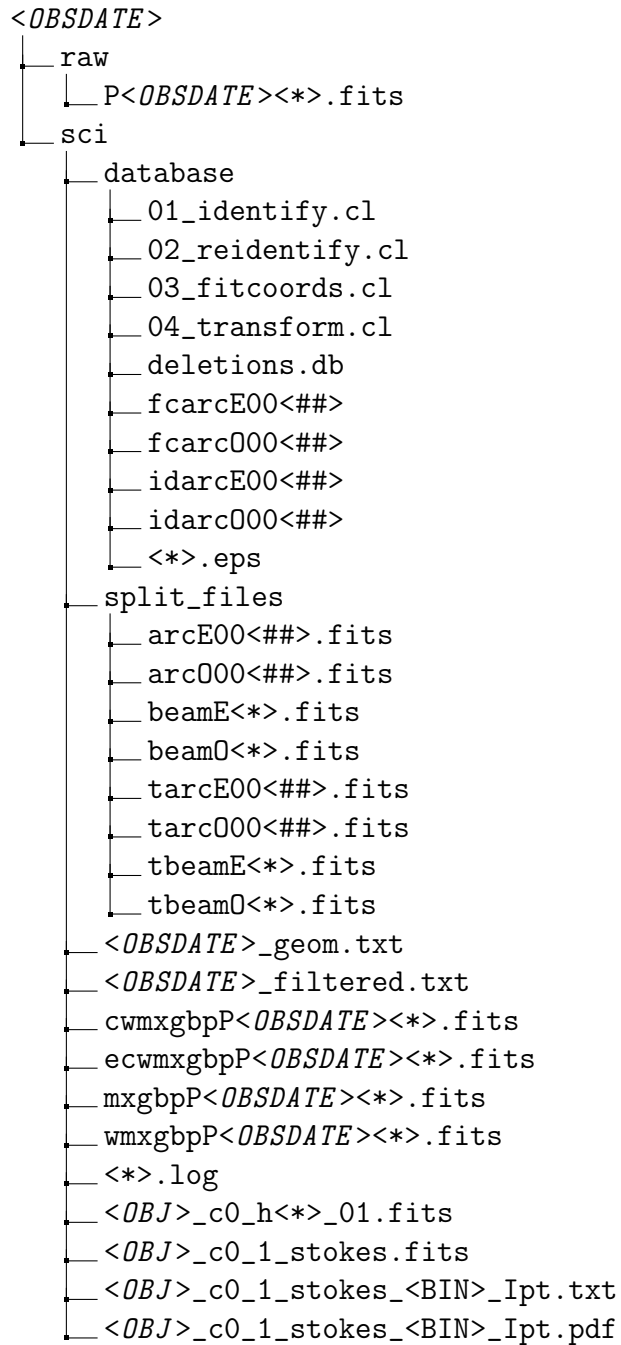


**Figure A.2:** The typical file structure after completing the reduction process.



# Appendix B

## STOPS Source Code

This section of Appendix includes all the major STOPS source code files related to the reduction process. Files such as those related to python initialization, testing directories, and other non-essential modules have been excluded for brevity and clarity.

**Listing B.1:** The source code for `__main__.py`

```
1 #!/usr/bin/env python3
2 # -*- coding: utf-8 -*-
3
4 """Argument parser for STOPS."""
5
6 # MARK: Imports
7 import sys
8 import argparse
9 import logging
10 from pathlib import Path
11
12 from STOPS import __version__
13 from STOPS import Split, Join, CrossCorrelate, Skylines
14 from STOPS.utils import ParserUtils as Parser
15 from STOPS.utils.Constants import SPLIT_ROW, PREFIX, PARSE, SAVE_CORR, SAVE_SKY
16
17 # MARK: Constants
18 PROG = "STOPS"
19 DESCRIPTION = """
20 Supplementary TOols for Polsalt Spectropolarimetry (STOPS) is a
21 collection of supplementary tools created for SALT's POLSALT pipeline,
22 allowing for wavelength calibrations with IRAF. The tools provide
23 support for splitting and joining polsalt formatted data as well as
24 cross correlating complementary polarimetric beams.
25
26 DOI: 10.22323/1.401.0056
27 """
28
29
30 # MARK: Universal Parser
31 parser = argparse.ArgumentParser(
32     prog=PROG,
33     description=DESCRIPTION,
34     formatter_class=argparse.RawDescriptionHelpFormatter,
35 )
36 parser.add_argument(
37     "-V",
38     "--version",
39     action="version",
40     version=f"%(prog)s as of {__version__}",
41 )
```

```

42 parser.add_argument(
43     "-v",
44     "--verbose",
45     action="count",
46     default=PARSE['VERBOSE'],
47     help=(
48         "Counter flag which enables and increases verbosity. "
49         "Use -v or -vv for greater verbosity levels."
50     ),
51 )
52 parser.add_argument(
53     "-l",
54     "--log",
55     action="store",
56     type=Parser.parse_logfile,
57     help=(
58         "Filename of the logging file. "
59         "File is created if it does not exist. Defaults to None."
60     ),
61 )
62 parser.add_argument(
63     "data_dir",
64     action="store",
65     nargs="?",
66     default=PARSE['DATA_DIR'],
67     type=Parser.parse_path,
68     help=(
69         "Path of the directory which contains the working data. "
70         f"Defaults to the cwd -> '{PARSE['DATA_DIR']}' (I.E. '..')."
71     ),
72 )
73
74
75 # MARK: Split\Join Parent
76 split_join_args = argparse.ArgumentParser(add_help=False)
77 split_join_args.add_argument(
78     "-n",
79     "--no_arc",
80     action="store_true",
81     help="Flag to exclude arc files from processing.",
82 )
83 split_join_args.add_argument(
84     "-s",
85     "--split_row",
86     default=SPLIT_ROW,
87     type=int,
88     help=(
89         "Row along which the O and E beams are split. "
90         f"Defaults to polsalt's default -> {SPLIT_ROW}."
91     ),
92 )
93 split_join_args.add_argument(
94     "-p",
95     "--save_prefix",
96     nargs=2,
97     default=PREFIX,
98     help=(
99         "Prefix appended to the filenames, "
100        "with which the O and E beams are saved. "
101        f"Defaults to {PREFIX}."
102     ),
103 )
104
105
106 # MARK: Correlate\Skylines Parent
107 corr_sky_args = argparse.ArgumentParser(add_help=False)
108 corr_sky_args.add_argument(
109     "filenames",
110     action="store",
111     nargs="+",
112     type=Parser.parse_file,
113     help=(
114         "File name(s) of FITS file(s) to be processed."

```

```

115     "A minimum of one filename is required."
116 ),
117 )
118 corr_sky_args.add_argument(
119     "-b",
120     "--beams",
121     choices=["O", "E", "OE"],
122     type=str.upper,
123     default=PARSE['BEAMS'],
124     help=(
125         "Beams to process."
126         f"Defaults to {PARSE['BEAMS']}, but "
127         "may be given 'O', 'E', or 'OE' to "
128         "determine which beams are processed."
129     ),
130 )
131 corr_sky_args.add_argument(
132     "-ccd",
133     "--split_ccd",
134     action="store_false",
135     help=(
136         "Flag to NOT split CCD's."
137         "Recommended to leave off unless the chip gaps "
138         "have been removed from the data."
139     ),
140 )
141 corr_sky_args.add_argument(
142     "-c",
143     "--continuum_order",
144     type=int,
145     default=PARSE['CONT_ORD'],
146     dest="cont_ord",
147     help=(
148         "Order of continuum to remove from spectra."
149         "Higher orders recommended to remove most variation, "
150         "leaving only significant features."
151     ),
152 )
153 corr_sky_args.add_argument(
154     "-p",
155     "--plot",
156     action="store_true",
157     help="Flag for additional plot outputs.",
158 )
159
160
161 # MARK: Create subparser modes
162 subparsers = parser.add_subparsers(
163     dest="mode",
164     help="Operational mode of supplementary tools",
165 )
166
167
168 # MARK: Split Subparser
169 split_parser = subparsers.add_parser(
170     "split",
171     aliases=["s"],
172     help="Split mode",
173     parents=[split_join_args],
174 )
175 # 'children' split args here
176 # Change defaults here
177 split_parser.set_defaults(
178     mode="split",
179     func=Split,
180 )
181
182
183 # MARK: Join Subparser
184 join_parser = subparsers.add_parser(
185     "join",
186     aliases=["j"],
187     help="Join mode",

```

```

188     parents=[split_join_args],
189 )
190 # 'children' join args here
191 join_parser.add_argument(
192     "-c",
193     "--coefficients",
194     dest="solutions_list",
195     nargs='*',
196     type=Parser.parse_file,
197     help=(
198         "Custom coefficients to use instead of the `IRAF` fitcoords "
199         "database. Use as either '-c <o_solution> <e_solution>' or "
200         "a regex descriptor '-c <*solution*extention>'."
201     ),
202 )
203 # Change defaults here
204 join_parser.set_defaults(
205     mode="join",
206     func=Join,
207 )
208
209
210 # MARK: Correlate Subparser
211 corr_parser = subparsers.add_parser(
212     "correlate",
213     aliases=["x"],
214     help="Cross correlation mode",
215     parents=[corr_sky_args],
216 )
217 # 'children' correlate args here
218 corr_parser.add_argument(
219     "-o",
220     "--offset",
221     type=int,
222     default=PARSE['OFFSET'],
223     help=(
224         "Introduces an offset when correcting for "
225         "known offset in spectra or for testing purposes. "
226         f"Defaults to {PARSE['OFFSET']}. "
227         "(For testing, not used during regular operation.)"
228     ),
229 )
230 corr_parser.add_argument(
231     "-s",
232     "--save_prefix",
233     action="store",
234     nargs="?",
235     type=lambda path: Path(path).expanduser().resolve(),
236     const=SAVE_CORR,
237     help=(
238         "Prefix used when saving plot. "
239         "Excluding flag does not save output plot, "
240         f"flag usage of option uses default prefix, "
241         "and a provided prefix overwrites default prefix."
242     ),
243 )
244 # Change defaults here
245 corr_parser.set_defaults(
246     mode="correlate",
247     func=CrossCorrelate,
248 )
249
250
251 # MARK: Skyline Subparser
252 sky_parser = subparsers.add_parser(
253     "skylines",
254     aliases=["sky"],
255     help="Sky line check mode",
256     parents=[corr_sky_args],
257 )
258 # 'children' skyline args here
259 sky_parser.add_argument(
260     "-t",

```

```

261     "--transform",
262     action="store_false",
263     help=(
264         "Flag to force transform images. "
265         "Recommended to use only when input image(s) "
266         "are prefixed 't' but are not yet transformed."
267     ),
268 )
269 sky_parser.add_argument(
270     "-s",
271     "--save_prefix",
272     action="store",
273     nargs="?",
274     type=lambda path: Path(path).expanduser().resolve(),
275     const=SAVE_SKY,
276     help=(
277         "Prefix used when saving plot. "
278         "Excluding flag does not save output plot, "
279         f"flag usage of option uses default prefix, "
280         "and a provided prefix overwrites default prefix."
281     ),
282 )
283 # Change defaults here
284 sky_parser.set_defaults(
285     mode="skyline",
286     func=Skylines,
287 )
288
289
290 # MARK: Keyword Clean Up
291 args = parser.parse_args()
292
293 if len(sys.argv) == 1:
294     parser.print_help(sys.stderr)
295     sys.exit(2)
296
297 args.verbose = Parser.parse_loglevel(args.verbose)
298
299 if 'log' in args and args.log not in [None]:
300     args.log = args.data_dir / args.log
301
302 if "filenames" in args:
303     args.filenames = Parser.flatten(args.filenames)
304
305 if "solutions_list" in args and isinstance(args.solutions_list, list):
306     args.solutions_list = Parser.flatten(args.solutions_list)
307
308 # MARK: Begin logging
309 logging.basicConfig(
310     filename=args.log,
311     format="%(asctime)s - %(module)s - %(levelname)s - %(message)s",
312     datefmt="%Y-%m-%d %H:%M:%S",
313     level=args.verbose,
314 )
315
316 # MARK: Call Relevant Class(Args)
317 logging.debug(f"Argparse namespace: {args}")
318 logging.info(f"Mode:{args.mode}")
319 args.func(**vars(args)).process()
320
321
322 # Confirm all processes completed and exit without error
323 logging.info("All done! Come again!\n")

```

---

Listing B.2: The source code for `split.py`

```

1 #!/usr/bin/env python3
2 # -*- coding: utf-8 -*-
3
4 """Module for splitting ``polsalt`` FITS files."""
5
6 # MARK: Imports
7 import os
8 import sys
9 import logging
10 from copy import deepcopy
11 from pathlib import Path
12
13 import numpy as np
14 from astropy.io import fits as pyfits
15
16 from STOPS.utils.SharedUtils import find_files, find_arc
17 from STOPS.utils.Constants import SAVE_PREFIX, CROP_DEFAULT, SPLIT_ROW
18
19
20 # MARK: Split Class
21 class Split:
22
23     #-----split0-----
24
25     """
26     The `Split` class allows for the splitting of `polsalt` FITS files
27     based on the polarization beam. The FITS files must have basic
28     `polsalt` pre-reductions already applied (`mxbgp...` FITS files).
29
30     Parameters
31     -----
32     data_dir : str / Path
33         The path to the data to be split
34     fits_list : list[str], optional
35         A list of pre-reduced `polsalt` FITS files to be split within `data_dir`.
36         (The default is None, `Split` will search for `mxbgp*.fits` files)
37     split_row : int, optional
38         The row along which to split the data of each extension in the FITS file.
39         (The default is SPLIT_ROW (See Notes), the SALT RSS CCD's middle row)
40     no_arc : bool, optional
41         Decides whether the arc frames should be recombined.
42         (The default is False, `polsalt` has no use for the arc after wavelength
43         ↩ calibrations)
44     save_prefix : dict[str, list[str]], optional
45         The prefix with which to save the O & E beams.
46         Setting `save_prefix` = ``None`` does not save the split O & E beams.
47         (The default is SAVE_PREFIX (See Notes))
48
49     Attributes
50     -----
51     arc : str
52         Name of arc FITS file within `data_dir`.
53         `arc` = ```` if `no_arc` or not detected in `data_dir`.
54     o_files, e_files : list[str]
55         A list of the `O`- and `E`-beam FITS file names.
56         The first entry is the arc file if `arc` defined.
57     data_dir
58     fits_list
59     split_row
60     save_prefix
61
62     Methods
63     -----
64     split_file(file: os.PathLike)
65         -> tuple[astropy.io.fits.HDUList]
66         Handles creation and saving the separated FITS files
67     split_ext(hdulist: astropy.io.fits.HDUList, ext: str = 'SCI')
68         -> astropy.io.fits.HDUList
69         Splits the data in the `ext` extension along the `split_row`
70     crop_file(hdulist: astropy.io.fits.HDUList, crop: int = CROP_DEFAULT (See Notes))
71         -> tuple[numumpy.ndarray]

```

```

71     Crops the data along the edge of the frame, that is,
72     `O`-beam cropped as [crop:], and
73     `E`-beam cropped as [: - crop].
74     update_beam_lists(o_name: str, e_name: str)
75         -> None
76         Updates `o_files` and `e_files`.
77     save_beam_lists(file_suffix: str = 'frames')
78         -> None
79         Creates (Overwrites if exists) and writes the `o_files` and `e_files` to files
80         ↳ named
81         `o_{file_suffix}` and `e_{file_suffix}`, respectively.
82     process()
83         -> None
84         Calls `split_file` and `save_beam_lists` on each file in `fits_list` for
85         ↳ automation.

86 Other Parameters
87 -----
88 **kwargs : dict
89     keyword arguments. Allows for passing unpacked dictionary to the class
90     ↳ constructor.

91 Notes
92 -----
93 Constants Imported (See utils.Constants):
94     SAVE_PREFIX
95     CROP_DEFAULT
96     SPLIT_ROW
97
98 """
99 #-----split1-----
100
101 # MARK: Split init
102 def __init__(
103     self,
104     data_dir: Path,
105     fits_list: list[str] = None,
106     split_row: int = SPLIT_ROW,
107     no_arc: bool = False,
108     save_prefix: Path | None = None,
109     **kwargs,
110 ) -> None:
111     self.data_dir = data_dir
112     self.fits_list = find_files(
113         data_dir=data_dir,
114         filenames=fits_list,
115         prefix="mxgbp",
116         ext="fits"
117     )
118     self.split_row = split_row
119     self.save_prefix = SAVE_PREFIX
120     if isinstance(save_prefix, dict):
121         self.save_prefix = save_prefix
122
123     self.arc = "" if no_arc else find_arc(self.fits_list)
124     self.o_files = []
125     self.e_files = []
126
127     logging.debug("__init__ - \n", self.__dict__)
128
129 # MARK: Split Files
130 def split_file(
131     self,
132     file: os.PathLike
133 ) -> tuple[pyfits.HDUList, pyfits.HDUList]:
134     """
135     Split the single FITS file into separated `O`- and `E`- FITS files.
136
137 Parameters
138 -----
139     file : os.PathLike
140

```

```

141     The name of the FITS file to be split.
142
143     Returns
144     -----
145     tuple[astropy.io.fits.HDUList, astropy.io.fits.HDUList]
146         Tuple containing the split O and E beam HDULists.
147
148     """
149     # Create empty HDUList
150     o_beam = pyfits.HDUList()
151     e_beam = pyfits.HDUList()
152
153     # Open file and split O & E beams
154     with pyfits.open(file) as hdul:
155         o_beam.append(hdul["PRIMARY"].copy())
156         e_beam.append(hdul["PRIMARY"].copy())
157
158     # Split specific extention
159     raw_split = self.split_ext(hdul, "SCI")
160
161     # o_beam[0].data = raw_split['SCI'].data[1]
162     # e_beam[0].data = raw_split['SCI'].data[0]
163     o_beam[0].data, e_beam[0].data = self.crop_file(raw_split)
164
165     # Handle prefix and names
166     pref = "arc" if file == self.arc else "beam"
167     o_name = self.save_prefix[pref][0] + file.name[-9:]
168     e_name = self.save_prefix[pref][1] + file.name[-9:]
169
170     # Add split data to O & E beam lists
171     self.update_beam_lists(o_name, e_name, pref == "arc")
172
173     # Handle don't save case
174     if self.save_prefix is None:
175         return o_beam, e_beam
176
177     # Handle save case
178     o_beam.writeto(o_name, overwrite=True)
179     e_beam.writeto(e_name, overwrite=True)
180
181     return o_beam, e_beam
182
183     # MARK: Split extensions
184     def split_ext(
185         self,
186         hdulist: pyfits.HDUList,
187         ext: str = "SCI"
188     ) -> pyfits.HDUList:
189         """
190             Split the data of the specified extension of `hdulist` into
191             its 'O'- and 'E'- beams.
192
193             Parameters
194             -----
195             hdulist : astropy.io.fits.HDUList
196                 The FITS HDUList to be split.
197             ext : str, optional
198                 The name of the extension to be split.
199                 (Defaults to 'SCI')
200
201             Returns
202             -----
203             astropy.io.fits.HDUList
204                 The HDUList with the split applied.
205
206             """
207             hdu = deepcopy(hdulist)
208             rows, cols = hdu[ext].data.shape
209
210             # if odd number of rows, strip off the last one
211             rows = int(rows / 2) * 2
212
213             # how far split is from center of detector

```

```

214     offset = int(self.split_row - rows / 2)
215
216     # split arc into o/e images
217     ind_rc = np.indices((rows, cols))[0]
218     padbins = (ind_rc < offset) | (ind_rc > rows + offset)
219
220     # Roll split_row to be centre row
221     image_rc = np.roll(hdu[ext].data[:rows, :], -offset, axis=0)
222     image_rc[padbins] = 0.0
223
224     # Split columns equally
225     hdu[ext].data = image_rc.reshape((2, int(rows / 2), cols))
226
227     return hdu
228
229 # MARK: Crop files
230 @staticmethod
231 def crop_file(
232     hdulist: pyfits.HDUList,
233     crop: int = CROP_DEFAULT
234 ) -> tuple[np.ndarray, np.ndarray]:
235     """
236         Crop the data with respect to the `O`/`E` beam.
237
238     Parameters
239     -----
240     hdulist : astropy.io.fits.HDUList
241         The HDUList containing the data to be cropped.
242     crop : int, optional
243         The number of rows to be cropped from the bottom and top
244         of the `O` and `E` beam, respectively.
245         (Defaults to 40)
246
247     Returns
248     -----
249     tuple[numpy.ndarray, np.ndarray]
250         Tuple containing the cropped O and E beam data arrays.
251
252     """
253     o_data = hdulist["SCI"].data[1, 0:-crop]
254     e_data = hdulist["SCI"].data[0, crop:]
255
256     return o_data, e_data
257
258 # MARK: Update beam lists
259 def update_beam_lists(
260     self,
261     o_name,
262     e_name,
263     arc: bool = True
264 ) -> None:
265     """
266         Update the `o_files` and `e_files` attributes.
267
268     Parameters
269     -----
270     o_name : str
271         The filename of the O beam.
272     e_name : str
273         The filename of the E beam.
274     arc : bool, optional
275         Indicates whether the first entry should be the arc frame.
276         (Defaults to True)
277
278     Returns
279     -----
280     None
281
282     """
283     if arc:
284         self.o_files.insert(0, o_name)
285         self.e_files.insert(0, e_name)
286     else:

```

```
287         self.o_files.append(o_name)
288         self.e_files.append(e_name)
289
290     return
291
292 # MARK: Save beam lists
293 def save_beam_lists(self, file_suffix: str = 'frames') -> None:
294     with open(f"o_{file_suffix}", "w+") as f_o, \
295             open(f"e_{file_suffix}", "w+") as f_e:
296         for i, j in zip(self.o_files, self.e_files):
297             f_o.write(i + "\n")
298             f_e.write(j + "\n")
299
300     return
301
302 # MARK: Process all Listed Images
303 def process(self) -> None:
304     """
305     Process all FITS images stored in the `fits_list` attribute
306
307     Returns
308     -----
309     None
310
311     """
312     for target in self.fits_list:
313         logging.debug(f"Processing {target}")
314         self.split_file(target)
315
316     self.save_beam_lists()
317
318     return
319
320
321 # MARK: Main function
322 def main(argv) -> None:
323     """Main function."""
324
325     return
326
327
328 if __name__ == "__main__":
329     main(sys.argv[1:])
```

**Listing B.3:** The source code for `join.py`

```

1 #!/usr/bin/env python3
2 # -*- coding: utf-8 -*-
3
4 """
5 Module for joining the split FITS files with an external wavelength solution.
6 """
7
8 # MARK: Imports
9 import os
10 import sys
11 import logging
12 import re
13 from pathlib import Path
14
15 import numpy as np
16 from numpy.polynomial.chebyshev import chebgrid2d as chebgrid2d
17 from numpy.polynomial.legendre import leggrid2d as leggrid2d
18 from astropy.io import fits as pyfits
19
20 # from lacosmic import lacosmic # Replaced: ccdproc is ~6x faster
21 from ccdproc import cosmicray_lacosmic as lacosmic
22
23 from STOPS.utils.specpolpy3 import read_wollaston, split_sci
24 from STOPS.utils.SharedUtils import find_files, find_arc
25 from STOPS.utils.Constants import DATADIR, SAVE_PREFIX, SPLIT_ROW, CR_PARAMS
26
27
28 # MARK: Join Class
29 class Join:
30
31     #-----join0-----
32
33     """
34     The `Join` class allows for the joining of previously split files and the
35     appending of an external wavelength solution in the `polsalt` FITS file format.
36
37     Parameters
38     -----
39     data_dir : str / Path
40         The path to the data to be joined
41     database : str, optional
42         The name of the `IRAF` database folder.
43         (The default is "database")
44     fits_list : list[str], optional
45         A list of pre-reduced `polsalt` FITS files to be joined within `data_dir`.
46         (The default is ``None``, `Join` will search for `mxbp*.fits` files)
47     solutions_list: list[str], optional
48         A list of solution filenames from which the wavelength solution is created.
49         (The default is ``None``, `Join` will search for `fc*` files within the
49         ↪ database` directory)
50     split_row : int, optional
51         The row along which the data of each extension in the FITS file was split.
52         Necessary when Joining cropped files.
53         (The default is 517, the SALT RSS CCD's middle row)
54     save_prefix : dict[str, list[str]], optional
55         The prefix with which the previously split `O`- & `E`-beams were saved.
56         Used for detecting if cropping was applied during the splitting procedure.
57         (The default is SAVE_PREFIX (See Notes))
58     verbose : int, optional
59         The level of verbosity to use for the Cosmic ray rejection
60         (The default is 30, I.E. logging.INFO)
61
62     Attributes
63     -----
64     fc_files : list[str]
65         Valid solutions found from `solutions_list`.
66     custom : bool
67         Internal flag for whether `solutions_list` uses the `IRAF` or a custom format.
68         See Notes for custom solution formatting.
69         (Default (inherited from `solutions_list`) is False)
70     arc : str

```

```

71     Deprecated. Name of arc FITS file within `data_dir`.
72     data_dir
73     database
74     fits_list
75     split_row
76     save_prefix
77
78
79     Methods
80     -----
81     get_solutions(wavlist: list | None, prefix: str = "fc") -> (fc_files, custom):
82         tuple[list[str], bool]
83             Parse `solutions_list` and return valid solution files and if they are
84             non-`IRAF` solutions.
85     parse_solution(fc_file: str, x_shape: int, y_shape: int) -> tuple[dict[str, int],
86         np.ndarray]
87         Loads the wavelength solution file and parses keywords necessary for creating
88         the wavelength extension.
89     join_file(file: os.PathLike) -> None
90         Joins the files,
91         attaches the wavelength solutions,
92         performs cosmic ray cleaning,
93         masks the extension,
94         and checks cropping performed in `Split`.
95         Writes the FITS file in a `polsalt` valid format.
96     check_crop(hdu: pyfits.HDUList, o_file: str, e_file: str) -> int
97         Opens the split `O`- and `E`-beam FITS files and returns the amount of cropping
98         that was performed.
99     process() -> None
100        Calls `join_file` on each file in `fits_list` for automation.
101
102
103     Other Parameters
104     -----
105     no_arc : bool, optional
106         Deprecated. Decides whether the arc frames should be processed.
107         (The default is False, `polsalt` has no use for the arc after wavelength
108         calibrations)
109     **kwargs : dict
110         keyword arguments. Allows for passing unpacked dictionary to the class
111         constructor.
112
113     Notes
114     -----
115     Constants Imported (See utils.Constants):
116         DATADIR, SAVE_PREFIX, SPLIT_ROW, CR_PARAMS
117
118     Custom wavelength solutions must be formatted containing:
119         `x`, `y`, *coefficients...
120     where a solution are of order (`x` by `y`) and must contain  $x \times y$  coefficients,
121     all separated by newlines. The name of the custom wavelength solution file
122     must contain either "cheb" or "leg" for Chebyshev or Legendre
123     wavelength solutions, respectively.
124
125     Cosmic ray rejection is performed using lacosmic [1]_ implemented in ccdproc via
126     astroscreappy [2]_.
127
128     References
129     -----
130     .. [1] van Dokkum 2001, PASP, 113, 789, 1420 (article :
131         <https://adsabs.harvard.edu/abs/2001PASP..113.1420V>
132     .. [2] https://zenodo.org/records/1482019
133
134     """
135
136     #-----join1-----
137
138     # MARK: Join init
139     def __init__(self,
140                  data_dir: Path,
141                  database: str = "database",
142                  fits_list: list[str] = None,
143

```

```

135     solutions_list: list[Path] = None,
136     split_row: int = SPLIT_ROW,
137     no_arc: bool = True,
138     save_prefix: Path | None = None,
139     verbose: int = 30,
140     **kwargs,
141 ) -> None:
142     self.data_dir = data_dir
143     self.database = Path(data_dir) / database
144     self.fits_list = find_files(
145         data_dir=self.data_dir,
146         filenames=fits_list,
147         prefix="mxgbp",
148         ext="fits",
149     )
150     self.fc_files, self.custom = self.get_solutions(solutions_list)
151     self.split_row = split_row
152     self.save_prefix = SAVE_PREFIX
153     if isinstance(save_prefix, dict):
154         self.save_prefix = save_prefix
155
156     self.no_arc = no_arc
157     self.arc = find_arc(self.fits_list)
158
159     self.verbose = verbose < 30
160
161     logging.debug("__init__ - \n", self.__dict__)
162
163
164 # MARK: Find 2D WAV Functions
165 def get_solutions(
166     self,
167     wavlist: list[str] | None,
168     prefix: str = "fc",
169     reverse: bool = False,
170 ) -> tuple[list[str], bool]:
171     """
172     Get the list of wavelength solution files.
173
174     Parameters
175     -----
176     wavlist : list[str] | None
177         A list of custom wavelength solutions files.
178         If ``None``, `Join` will search for wavelength solutions
179         in the `database` directory.
180     prefix : str, optional
181         The prefix of the wavelength solution files.
182         (Defaults to "fc")
183     reverse : bool, optional
184         Whether to reverse the wavelength solution files.
185         Necessary when `wavlist` ordered ['O', 'E']
186         (Defaults to False)
187
188     Returns
189     -----
190     tuple[list[str], bool]
191         A tuple containing the list of wavelength solutions files and
192         a boolean indicating whether custom solutions were provided.
193
194     """
195     # No custom solutions
196     if not wavlist:
197         # Handle finding solutions
198         ws = []
199         for fl in os.listdir(self.database):
200             if os.path.isfile(self.database / fl) and (prefix == fl[0:len(prefix)]):
201                 ws.append(fl)
202
203         if len(ws) != 2:
204             # Handle incorrect number of solutions found
205             msg = (
206                 f"Incorrect amount of wavelength solutions "
207                 f"({len(ws)} fc... files) found in the solution "

```

```

208             f"dir.: {self.database}"
209         )
210         logging.error(msg)
211         raise FileNotFoundError(msg)
212
213     sols = {
214         i: j for i, j in zip(['0', 'E'], sorted(ws, reverse=reverse))
215     }
216     logging.debug(f"get_solutions - Found {sols} in {self.database}")
217
218     return sorted(ws, reverse=reverse), False
219
220     # Custom solution
221     if len(wavlist) >= 2:
222         if len(wavlist) > 2:
223             logging.warning(f" Too many solutions, only {wavlist[:2]} are
224             ↪ considered")
225             wavlist = wavlist[:2]
226
227         for fl in wavlist:
228             if not os.path.isfile(os.path.join(self.data_dir, fl)):
229                 msg = (
230                     f"{fl} not found in the "
231                     f"data directory {self.data_dir}"
232                 )
233                 logging.error(msg)
234                 raise FileNotFoundError(msg)
235
236         sols = {
237             i: j for i, j in zip(['0', 'E'], sorted(wavlist, reverse=reverse))
238         }
239         logging.debug(f"get_solutions - Found {sols} in {self.database}")
240
241     return sorted(wavlist, reverse=reverse), True
242
243     # MARK: Parse 2D WAV Function
244     def parse_solution(
245         self,
246         fc_file: str,
247         x_shape: int,
248         y_shape: int
249     ) -> tuple[dict[str, int], np.ndarray]:
250         """
251             Parse the 2D wavelength solution function from `fc_file`.
252
253             Parameters
254             -----
255             fc_file : str
256                 The filename of the wavelength solutions file.
257             x_shape : int
258                 The x-order of the 2D solution.
259             y_shape : int
260                 The y-order of the 2D solution.
261
262             Returns
263             -----
264             tuple[dict[str, int], np.ndarray]
265                 A tuple containing a dictionary of
266                 the parameters of the solution function
267                 and the function coefficients.
268
269             fit_params = {}
270
271             if self.custom:
272                 # Load coefficients
273                 coeff = np.loadtxt(fc_file)
274
275                 fit_params["xorder"] = int(coeff[0].astype(int))
276                 fit_params["yorder"] = int(coeff[1].astype(int))
277                 coeff = coeff[2:]
278
279             f_type = 3

```

```

280         if "cheb" in str(fc_file):
281             f_type = 1
282         elif "leg" in str(fc_file):
283             f_type = 2
284         fit_params["function"] = f_type
285
286         fit_params["xmin"], fit_params["xmax"] = 1, x_shape
287         fit_params["ymin"], fit_params["ymax"] = 1, y_shape
288
289     else:
290         # Parse IRAF fc database files
291         file_contents = []
292         with open(self.database / fc_file) as fcfile:
293             for i in fcfile:
294                 file_contents.append(re.sub(r"\n\t\s*", "", i))
295
296         if file_contents[9] != "1.": # xterms - Cross-term type
297             msg = (
298                 "Cross-term not recognised (always 1 for "
299                 "'FITCOORDS'), redo FITCOORDS or change manually."
300             )
301             raise Exception(msg)
302
303         fit_params["function"] = int(file_contents[6][-1])
304
305         fit_params["xorder"] = round(float(file_contents[7][-1]), None)
306         fit_params["yorder"] = round(float(file_contents[8][-1]), None)
307
308         fit_params["xmin"] = int(file_contents[10][-1])
309         fit_params["xmax"] = x_shape
310         # int(file_contents[11][-1])# stretch fit over x
311         fit_params["ymin"] = int(file_contents[12][-1])
312         fit_params["ymax"] = y_shape
313         # int(file_contents[13][-1])# stretch fit over y
314
315         coeff = np.array(file_contents[14:], dtype=float)
316
317         coeff = np.reshape(
318             coeff,
319             (fit_params["xorder"], fit_params["yorder"]))
320
321     return fit_params, coeff
322
323
324 # MARK: Join Files
325 def join_file(self, file: os.PathLike) -> None:
326     """
327     Join the `O`- and `E`-beams, attach the wavelength solutions,
328     perform cosmic ray cleaning, mask the extensions,
329     and checks cropping performed by `Split`.
330     Write the FITS file in a `polsalt` valid format.
331
332     Parameters
333     -----
334     file : os.PathLike
335         The path of the FITS file to be joined.
336
337     See Also
338     -----
339     IRAF - `fitcoords` task
340         https://iraf.net/irafdocs/formats/fitcoords.php,
341     numpy 2D grid functions
342         https://numpy.org/doc/stable/reference/generated/numpy.polynomial.chebyshev.chebgrid2d.html,
343         https://numpy.org/doc/stable/reference/generated/numpy.polynomial.legendre.leggrid2d.html
344
345     """
346
347     # Create empty wavelength appended hdu list
348     whdu = pyfits.HDUList()
349
350     # Handle prefix and names
351     pref = "arc" if file == self.arc else "beam"
352     o_file = self.save_prefix[pref][0] + file.name[-9:]

```

```

353     e_file = self.save_prefix[pref][1] + file.name[-9:]
354
355     # Open file
356     with pyfits.open(file) as hdu:
357         # Check if file has been cropped
358         cropsize = self.check_crop(hdu, o_file, e_file)
359
360         y_shape = int(hdu["SCI"].data.shape[0] / 2) - cropsize
361         x_shape = hdu["SCI"].data.shape[1]
362
363         # No differences in "PRIMARY" extention header
364         primary_ext = hdu["PRIMARY"]
365         primary_ext.header["HISTORY"] = f"CRCLEAN: {CR_PARAMS}"
366         whdu.append(primary_ext)
367
368         for ext in ["SCI", "VAR", "BPM"]:
369             whdu.append(pyfits.ImageHDU(name=ext))
370             whdu[ext].header = hdu[ext].header.copy()
371             whdu[ext].header["CTYPE3"] = "O,E"
372
373             # Create empty extentions with correct order and format
374             if ext == "BPM":
375                 whdu[ext].data = np.zeros(
376                     (2, y_shape, x_shape),
377                     dtype="uint8"
378                 )
379                 whdu[ext].header["BITPIX"] = "-uint8"
380             else:
381                 whdu[ext].data = np.zeros(
382                     (2, y_shape, x_shape),
383                     dtype=">f4"
384                 )
385                 whdu[ext].header["BITPIX"] = "-32"
386
387             # Fill in empty extentions
388             if cropsize:
389                 temp_split = split_sci(
390                     hdu,
391                     self.split_row,
392                     ext=ext
393                 )[ext].data
394                 whdu[ext].data[0] = temp_split[0, cropsize:]
395                 whdu[ext].data[1] = temp_split[1, 0:-cropsize]
396
397             else:
398                 whdu[ext].data = split_sci(
399                     hdu,
400                     self.split_row,
401                     ext=ext
402                 )[ext].data
403             # End of hdu calls, close hdu
404
405             # MARK: Join (Wav. Ext.)
406             whdu.append(pyfits.ImageHDU(name="WAV"))
407             wav_header = whdu["SCI"].header.copy()
408             wav_header["EXTNAME"] = "WAV"
409             wav_header["CTYPE3"] = "O,E"
410             whdu["WAV"].header = wav_header
411
412             whdu["WAV"].data = np.zeros(
413                 whdu["SCI"].data.shape,
414                 dtype=">f4"
415             )
416
417             for num, fname in enumerate(self.fc_files):
418                 params, coeffs = self.parse_solution(
419                     fname,
420                     x_shape,
421                     y_shape
422                 )
423
424                 if params["function"] == 1: # Function type (1 = chebyshev)
425                     # Set wavelength extention values to function

```

```

426         whdu["WAV"].data[num] = chebgrid2d(
427             x=np.linspace(-1, 1, params["ymax"]),
428             y=np.linspace(-1, 1, params["xmax"]),
429             c=coeffs,
430         )
431
432     elif params["function"] == 2: # Function type (2 = legendre)
433         # Set wavelength extention values to function
434         whdu["WAV"].data[num] = leggrid2d(
435             x=np.linspace(-1, 1, params["ymax"]),
436             y=np.linspace(-1, 1, params["xmax"]),
437             c=coeffs,
438         )
439
440     else:
441         msg = (
442             "Function type not recognised, please wavelength "
443             "calibrate using either Chebyshev or Legendre."
444         )
445         raise Exception(msg)
446
447     # MARK: Cosmic Ray Cleaning
448     # See utils.Constants for `CR_PARAMS` discussion
449     whdu["SCI"].data[num] = lacosmic(
450         whdu["SCI"].data[num],
451         # contrast=CR_PARAMS['CR_CONTRAST'],
452         # threshold=CR_PARAMS['CR_THRESHOLD'],
453         # neighbor_threshold=CR_PARAMS['CR_NEIGH_THRESH'],
454         # effective_gain=CR_PARAMS['GAIN'],
455         # background=CR_PARAMS['BACKGROUND'],
456         readnoise=CR_PARAMS['READNOISE'],
457         gain=CR_PARAMS['GAIN'],
458         verbose=self.verbose,
459     )[0]
460
461     # MARK: WAV masking
462     # Left & Right Crop
463     whdu["WAV"].data[whdu["WAV"].data[:] < 3_000] = 0.0
464     whdu["WAV"].data[whdu["WAV"].data[:] >= 10_000] = 0.0
465
466     # Top & Bottom Crop (shift\tilt)
467     rpix_oc, cols, rbin, lam_c = read_wollaston(
468         whdu,
469         DATADIR + "wollaston.txt"
470     )
471
472     drow_oc = (rpix_oc - rpix_oc[:, int(cols / 2)][:, None]) / rbin
473
474     # Cropping as suggested
475     for c, col in enumerate(drow_oc[0]):
476         if np.isnan(col):
477             continue
478
479         if int(col) < 0:
480             whdu["WAV"].data[0, int(col):, c] = 0.0
481         elif int(col) > cropsize:
482             whdu["WAV"].data[0, 0: int(col) - cropsize, c] = 0.0
483
484     for c, col in enumerate(drow_oc[1]):
485         if np.isnan(col):
486             continue
487
488         if int(col) > 0:
489             whdu["WAV"].data[1, 0: int(col), c] = 0.0
490         elif (int(col) < 0) & (abs(int(col)) > cropsize):
491             whdu["WAV"].data[1, int(col) + cropsize:, c] = 0.0
492
493     # MARK: BPM masking
494     whdu["BPM"].data[0] = np.where(
495         whdu["WAV"].data[0] == 0,
496         1,
497         whdu["BPM"].data[0]
498     )

```

```

499     whdu["BPM"].data[1] = np.where(
500         whdu["WAV"].data[1] == 0,
501         1,
502         whdu["BPM"].data[1]
503     )
504
505     whdu.writeto(f"w{os.path.basename(file)}", overwrite="True")
506
507     return
508
509 # MARK: Check Crop
510 @staticmethod
511 def check_crop(
512     hdu: pyfits.HDUList,
513     o_file: str,
514     e_file: str
515 ) -> int:
516     """
517     Check if cropping is necessary when joining `O`- and `E`-beams.
518
519     Parameters
520     -----
521     hdu : astropy.io.fits.HDUList
522         The HDUList to check for cropping.
523     o_file : str
524         The name of the previously split `O`-beam FITS file.
525     e_file : str
526         The name of the previously split `E`-beam FITS file.
527
528     Returns
529     -----
530     int
531         The number of rows which were cropped by `Split`.
532
533     """
534     cropsize = 0
535
536     with pyfits.open(o_file) as o, \
537         pyfits.open(e_file) as e:
538         o_y = o[0].data.shape[0]
539         e_y = e[0].data.shape[0]
540
541     if hdu["SCI"].data.shape[0] != (o_y + e_y):
542         # Get crop size, assuming crop same on both sides
543         cropsize = int((hdu["SCI"].data.shape[0] - o_y - e_y) / 2)
544
545     return cropsize
546
547 # MARK: Process all Listed Images
548 def process(self) -> None:
549     """
550     Process all FITS images stored in the `fits_list` attribute
551     """
552     for target in self.fits_list:
553         logging.debug(f"Processing {target}")
554         self.join_file(target)
555
556
557 def main(argv) -> None:
558     """
559     Main function.
560     """
561
562
563 if __name__ == "__main__":
564     main(sys.argv[1:])

```

Listing B.4: The source code for `cross_correlate.py`

```

1 #!/usr/bin/env python3
2 # -*- coding: utf-8 -*-
3
4 """Module for cross correlating polarization beams."""
5
6 # MARK: Imports
7 import sys
8 import logging
9 import itertools as iters
10 from pathlib import Path
11 from importlib.resources import files
12 from typing import Callable
13
14 import numpy as np
15 from numpy.polynomial import chebyshev
16 import matplotlib.pyplot as plt
17 import matplotlib.axes
18 from astropy.io import fits as pyfits
19 from scipy import signal
20
21 from STOPS.utils.SharedUtils import find_files, continuum
22 from STOPS.utils.Constants import SAVE_CORR, OFFSET
23 import STOPS.utils
24
25 mpl_logger = logging.getLogger('matplotlib')
26 mpl_logger.setLevel(logging.INFO)
27
28
29 # MARK: Correlate class
30 class CrossCorrelate:
31
32     #-----corr0-----
33
34     """
35     Cross correlate allows for comparing the extensions of multiple
36     FITS files, or comparing the O and E beams of a single FITS file.
37
38     Parameters
39     -----
40     data_dir : str / Path
41         The path to the data to be cross correlated
42     filenames : list[str]
43         The ecwmxgbp*.fits files to be cross correlated.
44         If only one filename is defined, correlation is done against the two
45         ↪ polarization beams.
46     split_ccd : bool, optional
47         Decides whether the CCD regions should each be individually cross correlated.
48         (The default is True, which splits the spectrum up into its separate CCD regions)
49     cont_ord : int, optional
50         The degree of a chebyshev to fit to the continuum.
51         (The default is 11)
52     plot : bool, optional
53         Decides whether the continuum fitting should be plotted
54         (The default is False, so no continua plots are displayed)
55     save_prefix : str, optional
56         The name or directory to save the figure produced to.
57         "." saves a default name to the current working. A default name is also used
58         ↪ when save_prefix is a directory.
59         (The default is None, I.E. The figure is not saved, only displayed)
60
61     Attributes
62     -----
63     data_dir
64     fits_list
65     beams : str
66         The mode of correlation.
67         'OE' for same file, and 'O' or 'E' for different files but same extension.
68     ccds : int
69         The number of CCD's in the data. Used to split the CCD's if split_ccd is True.
70     cont_ord : int
71         The degree of the chebyshev to fit to the continuum.

```

```

70     can_plot : bool
71         Decides whether the continuum fitting should be plotted
72     offset : int
73         The amount the spectrum is shifted, mainly to test the effect of the cross
74         ↵ correlation
75         (The default is 0, I.E. no offset introduced)
76     save_prefix
77     wav_unit : str
78         The units of the wavelength axis.
79         (The default is Angstroms)
80     wav_cdelt : int
81         The wavelength increment.
82         (The default is 1)
83     alt : Callable
84         An alternate method of cross correlating the data.
85         (The default is None)

86     Methods
87     -----
88     load_file(filename: Path) -> tuple[np.ndarray, np.ndarray, np.ndarray]
89         Loads the data from a FITS file.
90     get_bounds(bpm: np.ndarray) -> np.ndarray
91         Finds the bounds for the CCD regions.
92     remove_cont(spec: list, wav: list, bpm: list, plot_cont: bool) -> None
93         Removes the continuum from the data.
94     correlate(filename1: Path, filename2: Path | None = None) -> None
95         Cross correlates the data.
96     ftcs(filename1: Path, filename2: Path | None = None) -> None
97         Cross correlates the data using the Fourier Transform.
98     plot(spec, wav, bpm, corrdb, lagsdb) -> None
99         Plots the data.
100    process() -> None
101        Processes the data.

102    Other Parameters
103    -----
104    offset : int, optional
105        The amount the spectrum is shifted, mainly to test the effect of the cross
106        ↵ correlation
107        (The default is 0, I.E. no offset introduced)
108    **kwargs : dict
109        keyword arguments. Allows for passing unpacked dictionary to the class
110        ↵ constructor.
111    ftcs : bool, optional
112        Decides whether the Fourier Transform should be used for cross correlation.

113    See Also
114    -----
115    scipy
116        https://docs.scipy.org/doc/scipy/reference/generated/scipy.signal.correlate.html
117

118    Notes
119    -----
120    Constants Imported (See utils.Constants):
121        SAVE_CORR
122
123    """
124
125    #-----corr1-----
126
127    # MARK: Correlate init
128
129    def __init__(
130        self,
131        data_dir: Path,
132        filenames: list[str],
133        beams: str = "OE",
134        split_ccd: bool = True,
135        cont_ord: int = 11,
136        plot: bool = False,
137        offset: int = 0,
138        save_prefix: Path | None = None,
139

```

```

140         **kwargs,
141     ) -> None:
142         self.data_dir = data_dir
143         self.fits_list = find_files(
144             data_dir=self.data_dir,
145             filenames=filenames,
146             prefix="ecwmxgbp",
147             ext="fits",
148         )
149         self._beams = None
150         self.beams = beams
151         self.ccds = 1
152         if split_ccd:
153             # BPM == 2 near center of CCD if CCD count varies
154             with pyfits.open(self.fits_list[0]) as hdu:
155                 self.ccds = sum(hdu["BPM"].data.sum(axis=1)[0] == 2)
156
157         if self.ccds == 0:
158             self.ccds = 3
159             err_msg = f"BPM ext. of {self.fits_list[0].name} contains no `2` near
160             ↪ center of CCD."
161             logging.warning(err_msg)
162
163         self.cont_ord = cont_ord
164         self.can_plot = plot
165         self.offset = offset
166         if offset != 0:
167             logging.warning("'offset' is only for testing.")
168
169         err_msg = "Offset removed after finalizing testing."
170         logging.error(err_msg)
171         raise ValueError(err_msg)
172         # # Add an offset to the spectra to test cross correlation
173         # self.spec1 = np.insert(
174         #     self.spec1, [0] * offset, self.spec1[:, :offset], axis=-1
175         # )[:, : self.spec1.shape[-1]]
176
177         self.save_prefix = save_prefix
178         # Handle directory save name
179         if self.save_prefix and self.save_prefix.is_dir():
180             self.save_prefix /= SAVE_CORR
181             logging.warning((
182                 f"Correlation save name resolves to a directory. "
183                 f"Saving under {self.save_prefix}"
184             ))
185
186         self.wav_unit = "$\\AA$"
187         self.wav_cdelt = 1
188
189         self.alt = self.ftcs if kwargs.get("ftcs") else None
190
191         logging.debug("__init__ - \n", self.__dict__)
192         return
193
194     # MARK: Beams property
195     @property
196     def beams(self) -> str:
197         return self._beams
198
199     @beams.setter
200     def beams(self, mode: str) -> None:
201         if mode not in ['O', 'E', 'OE']:
202             err_msg = f"Correlation mode '{mode}' not recognized."
203             logging.error(err_msg)
204             raise ValueError(err_msg)
205
206         self._beams = mode
207
208         return
209
210     # MARK: Load file
211     def load_file(
212         self,

```

```

212         filename: Path
213     ) -> tuple[np.ndarray, np.ndarray, np.ndarray]:
214         """
215             Load the data from a FITS file.
216
217         Parameters
218         -----
219         filename : Path
220             The name of the FITS file to load.
221
222         Returns
223         -----
224         tuple[np.ndarray, np.ndarray, np.ndarray]
225             The spectrum, wavelength, and bad pixel mask.
226
227         """
228
229
230     # Open HDU
231     with pyfits.open(filename) as hdul:
232         spec = hdul["SCI"].data.sum(axis=1)
233         wav = (
234             np.arange(spec.shape[-1])
235             * hdul["SCI"].header["CDELT1"]
236             + hdul["SCI"].header["CRVAL1"]
237         )
238         wav = np.array((wav, wav))
239         bpm = hdul["BPM"].data.sum(axis=1)
240
241         self.wav_cdel = float(hdul["SCI"].header["CDELT1"])
242
243         if hdul["SCI"].header["CTYPE1"] != 'Angstroms':
244             self.wav_unit = hdul["SCI"].header["CTYPE1"]
245
246     return spec, wav, bpm
247
248     # MARK: Get bounds
249     def get_bounds(self, bpm: np.ndarray) -> np.ndarray:
250         """
251             Find the bounds for a file based on the CCD count.
252
253         Parameters
254         -----
255         bpm : np.ndarray
256             The bad pixel mask.
257
258         Returns
259         -----
260         np.ndarray
261             The bounds for the CCD regions.
262
263         """
264         # bounds.shape -> (0/E, CCD's, low./up. bound)
265         if self.ccds == 1:
266             return np.array(
267                 [(0, bpm[0].shape[-1]), (0, bpm[1].shape[-1])]
268             ).astype(int)
269
270         bounds = np.zeros((2, self.ccds, 2))
271
272         # Get lower and upper bound for each ccd, save to bounds
273         # Lower -> min is zero, Upper -> max is bpm length
274         for ext, ccd in iter.product(range(2), range(self.ccds)):
275             mid = np.where(bpm[ext] == 2)[0][ccd]
276             ccds = self.ccds * 2
277             bounds[ext, ccd] = (
278                 max(mid - bpm.shape[-1] // ccds, 0),
279                 min(mid + bpm.shape[-1] // ccds, bpm.shape[-1])
280             )
281
282         return bounds.astype(int)
283
284     # MARK: Remove Continua
285     def remove_cont(

```

```

285         self,
286         spec: np.ndarray,
287         wav: np.ndarray,
288         bpm: np.ndarray,
289         plot_cont: bool
290     ) -> np.ndarray:
291         """
292             Remove the continuum from the data.
293
294         Parameters
295         -----
296         spec : np.ndarray
297             The spectrum to remove the continuum from.
298         wav : np.ndarray
299             The wavelength of the spectrum.
300         bpm : np.ndarray
301             The bad pixel mask.
302         plot_cont : bool
303             Decides whether the continuum fitting should be plotted
304
305         Returns
306         -----
307         spec : np.ndarray
308
309         """
310         # Mask out the bad pixels for fitting continua
311         okwav = np.where(bpm != 1)
312
313         # Define continua
314         ctm = continuum(
315             wav[okwav],
316             spec[okwav],
317             deg=self.cont_ord,
318             plot=plot_cont,
319         )
320
321         # Normalise spectra
322         spec /= chebyshev.chebval(wav, ctm)
323         spec -= 1
324
325         return spec
326
327     # MARK: Correlate
328     def correlate(
329         self,
330         filename1: Path,
331         filename2: Path | None = None,
332         alt: Callable = None
333     ) -> tuple[np.ndarray, np.ndarray, np.ndarray, list[list], list[list]]:
334         """
335             Cross correlates the data.
336
337         Parameters
338         -----
339         filename1 : Path
340             The name of the first FITS file to cross correlate.
341         filename2 : Path, optional
342             The name of the second FITS file to cross correlate.
343             (Defaults to None)
344         alt : Callable, optional
345             An alternate method of cross correlating the data.
346             (Defaults to None)
347
348         Returns
349         -----
350         spec, wav, bpm, lagsdb, corrdb: tuple[np.ndarray, np.ndarray, np.ndarray,
351             list[list], list[list]]
352
353         """
354         # mode: 0E -> '01' & 'E1', 0 -> '01' & '02', E -> 'E1' & 'E2'
355         # Load data
356         spec, wav, bpm = self.load_file(filename1)
357         if filename2 and self.beams != '0E':

```

```

357     def unpack(exts, *args):
358         return [arr[exts] for arr in args]
359
360         if self.beams == '0':
361             spec[-1], wav[-1], bpm[-1] = unpack(
362                 0, *self.load_file(filename2)
363             )
364
365         else:
366             spec[0], wav[0], bpm[0] = spec[-1], wav[-1], bpm[-1]
367             spec[-1], wav[-1], bpm[-1] = unpack(
368                 -1, *self.load_file(filename2)
369             )
370
371         bounds = self.get_bounds(bpm)
372
373         logging.debug(
374             f"correlate - data shape:\n{spec/wav/bpm: {spec.shape}}"
375         )
376
377         corrdb = [[] for _ in range(self.ccds)]
378         lagsdb = [[] for _ in range(self.ccds)]
379         for ccd in range(self.ccds):
380             sig = []
381             for ext in range(2):
382                 lb, ub = bounds[ext, ccd]
383
384                 if self.cont_ord > 0:
385                     spec[ext, lb:ub] = self.remove_cont(
386                         spec[ext, lb:ub],
387                         wav[ext, lb:ub],
388                         bpm[ext, lb:ub],
389                         self.can_plot
390                     )
391
392                     # Invert BPM (and account for 2); zero bad pixels
393                     sig.append((
394                         spec[ext, lb:ub]
395                         * abs(bpm[ext, lb:ub].astype(np.int8) * -1 + 1)
396                     ))
397
398                     # Finally(!!!) cross correlate signals and scale max -> 1
399                     corrdb[ccd] = signal.correlate(*sig) if not alt else alt(*sig)
400                     corrdb[ccd] /= np.max(corrdb[ccd])
401                     # noinspection PyTypeChecker
402                     lagsdb[ccd] = signal.correlation_lags(
403                         sig[0].shape[-1],
404                         sig[1].shape[-1]
405                     ) * self.wav_cdelt
406
407         return spec, wav, bpm, corrdb, lagsdb
408
409         # MARK: ftcs alternate
410         def ftcs(
411             self,
412             signal1: np.ndarray,
413             signal2: np.ndarray
414         ) -> np.ndarray:
415             """
416                 Cross correlates the data using the Fourier Transform.
417
418                 Parameters
419                 -----
420                 signal1 : np.ndarray
421                     The first signal to cross correlate.
422                 signal2 : np.ndarray
423                     The second signal to cross correlate.
424
425                 Returns
426                 -----
427                 np.ndarray
428                     The correlation data using the Fourier Transform.
429

```

```

430     """
431     logging.debug(
432         f"ftcs - data shape:\n{tspec.wav/bpm: {signal1.shape}}"
433     )
434
435     # Invert BPM (and account for 2); zero bad pixels
436     ft_spec1 = np.fft.fft(signal1)
437     ft_spec2 = np.fft.fft(signal2)
438
439     if self.can_plot:
440         plt.plot(ft_spec1)
441         plt.plot(ft_spec2)
442         plt.show()
443
444     # Cross correlate signals
445     # ft_spectrum1 * np.conj(ft_spectrum2)
446     corr_entry = signal.correlate(ft_spec1, ft_spec2)
447
448     return np.fft.ifft(corr_entry)
449
450 # MARK: Plot
451 def plot(self, spec, wav, bpm, corrdb, lagsdb) -> None:
452     """
453     Plot the data.
454
455     Parameters
456     -----
457     spec : np.ndarray
458         The spectrum.
459     wav : np.ndarray
460         The wavelength.
461     bpm : np.ndarray
462         The bad pixel mask.
463     corrdb : np.ndarray
464         The cross correlation data.
465     lagsdb : np.ndarray
466         The `lags` data.
467
468     Returns
469     -----
470     None
471
472     """
473     plt.style.use([
474         files(STOPS.utils).joinpath('STOPS.mplstyle'),
475         files(STOPS.utils).joinpath('STOPS_correlate.mplstyle'),
476     ])
477     bounds = self.get_bounds(bpm)
478
479     fig, axs = plt.subplots(2, self.ccds, sharey="row")
480
481     if self.ccds == 1:
482         # Convert axs to a 2D array
483         # noinspection PyTypeChecker
484         axs: np.ndarray[matplotlib.axes.Axes] = np.swapaxes(np.atleast_2d(axs), 0, 1)
485
486     # for ext, ccd in iters.product(range(2), range(self.ccds)):
487
488     for ccd in range(self.ccds):
489         axs[0, ccd].plot(
490             lagsdb[ccd],
491             corrdb[ccd] * 100,
492             color='C4',
493             label=f"max lag @ {lagsdb[ccd][corrdb[ccd].argmax()]} - (bounds[1, ccd, "
494             "0] - bounds[0, ccd, 0])}",
495         )
496
497         for ext in range(2):
498             lb, ub = bounds[ext, ccd]
499             logging.debug(f"fl-{ext}: {wav[ext, lb]}:{wav[ext, ub - 1]}")
500
501             axs[1, ccd].plot(
502                 wav[ext, lb:ub],
503             )

```

```

502     spec[ext, lb:ub]
503     * abs(bpm[ext, lb:ub].astype(np.int8) * -1 + 1)
504     + OFFSET * ext,
505     label=(
506         f"${self.beams} if self.beams != 'OE' else self.beams[{ext}]}"
507         f"_{ext + 1} if self.beams != 'OE' else 1}"
508         f"{' (' + str(OFFSET * ext) + ')') if ext > 0 else ''}"
509     ),
510 )
511
512     axs[0, 0].set_ylabel("Normalised Correlation\n($\\%$)")
513     for ax in axs[1:, 0]:
514         ax.set_ylabel("Normalised Intensity\n(Counts)")
515     xcol = int(self.ccds != 1)
516     axs[0, xcol].set_xlabel(f"Signal Lag ({self.wav_unit})")
517     axs[-1, xcol].set_xlabel(f"Wavelength ({self.wav_unit})")
518     for ax in axs.flatten():
519         leg = ax.legend()
520         leg.set_draggable(True)
521
522     # plt.tight_layout()
523     # fig1 = plt.gcf()
524     # DPI = fig1.get_dpi()
525     # fig1.set_size_inches(700.0/float(DPI), 250.0/float(DPI))
526     plt.show()
527
528     # Handle do not save
529     if not self.save_prefix:
530         return
531
532     # Handle save
533     fig.savefig(fname=self.save_prefix)
534
535     return
536
537 # MARK: Process all listed images
538 def process(self) -> None:
539     """
540     Process the data.
541
542     Returns
543     -----
544     None
545
546     """
547     if self.beams != 'OE' and len(self.fits_list) == 1:
548         # change mode to OE with warning
549         logging.warning((
550             f"`{self.beams}` correlation not possible for "
551             "a single file. correlation `mode` changed to 'OE'."
552         ))
553         self.beams = 'OE'
554
555     # OE `mode` (same file, diff. ext.)
556     if self.beams == 'OE':
557         for fl in self.fits_list:
558             logging.info(f"'OE' correlation of {fl}.")
559             spec, wav, bpm, corr, lags = self.correlate(fl, alt=self.alt)
560             self.plot(spec, wav, bpm, corr, lags)
561
562     return
563
564     # OE `mode` (diff. files, same ext.)
565     for fl1, fl2 in iters.combinations(self.fits_list, 2):
566         logging.info(f"{self.beams} correlation of {fl1} vs {fl2}.")
567         spec, wav, bpm, corr, lags = self.correlate(fl1, fl2, alt=self.alt)
568         self.plot(spec, wav, bpm, corr, lags)
569
570     return
571
572
573 # MARK: Main function
574 def main(argv) -> None:

```

```
575     return
576
577
578 if __name__ == "__main__":
579     main(sys.argv[1:])
```

Listing B.5: The source code for `skylines.py`

```

1 #!/usr/bin/env python3
2 # -*- coding: utf-8 -*-
3
4 """
5 Module for analyzing the sky lines of a wavelength calibrated image.
6 """
7
8 # MARK: Imports
9 import sys
10 import logging
11 from pathlib import Path
12 from importlib.resources import files
13
14 import numpy as np
15 import matplotlib.pyplot as plt
16 import matplotlib.axes
17 from astropy.io import fits as pyfits
18 from scipy import signal
19
20 from STOPS.utils.SharedUtils import find_files, get_arc_lamp
21 from STOPS.utils.Constants import SAVE_SKY, FIND_PEAK_PARAMS
22 import STOPS.data
23 import STOPS.utils
24 import STOPS.data.RSS_arc
25
26 # print(
27 #     [logging.getLogger(name) for name in logging.root.manager.loggerDict]
28 # )
29 mpl_logger = logging.getLogger('matplotlib')
30 mpl_logger.setLevel(logging.INFO)
31 pil_logger = logging.getLogger('PIL')
32 pil_logger.setLevel(logging.INFO)
33
34
35 # MARK: Skylines Class
36 class Skylines:
37
38     #-----sky0-----
39
40     """
41         Class representing the Skylines object.
42
43     Parameters
44     -----
45     data_dir : Path
46         The directory containing the data files.
47     filenames : list[str]
48         The list of filenames to be processed.
49     beam : str, optional
50         The beam mode, by default "0E".
51     plot : bool, optional
52         Flag indicating whether to plot the continuum, by default False.
53     save_prefix : Path / None, optional
54         The prefix for saving the data, by default None.
55     **kwargs
56         Additional keyword arguments.
57
58     Attributes
59     -----
60     data_dir : Path
61         The directory containing the data files.
62     fits_list : list[str]
63         The list of fits file paths.
64     beams : str
65         The beam mode.
66     can_plot : bool
67         Flag indicating whether to plot the continuum.
68     save_prefix : Path / None
69         The prefix for saving the data.
70     wav_unit : str
71         The unit of wavelength.

```

```

72
73     Methods
74     -----
75     checkLoad(self, path1: str) -> np.ndarray:
76         Checks and loads the data from the given path.
77     transform(self, wav_sol: np.ndarray, spec: np.ndarray) -> np.ndarray:
78         Transforms the input wavelength and spectral data based on
79         the given wavelength solution.
80     rmvCont(self) -> np.ndarray:
81         Removes the continuum from the spectrum.
82     process(self) -> None:
83         Placeholder method for processing the data.
84     """
85
86     #-----sky1-----
87
88     # MARK: Skylines init
89     def __init__(self,
90                  data_dir: Path,
91                  filenames: list[str],
92                  beams: str = "OE",
93                  split_ccd: bool = False,
94                  cont_ord: int = 11,
95                  plot: bool = False,
96                  transform: bool = True,
97                  save_prefix: Path | None = None,
98                  **kwargs,
99                  ) -> None:
100        self.data_dir = data_dir
101        self.fits_list, self.arc_list = find_files(
102            data_dir=self.data_dir,
103            filenames=filenames,
104            prefix="wmxgbp", # t[o/e]beam
105            ext="fits",
106            sep_arc=True,
107        )
108        if self.arc_list:
109            self.arc_lamp = get_arc_lamp(self.arc_list[0])
110
111        self._beams = None
112        self.beams = beams
113        self.ccds = 1
114        if split_ccd:
115            # See cross_correlate for initial implementation
116            self.ccds = 3
117
118        self.cont_ord = cont_ord
119        self.can_plot = plot
120        self.must_transform = transform
121
122        self.save_prefix = save_prefix
123        # Handle directory save name
124        if self.save_prefix and self.save_prefix.is_dir():
125            self.save_prefix /= SAVE_SKY
126            logging.warning((
127                f"Skylines save name resolves to a directory. "
128                f"Saving under {self.save_prefix}"
129            ))
130
131        self.max_difference = 5
132
133        self.wav_unit = "$\\AA$"
134
135        logging.debug("__init__ - \n", self.__dict__)
136
137        return
138
139    # MARK: Beams property
140    @property
141    def beams(self) -> str:
142        return self._beams
143
144

```

```

145     @beams.setter
146     def beams(self, mode: str) -> None:
147         if mode not in ['0', 'E', 'OE']:
148             err_msg = f"Correlation mode '{mode}' not recognized."
149             logging.error(err_msg)
150             raise ValueError(err_msg)
151
152         self._beams = mode
153
154     return
155
156 # MARK: Find Peaks
157 def find_peaks(
158     self,
159     spec: np.ndarray,
160     axis: int | None = None,
161     min_height: float = 0.5,
162     **kwargs,
163 ) -> tuple[list[np.ndarray], list[dict]]:
164     """
165     Finds the peaks in the given spectral data.
166
167     Parameters
168     -----
169     spec : np.ndarray
170         The spectral data.
171     axis: int / None, optional
172         The axis along which the peaks are found.
173     min_height : float, optional
174         The minimum height of the peaks, by default 0.5.
175
176     Returns
177     -----
178     peaks, properties : tuple[list[np.ndarray], list[dict]]
179         The peaks and their properties.
180
181     """
182     peaks = []
183     props = []
184     row_means = []
185
186     for ext in range(len(self.beams)):
187         row_mean = spec[ext] if axis is None else np.mean(spec[ext], axis=axis)
188
189         peak, prop = signal.find_peaks(
190             row_mean,
191             prominence=min_height * np.max(row_mean),
192             width=0,
193             **kwargs,
194         )
195         peaks.append(peak)
196         props.append(prop)
197         row_means.append(row_mean)
198
199     if self.can_plot:
200         fig, axs = plt.subplots(2, 1)
201         for ext in range(len(self.beams)):
202             axs[ext].plot(
203                 row_means[ext],
204                 label=f"'E' if ext else '0'")
205             )
206             axs[ext].plot(
207                 peaks[ext],
208                 row_means[ext][peaks[ext]],
209                 "x",
210                 label=f"'E' if ext else '0'" peaks"
211             )
212             axs[ext].legend()
213             plt.show()
214
215     logging.debug(f"find_peaks - peaks: {[len(i) for i in peaks]}")
216     logging.debug(f"find_peaks - props: {[key for key in props[0].keys()]}")
217

```

```

218     return peaks, props
219
220     # MARK: Min. of Diff. Matrix
221     @staticmethod
222     def min_diff_matrix(
223         a: np.ndarray,
224         b: np.ndarray,
225         max_diff: int = 100
226     ) -> tuple[np.ndarray, np.ndarray, np.ndarray]:
227         """
228             Find the minimum difference between the elements of two arrays.
229
230             Parameters
231             -----
232             a : np.ndarray
233                 The first 1d array.
234             b : np.ndarray
235                 The second 1d array.
236             max_diff : int, optional
237                 The maximum difference allowed, by default 100.
238
239             Returns
240             -----
241             a : np.ndarray (len(a))
242                 The elements of the first array.
243             min_vals : np.ndarray (len(a))
244                 The minimum difference between the elements of the two arrays.
245             min_idxs : np.ndarray (len(a))
246                 The indices of the minimum difference between
247                 the elements of the two arrays.
248
249         """
250         # Compute the difference matrix using transpose
251         diff = a - b[:, np.newaxis]
252
253         # Find the minimum value in each row (A) of `diff`
254         min_idxs = np.abs(diff).argmin(axis=0)
255         print(min_idxs.shape, diff.shape)
256         min_vals = np.array([diff[j, i] for i, j in enumerate(min_idxs)])
257         # TODO: Recalculate min_val after selecting best min_val and
258         # TODO: removing the corresponding row/column
259
260         logging.debug(f"min_diff_matrix - min_vals: {np.round(min_vals, 2)}")
261         logging.debug(f"min_diff_matrix - min_idxs: {min_idxs}")
262
263         max_mask = (min_vals <= max_diff) & (min_vals >= -1 * max_diff)
264
265         return a[max_mask], min_vals[max_mask], min_idxs[max_mask]
266
267     # MARK: Load File Data
268     def load_file_data(
269         self,
270         filename: Path
271     ) -> tuple[np.ndarray, np.ndarray, np.ndarray]:
272         """
273             Loads the data from the given file.
274
275             Parameters
276             -----
277             filename : Path
278                 The path to the file to be loaded.
279
280             Returns
281             -----
282             spec, wav, bpm : tuple[np.ndarray, np.ndarray, np.ndarray]
283                 The wavelength, spectral, and bad pixel mask data.
284
285         """
286         # Load data from self.beams extension
287         with pyfits.open(filename) as hdul:
288             exts = [0, 1] if len(self.beams) == 2 else 0 + int(self.beams == 'E')
289             spec2d = np.atleast_3d(hdul["SCI"].data[exts])
290             wav2d = np.atleast_3d(hdul["WAV"].data[exts])

```

```

291         bpm2d = np.atleast_3d(hdul["BPM"].data[exts].astype(bool))
292
293     logging.info(
294         f"load_file_data - {filename.name} - shape: {spec2d.shape}"
295     )
296
297     return spec2d, wav2d, bpm2d
298
299 # MARK: Load Sky or Arc Lines
300 @staticmethod
301 def load_lines(
302     filename: str | Path | None = None,
303     dtype: list[tuple] = [('wav', float), ('flux', float)],
304     skip_header: int = 3,
305     skip_footer: int = 1
306 ) -> np.ndarray:
307     """
308         Loads the sky or arc lines from the given file.
309
310     Parameters
311     -----
312     filename : str / Path / None, optional
313         The path to the file to be loaded.
314         Defaults to loading the skylines from `data/sky.salt`.
315     dtype : list[tuple], optional
316         The data type of the sky lines.
317         (Default is [('wav', float), ('flux', float)])
318     skip_header : int, optional
319         The amount of lines to skip of the `filenames` header.
320         (Default is 3)
321     skip_footer : int, optional
322         The amount of lines to skip of the `filename`'s footer.
323         (Default is 1)
324
325     Returns
326     -----
327     sky_lines : np.ndarray['wav', 'flux']
328         The sky lines from the file.
329
330     """
331     lines: np.ndarray = None
332
333     usecols = None
334     if filename:
335         filename = files(STOPS.data.RSS_arc).joinpath(filename)
336         usecols = (0, 1)
337     else:
338         filename = files(STOPS.data).joinpath('sky.salt')
339
340     lines = np.genfromtxt(
341         filename,
342         dtype=dtype,
343         skip_header=skip_header,
344         skip_footer=skip_footer,
345         usecols=usecols
346     )
347
348     logging.debug(
349         f"load_lines - {filename.name} - shape: {lines.shape}"
350     )
351
352     return lines
353
354 # MARK: Mask Traces
355 def mask_traces(
356     self,
357     spec: np.ndarray,
358     bpm: np.ndarray,
359     max_traces: int = 1,
360     tr_pad: int = 5,
361     bg_margin: int = 10,
362     lr_margins: list[int] = [10, 10],
363     h_min: float = 0.5,

```

```

364         h_rel: float = 1 - 0.05,
365     ) -> np.ndarray:
366         """
367             Masks the traces in the bad pixel mask.
368
369         Parameters
370         -----
371         spec : np.ndarray
372             The spectral data.
373         bpm : np.ndarray
374             The bad pixel mask.
375         max_traces : int, optional
376             The maximum number of traces to be masked.
377             (Default is 1)
378         tr_pad : int, optional
379             The amount to pad traces by.
380             (Default is 5)
381         bg_margin : int, optional
382             The margin size for the background.
383             (Default is 10)
384         lr_margins : list[int, int], optional
385             The left and right background margins at the spectrum edge.
386             (Default is [10, 10])
387         h_min: float, optional
388             The minimum height of a detected peak.
389             (Default is 0.5)
390         h_rel: float, optional
391             The relative height for the properties of a detected peak.
392             (Default is 1)
393
394         Returns
395         -----
396         bpm : np.ndarray
397             The updated bad pixel mask.
398
399         """
400         # Base mask
401         bpm[:, :bg_margin] = True
402         bpm[:, -bg_margin:] = True
403         bpm[:, :, :lr_margins[0]] = True
404         bpm[:, :, -lr_margins[1]:] = True
405
406         # Get the traces
407         traces, tr_props = self.find_peaks(
408             spec,
409             axis=1,
410             min_height=h_min,
411             rel_height=h_rel
412         )
413
414         for ext in range(len(self.beams)):
415             # Mask the traces
416             for i in range(len(traces[ext])[:max_traces]):
417                 lb = max(
418                     0,
419                     int(tr_props[ext]['left_ips'][i]) - tr_pad
420                 )
421                 ub = min(
422                     spec.shape[-1],
423                     int(tr_props[ext]['right_ips'][i]) + tr_pad
424                 )
425                 bpm[ext, lb: ub] = True
426             # TODO: Relocate targets after initial masking
427
428             logging.info(f"mask_traces - {min(max_traces, len(traces))} of {len(traces)}"
429                         " traces masked.")
430
431         return bpm
432
433         # MARK: Transform Spectra
434         def transform(
435             self,
436             spec: np.ndarray,

```

```

436         wav_sol: np.ndarray,
437         row_max: int | None = None,
438         res_plot: bool = False,
439     ) -> tuple[np.ndarray, np.ndarray]:
440     """
441         Transforms the input wavelength and spectral data
442         based on the given wavelength solution.
443
444     Parameters
445     -----
446     spec : np.ndarray
447         The spectral data.
448     wav_sol : np.ndarray
449         The wavelength solution.
450     row_max : int, optional
451         The row along which the spectral data is to be transformed.
452         (Default is None)
453     res_plot : bool, optional
454         Flag indicating whether to plot the results.
455         (Default is False)
456
457     Returns
458     -----
459     spec, wav : np.ndarray
460         The transformed wavelength and spectral data.
461
462     """
463     # Create arrays to return
464     cs = np.zeros_like(spec)
465     cw = np.zeros_like(wav_sol.mean(axis=1))
466
467     for ext in range(len(self.beams)):
468
469         if row_max:
470             avg_max = row_max
471         else:
472             # Get middle row (to interpolate the rest of the rows to)
473             avg_max = np.mean(spec[ext], axis=1).argmax()
474
475         # Correct extensions based on wavelength
476         # Get wavelength values at row with most trace
477         cw[ext] = wav_sol[ext, avg_max]
478
479         # Spec ext
480         for row in range(cs.shape[1]):
481             cs[ext, row] = np.interp(
482                 cw[ext],
483                 wav_sol[ext, row],
484                 spec[ext, row]
485             )
486             # f_2d = interpolate.interp2d(
487             #     wav_sol[ext, row],
488             #     np.arange(rows),
489             #     spec[ext],
490             # )
491             # cs[ext] = f_2d(cw[ext, row], np.arange(rows))
492
493         # Plot results
494         if res_plot:
495             fig, axs = plt.subplots(2, 1, figsize=[20, 4])
496             for ext in range(len(self.beams)):
497                 axs[ext].imshow(
498                     cs[ext],
499                     vmax=cs[ext].mean() + 2 * cs[ext].std(),
500                     vmin=cs[ext].mean() - 2 * cs[ext].std()
501                 )
502
503             logging.debug(f"'E' if ext else 'O' Average continuum =
504             ↪ {np.median(np.median(cs[ext], axis=0)):4.3f}")
505
506             axx = axs[ext].twinx()
507             axx.hlines(
508                 np.median(np.median(cs[ext], axis=0)),

```

```

508         0,
509         cs[ext].shape[-1],
510         colors='black',
511     )
512     axx.plot(
513         cs[ext].mean(axis=0),
514         "k",
515         label=f"mean {'E' if ext else '0'}"
516     )
517     axx.plot(
518         np.median(cs[ext], axis=0),
519         "r",
520         label=f"median {'E' if ext else '0'}"
521     )
522     axx.legend()
523 plt.show()
524
525 logging.info(f"transform - {cs.shape} transformed.")
526
527 return cs, cw
528
529 # MARK: Plot
530 def plot(
531     self,
532     spectra,
533     wavelengths,
534     peaks,
535     properties,
536     arc: bool = False,
537 ) -> None:
538     plt.style.use([
539         files(STOPS.utils).joinpath('STOPS.mplstyle'),
540         files(STOPS.utils).joinpath('STOPS_skylines.mplstyle'),
541     ])
542     plt.rcParams['figure.subplot.hspace'] *= len(self.beams)
543
544     def norm(vals):
545         return (vals - np.min(vals)) / (np.max(vals) - np.min(vals))
546
547     # Load known lines
548     if arc:
549         lines = self.load_lines(filename=self.arc_lamp)
550     else:
551         lines = self.load_lines()
552
553     # noinspection PyTypeChecker
554     lines = lines[
555         (lines['wav'] > wavelengths[1][0][0].min()) &
556         (lines['wav'] < wavelengths[1][0][0].max())
557     ]
558
559     # Create plot for results
560     fig, axs = plt.subplots(2, self.ccds, sharex='col', sharey='row')
561
562     # Convert axs to a 2D array if ccd count is 1
563     if self.ccds == 1:
564         # noinspection PyTypeChecker
565         axs: np.ndarray[matplotlib.axes.Axes] = np.swapaxes(np.atleast_2d(axs), 0, 1)
566
567     for fl in range(len(self.arc_list if arc else self.fits_list)):
568
569         # set color cycle
570         # color = next(axs[0, 0]._get_lines.prop_cycler)['color'] # private
571         # deprecate
572         color = axs[0, 0]._get_lines.get_next_color()
573
574         for ext in range(len(self.beams)):
575
576             ccdrange = spectra[1][fl][ext].shape[-1] // self.ccds
577             for ccd in range(self.ccds):
578                 # MARK: plot spectrum
579                 # (transformed)
580                 axs[0, ccd].plot(

```

```

580         wavelengths[1][fl][ext][
581             ccdrange * ccd:ccdrange * (ccd + 1)
582         ],
583         norm(spectra[1][fl][ext][
584             ccdrange * ccd:ccdrange * (ccd + 1)
585         ]) * 100 + 10 * ext + 30 * fl,
586         color=color,
587         linestyle='dashed' if ext else 'solid',
588         label=f"${{self.beams[ext]}}_{{{{fl} + 1}}})^{+ {10 * ext + 30 * fl}}$"
589     ) if ccd == 0 else None,
590 )
591
592     # MARK: plot dev
593     # noinspection PyTypeChecker
594     sky_wavs, dev, peak_idx = self.min_diff_matrix(
595         lines['wav'],
596         wavelengths[1][fl][ext][peaks[1][fl][ext]],
597         max_diff=self.max_difference,
598     )
599
600     # # MARK: width/width_init
601     # width = properties[1][fl][ext]['widths'][peak_idx]
602     # width_i = np.zeros_like(width)
603
604     # sky_i, i_dev, i_idx = self.min_diff_matrix(
605     #     lines['wav'],
606     #     wavelengths[0][fl][ext][peaks[0][fl][ext]],
607     #     max_diff=self.max_difference,
608     # )
609
610     # width_i = np.array([
611     #     properties[0][fl][ext]['widths'][
612     #         np.where(wav == sky_i)[0][0]
613     #     ]
614     #     if wav in sky_i else 1000
615     #     for wav in sky_wavs
616     # ])
617     # width_ratio = (width / width_i) - 1
618     # width_ratio[width_ratio < 0] = 0
619
620     # ylolims = width_ratio > self.max_difference
621     # width_ratio[
622     #     width_ratio > self.max_difference
623     # ] = self.max_difference // 2
624
625     ok = np.where(
626         (sky_wavs >= wavelengths[1][fl][ext].data[ccdrange * ccd]) &
627         (sky_wavs <= wavelengths[1][fl][ext].data[ccdrange * (ccd + 1)])
628     )
629     axs[1, ccd].plot(
630         sky_wavs[ok],
631         dev[ok],
632         # yerr=(width_ratio[ok] * 0, width_ratio[ok]),
633         # lolims=ylolims[ok],
634         "." if ext else "x",
635         # fmt=". " if ext else "x",
636         alpha=0.8,
637         color=color,
638         # markeredgecolor='white',
639         # markeredgewidth=0.5,
640         # label=f"${{self.beams[ext]}}_{{{{fl} + 1}}})$",
641     )
642
643     logging.debug(f"plot - RMS: {np.sqrt(np.mean(dev[ok] ** 2)):.2f}")
644
645     for ccd in range(self.ccds):
646         ccdrange = spectra[1][0][0].shape[-1] // self.ccds
647
648         # spectrum
649         # noinspection PyTypeChecker
650         ok = np.where(
651             (lines['wav'] >= wavelengths[1][0][0].data[ccdrange * ccd]) &
652             (lines['wav'] <= wavelengths[1][0][0].data[ccdrange * (ccd + 1)])
653         )

```

```

652     )
653     # noinspection PyTypeChecker
654     axs[0, ccd].plot(
655         lines['wav'][ok],
656         lines['flux'][ok] * 0,
657         'x',
658         color='C4',
659         label="\text{sc}{{salt}}\nModel" if ccd == 0 else None,
660     )
661     # noinspection PyTypeChecker
662     for x in lines['wav'][ok]:
663         axs[0, ccd].axvline(x, ls='dashed', c='0.7')
664
665     axs[0, 0].set_ylabel("Rel. Intensity ($\\%$)")
666     axs[1, 0].set_ylabel(
667         "Closest Peak ($\\Delta\\lambda$)")
668     )
669     # for ax in axs[:, 0]:
670     #     ax.legend(loc='upper left', ncols=(fl + 1) * (ext + 1) + 1)
671     leg = fig.legend(
672         loc='center',
673         ncol=min(8, len(spectra[0])) + 1,
674         columnspacing=0.5,
675         bbox_to_anchor=(
676             np.mean((
677                 plt.rcParams['figure.subplot.left'],
678                 plt.rcParams['figure.subplot.right']
679             )),
680             np.mean((
681                 plt.rcParams['figure.subplot.bottom'],
682                 plt.rcParams['figure.subplot.top']
683             )))
684         ),
685     )
686     leg.set_draggable(True)
687     for ax in axs[1, :]:
688         ax.grid(axis='y')
689
690     # fig.add_subplot(111, frameon=False)
691     # # hide tick and tick label of the big axis
692     # plt.tick_params(
693     #     labelcolor='none',
694     #     which='both',
695     #     top=False,
696     #     bottom=False,
697     #     left=False,
698     #     right=False
699     # )
700     axs[-1, 0 if self.ccds == 1 else 1].set_xlabel(
701         f"Wavelength ({self.wav_unit})"
702     )
703
704     # plt.tight_layout()
705
706     plt.show()
707
708     # Save results
709     if self.save_prefix:
710         fig.savefig(fname=self.save_prefix)
711
712     return
713
714     # MARK: Process all listed images
715
716     def process(self, arc: bool = False) -> None:
717         files = self.fits_list
718         if arc:
719             files = self.arc_list
720
721         logging.info(f"Processing '{self.beams}' lines.")
722
723         spectra = [[], []]
724         wavs = [[], []]

```

```

725     peaks = [[], []]
726     peak_props = [[], []]
727
728     for fl in files:
729         # Load data
730         spec2d, wav2d, bpm2d = self.load_file_data(fl)
731
732         # Mask traces in BPM
733         bpm2d = self.mask_traces(
734             spec2d,
735             bpm2d,
736             max_traces=0,
737             bg_margin=15,
738             h_min=0.05
739         )
740         m_spec2d = np.ma.masked_array(spec2d, mask=bpm2d) # spec2d
741         m_wav2d = np.ma.masked_array(wav2d, mask=bpm2d) # wav2d
742
743         # Initial spectra
744         spec_i = np.mean(m_spec2d, axis=-2)
745         wav_i = np.mean(m_wav2d, axis=-2)
746
747         # Transform data
748         t_spec2d, t_wav = self.transform(
749             m_spec2d,
750             m_wav2d,
751             res_plot=self.can_plot
752         )
753
754         # Final spectra
755         spec_f = np.mean(t_spec2d, axis=-2)
756         wav_f = t_wav
757
758         # Find peaks
759         peaks_i, props_i = self.find_peaks(
760             spec_i,
761             **FIND_PEAK_PARAMS
762         )
763         peaks_f, props_f = self.find_peaks(
764             spec_f,
765             **FIND_PEAK_PARAMS
766         )
767
768         spectra[0].append([*spec_i])
769         spectra[1].append([*spec_f])
770         wavs[0].append([*wav_i])
771         wavs[1].append([*wav_f])
772         peaks[0].append([*peaks_i])
773         peaks[1].append([*peaks_f])
774         peak_props[0].append([*props_i])
775         peak_props[1].append([*props_f])
776
777         # Plot results
778         self.plot(spectra, wavs, peaks, peak_props, arc=arc)
779
780         if arc:
781             return
782         elif self.arc_list:
783             self.process(arc=True)
784
785         return
786
787
788 # MARK: Main function
789 def main(argv) -> None:
790     return
791
792
793 if __name__ == "__main__":
794     main(sys.argv[1:])

```

# Appendix C

## Proceedings

Development of STOPS and it's application to spectropolarimetric observations was presented at conferences, with the following proceedings included here.

- HEASA 2021 - Cooper, van Soelen, and Britto (2022)
- HEASA 2022 - Cooper and van Soelen (2023)

# Development of tools for the SALT/RSS spectropolarimetry reductions: application to the blazar 3C 279

---

**Justin Cooper,<sup>a,\*</sup> Brian van Soelen<sup>a</sup> and Richard J. Britto<sup>a</sup>**

<sup>a</sup>*University of the Free State,  
205 Nelson Mandela Drive, Bloemfontein, South Africa*

*E-mail:* [CooperJ@ufs.ac.za](mailto:CooperJ@ufs.ac.za), [VanSoelenB@ufs.ac.za](mailto:VanSoelenB@ufs.ac.za)

Blazars represent a subset of AGN with relativistic jets, where the direction of the jet lies very close to our line of sight. The highly Doppler boosted emission from the blazar's jet results in high apparent luminosities, and blazars display variability on periods from less than one day up to years. At optical wavelengths, the observed emission of the blazar is a superposition of the polarised non-thermal synchrotron emission, arising from the jet, and the unpolarised thermal emission, arising from the accretion disc, broad line region, torus and host galaxy. Polarimetry observations can serve as an important tool for diagnosing the emission from blazars. The RSS spectrograph, on SALT, can operate in spectropolarimetry mode and is currently being used to undertake spectropolarimetric observations of transient blazar sources. We present additional tools developed to work in conjunction with the current SALT spectropolarimetry reduction pipeline, POLSALT, that aims to streamline the reduction of the SALT polarisation data, including the testing of the wavelength calibration of the individual O and E beams. This was applied to observations of 3C 279 during 2017.

\*\*\* *High Energy Astrophysics in Southern Africa (HEASA2021)* \*\*\*

\*\*\* *13 - 17 September, 2021* \*\*\*

\*\*\* *Online* \*\*\*

---

\*Speaker

## 1. Introduction

Active Galactic Nuclei (AGN) are the centres of galaxies powered by accretion onto a supermassive black hole. The accretion can power relativistic jets which produce non-thermal emission over multiple wavelengths [1]. Blazars are a subclass of AGN where the direction of the jet lies very close to our line of sight. The highly Doppler boosted emission from the jet results in high apparent luminosities.

At optical wavelengths the observed emission is a superposition of polarised non-thermal synchrotron emission, arising from the jet, and unpolarised thermal emission, arising from the disc, broad line region, torus, and host galaxy [2].

The Robert Stobie Spectrograph (RSS) on the Southern African Large Telescope (SALT) [3] [4] is capable of long-slit spectropolarimetry and has been used to observe blazars in flaring and quiescent states. Data reduction of these observations is processed using the SALT spectropolarimetry reduction package POLSALT.<sup>1</sup> POLSALT allows for the full reduction, from pre-reduction to the extraction of the target spectra, and the measuring of the polarisation. However, it does not allow for much flexibility with the wavelength calibrations, nor does it provide tools to confirm that the wavelength calibrations lead to similar wavelength calibrated spectra for the O and E beams.

In order to streamline the data reduction we are developing additional tools to work in conjunction with POLSALT. We present the overview of this pipeline and demonstrate its application to an observation of 3C 279 taken in 2017.

## 2. Pipeline Overview

The tools being developed are designed to work in conjunction with POLSALT and provide a method to perform the wavelength calibrations using conventional `IRAF` methods [5]. They also allow easy comparisons to be made between the wavelength solutions of the O and E beam, to determine their quality and reliability.

The workflow for reductions is depicted in figure 1. It summarises the steps followed to reduce spectropolarimetric data. Steps that are performed using POLSALT are indicated in blue; steps performed by the new tools are shown in orange, while the `IRAF` calibration is shown in green.

If the wavelength solutions are found with `IRAF`, the tools split the multi-extension FITS files into the correct format for `IRAF` and the `IRAF` wavelength calibration is performed. The files are then written back into multi-extension FITS files in the correct format for POLSALT to complete the extraction and measurement of polarisation.

The cross-correlation between the O and E beam spectra, named correlation in figure 1, and relative flux calibrations are optional, though correlation is suggested. Relative flux calibrations may be performed assuming a standard and published standard spectra can be acquired. We performed the relative flux calibrations using the `ASTROPY` [6, 7] and `SCIPY`<sup>2</sup> packages.

---

<sup>1</sup><https://github.com/saltastro/polsalt>

<sup>2</sup><http://www.scipy.org/>

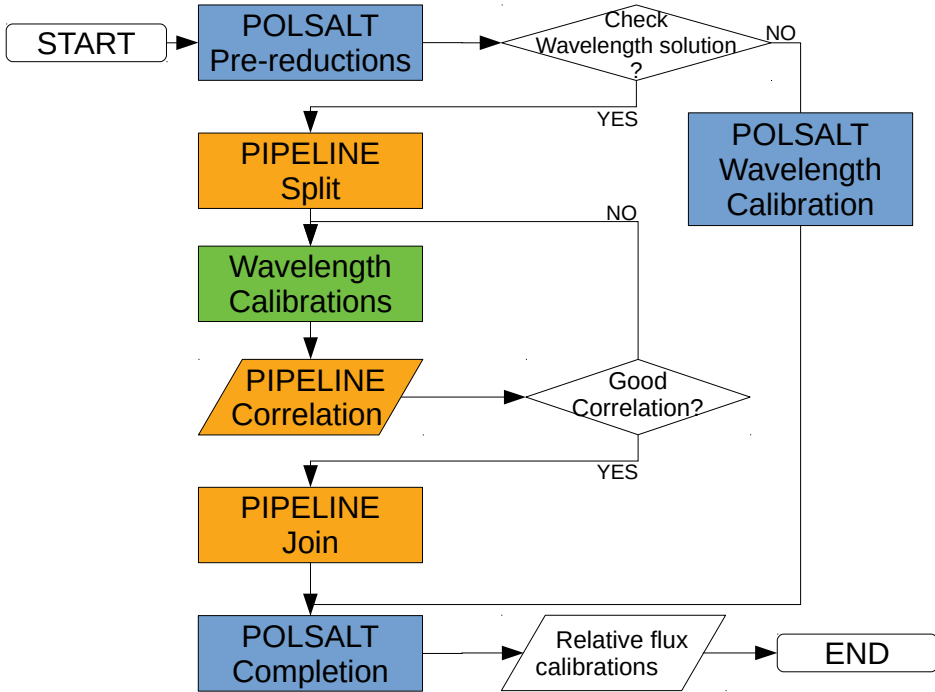


**Figure 1:** The flow diagram of the SALT RSS spectropolarimetry reductions steps.

POS (HEAS2021) 056

## 2.1 Pre-reduction

The first step in the pipeline uses **POLSLT** and this performs the pre-reductions, the over-scan subtraction, gain and cross talk corrections, and mosaicing. After the pre-reduction is performed, the next step is to either undertake the wavelength calibration with **POLSLT**, or to split the files into the correct format for **IRAF**.

## 2.2 FITS split

Once all pre-reductions are complete, the tool **SPLIT** converts the multi-extension FITS files into multiple, single extension O or E beam FITS files. This is done as some **IRAF** tasks do not handle multi-extension FITS files well. The O and E beam frames are cropped to remove any non-exposed rows to accommodate the standard **IRAF** tasks and the FITS files saved with updated header information.

## 2.3 Wavelength calibration

If the **POLSLT** pipeline is used, the wavelength calibration is performed using the wavelength calibration tools which form part of **PYSALT** [8].

If the files have been formatted for **IRAF**, standard wavelength calibration methods are followed, using the **NOAO** package and the **identify**, **re-identify**, and **fitcoords** tasks. This allows greater control of the resultant wavelength solution.

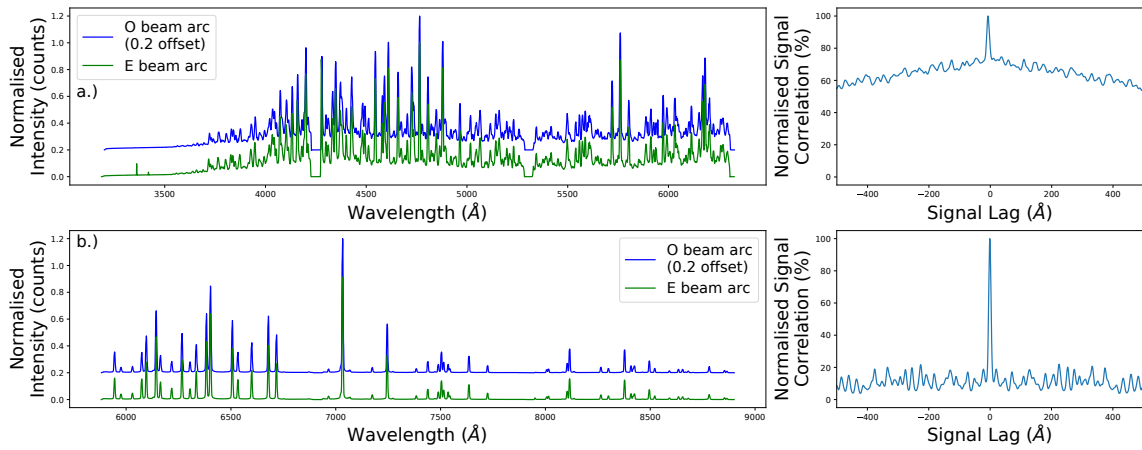


**Figure 2:** Comparison of the O and E beams for a.) ThAr and b.) Ne arc lamp spectra as well as the cross-correlation of their O and E beams.

## 2.4 Correlation

Our tool CORRELATE allows a comparison to be made between the O and E beam solutions, by performing a cross-correlation between the two arc or target observations, after the wavelength solution as been applied by `IRAF`. This is important as the polarisation is calculated from the difference between the O and E beam and, therefore, accurate wavelength solutions are required. The comparison between the O and E beams for a ThAr and Ne arc spectra and their cross-correlations, with a near zero lag, are shown in figure 2.a) and figure 2.b), respectively. Figure 2's Signal Lag plots show a clear peak at zero lag but also show an important distinction between noisy and quiet spectra in the non-peaking region.

## 2.5 FITS join

Once the `IRAF` wavelength calibrations are complete, the tool JOIN performs cosmic-ray cleaning using the LACOSMIC package [9], applies a wollaston correction which accounts for the physical shift of the spectra on the CCD, and then formats the single extension O and E beam FITS files into the multi-extension format required by `POLSALT`. This includes saving the wavelength solution found in `IRAF` as an additional extension. Currently only wavelength solutions fit with a Chebychev function are recognised but further development is planned to recognise Legendre functions.

## 2.6 Completion - extraction and polarisation measurement

After the wavelength solution is found, the final step is performed using `POLSALT`, which performs the curvature corrections, background subtraction, spectral extraction, and the raw and final stokes calculations. The binning and plotting also form part of the `POLSALT` completion.

## 3. Application to 3C 279

The blazar 3C 279 was observed in linear spectropolarimetry mode, on 2017 May 17, using the the PG0900 grating with two different grating angles ( $12.5^\circ$  and  $19.5^\circ$ ). The spectrophotometric

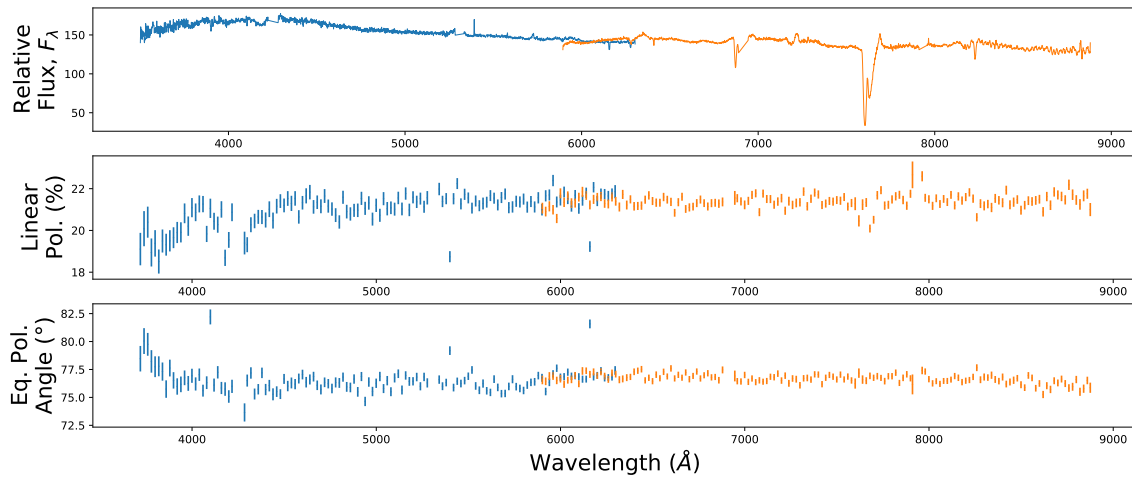


**Figure 3:** Reduced observations of 3C 279, taken with grating angle  $12.5^\circ$  (blue line) and  $19.5^\circ$  (orange line). Top: relative flux calibrated spectra. Middle: degree of linear polarisation. Bottom: Polarisation angle (relative to instrument).

standard star Hiltner 600 was observed on 2017 February 24, using the same configuration and was used for relative flux calibrations.

The target and standard were reduced following the steps discussed about. The flux correction was performed using `ASTROPY` and `SCIPY` python packages to correct the flux shape.

The results are shown in figure 3, indicating a good overlap between the observations taken at two different grating angles, with the polarisation measurements generally agree well where the observations overlap.

Figure 2 shows the comparison of the O and E beams for this observations. The cross-correlation is very close to zero lag, indicating the wavelength solution is similar for both the O and E beams.

#### 4. Discussion and Conclusions

Creating an independent 2D wavelength solution for the O and E beams using `IRAF` allows for more flexibility in obtaining the wavelength solutions and provides a tool to directly compare the O and E beam solutions. This is useful for difficult cases, such as arc line identification for the PG0300 spectral grating, because there are fewer arc lines in some parts of the spectra and it is more complicated to create a consistent solution across the full wavelength range covered.

The cross-correlation plot cannot only be considered when deciding on whether to proceed onward with the reductions or to return to wavelength calibrations as depicted in figure 1. The comparison of the spectra is as important since the cross-correlation may show zero lag but lines in the spectra could still be mis-identified in both beams. The cross-correlation serves as a method to check the similarity of the wavelength solutions but not the accuracy of said solutions.

The tools developed create an alternative to the `POLSALT` wavelength calibration and add a method to check the consistency of the wavelength solutions, as can be seen with the application to 3C 279. These assist with the wavelength calibration, in particular for observations taken with

the PG0300 and PG0900 RSS gratings, that have been used for numerous observations of blazar sources.

## Acknowledgments

The observational data presented was obtained with the Southern African Large Telescope (SALT) under the proposal 2016-2-LSP-001 (PI: D.A.H. Buckley). This work is based on the research supported in part by the National Research Foundation of South Africa (Grant Numbers: 116300).

## References

- [1] C.M. Urry and P. Padovani, *Unified Schemes for Radio-Loud Active Galactic Nuclei*, *PASP* **107** (1995) 803 [[astro-ph/9506063](#)].
- [2] M. Böttcher, B. Van Soelen, R.J. Britto, D.A.H. Buckley, J.P. Marais and H. Schutte, *Salt spectropolarimetry and self-consistent sed and polarization modeling of blazars*, *Galaxies* **5** (2017) .
- [3] E.B. Burgh, K.H. Nordsieck, H.A. Kobulnicky, T.B. Williams, D. O'Donoghue, M.P. Smith et al., *Prime focus imaging spectrograph for the southern african large telescope: optical design*, in *Instrument Design and Performance for Optical/Infrared Ground-based Telescopes*, vol. 4841, pp. 1463–1471, International Society for Optics and Photonics, 2003.
- [4] H.A. Kobulnicky, K.H. Nordsieck, E.B. Burgh, M.P. Smith, J.W. Percival, T.B. Williams et al., *Prime Focus Imaging Spectrograph for the Southern African Large Telescope: operational modes*, in *Instrument Design and Performance for Optical/Infrared Ground-based Telescopes*, M. Iye and A.F.M. Moorwood, eds., vol. 4841, pp. 1634 – 1644, International Society for Optics and Photonics, SPIE, 2003, [DOI](#).
- [5] D. Tody, *The IRAF Data Reduction and Analysis System*, in *Instrumentation in astronomy VI*, D.L. Crawford, ed., vol. 627 of *Society of Photo-Optical Instrumentation Engineers (SPIE) Conference Series*, p. 733, Jan., 1986, [DOI](#).
- [6] Astropy Collaboration, T.P. Robitaille, E.J. Tollerud, P. Greenfield, M. Droettboom, E. Bray et al., *Astropy: A community Python package for astronomy*, *A&A* **558** (2013) A33 [[1307.6212](#)].
- [7] Astropy Collaboration, A.M. Price-Whelan, B.M. Sipőcz, H.M. Günther, P.L. Lim, S.M. Crawford et al., *The Astropy Project: Building an Open-science Project and Status of the v2.0 Core Package*, *AJ* **156** (2018) 123 [[1801.02634](#)].
- [8] S.M. Crawford, M. Still, P. Schellart, L. Balona, D.A.H. Buckley, G. Dugmore et al., *PySALT: the SALT science pipeline*, in *Observatory Operations: Strategies, Processes, and Systems III*, D.R. Silva, A.B. Peck and B.T. Soifer, eds., vol. 7737 of *Society of Photo-Optical Instrumentation Engineers (SPIE) Conference Series*, p. 773725, July, 2010, [DOI](#).

- [9] P.G. Van Dokkum, *Cosmic-ray rejection by laplacian edge detection*, *Publications of the Astronomical Society of the Pacific* **113** (2001) 1420.

POS (HEASA2021) 056

## SALT Spectropolarimetric Pipeline Comparisons

J. Cooper<sup>a,\*</sup> and B. van Soelen<sup>a</sup>

<sup>a</sup>*University of the Free State, Physics Dept.,*

*PO Box 339, Bloemfontein, 9300*

*E-mail:* [Justin.jb78@gmail.com](mailto:Justin.jb78@gmail.com), [vanSoelenB@ufs.ac.za](mailto:vanSoelenB@ufs.ac.za)

Blazars are active galactic nuclei (AGN) with jets aligned very closely to our line of sight. The optical emission of blazars is often dominated by the polarised, non-thermal emission arising in the jets, with an underlying unpolarised, thermal emission component arising from the host galaxy, dusty torus, and accretion disk components.

Coupled with multi-wavelength observations, optical spectropolarimetry of blazars during both flaring and quiescent states can be used to disentangle the polarised and unpolarised components in their spectral energy distributions, providing better constraints for the non-thermal particle distribution. To this end, spectropolarimetry of blazars during different states of activity was taken with the Southern African Large Telescope (SALT) using the Robert Stobie Spectrograph (RSS). For RSS spectropolarimetry, reductions are performed using the POLSALT pipeline. In order to streamline the spectropolarimetric reductions, we have implemented supplementary interactive tools which provides additional wavelength calibration to improve the accuracy of the wavelength calibration for the O & E beam.

Here we present a brief overview of the tools and the results for Hiltner 652, a spectropolarimetric standard, as well as results for the blazars 3C 279. The reduced,  $P_Q$  and  $P_U$ , Stokes parameters of Hiltner 652 show no major deviation from previously published results which reassures us that there is no interference introduced into the Stokes parameter calculations when wavelength calibrations are handled by our supplementary tools. The  $\sim 6000 - 9000 \text{ \AA}$  range of 3C 279 shows a notable dip in the normalized spectrum during a period of flaring when compared to epochs of enhanced activity. The degree of polarisation for 3C 279 of 13.2%, 9.5%, and 21.2% for the epochs 2017 March 28, 2017 March 31, and 2017 May 17, respectively, remains fairly constant across the observed wavelength ranges while still varying with the blazars' state of quiescence or flaring.

*High Energy Astrophysics in Southern Africa 2022 - HEASA2022*  
*28 September - 1 October 2022*  
*Brandfort, South Africa*

---

\*Speaker

## 1. Introduction

Blazars are a radio-loud sub-set of Active Galactic Nuclei (AGN), where the jet is aligned very closely to our line of sight and whose observed emission varies over time scales from hours to decades [1]. The optical emission observed from blazars is often dominated by the polarised, non-thermal emission arising in the jets, but there is also underlying non-polarised, thermal emission arising from the host galaxy, dusty torus, and accretion disk components [2]. When a blazar varies between flaring and quiescent states, the relative strength of the thermal component to the non-thermal component changes.

The Spectral Energy Distribution (SED) of blazars shows two clear components: a lower energy component produced through leptonic synchrotron processes (covering the radio to the UV/soft X-ray regimes) and a higher energy component (covering the X-ray to the  $\gamma$ -ray regimes) which can be produced through either leptonic or hadronic processes [3]. Optical spectropolarimetry observations, coupled with multi-wavelength observations during both flaring and quiescent states, can be used to disentangle the polarised and non-polarised components in the blazar's SED, providing better constraints for the non-thermal particle distribution [4, 5].

To this end, spectropolarimetric observations of blazars during different states of activity were taken using SALT [6] and the RSS [7]. RSS spectropolarimetry data is reduced with the dedicated POLSALT pipeline [8]. In order to facilitate the blazar observations we have developed supplementary tools to provide a more interactive approach to the wavelength calibration, allowing for improved accuracy for the O & E beam wavelength solutions [9]. Furthermore, spectropolarimetric standards, which were also observed with SALT and the RSS, were reduced alongside the blazar observations to test that the developed tools correctly performed the wavelength calibration. Here we present an overview of the pipeline as well as the preliminary results of a spectropolarimetric standard, namely Hiltner 652, and for the blazar 3C 279.

## 2. Pipeline Overview

RSS spectropolarimetry data is currently reduced using the POLSALT pipeline [8]. This python package allows for a full reduction from pre-reduction to extracted spectrum, and measured polarisation. However, the wavelength calibration component of the package does not allow for flexibility, nor provide a tool to confirm that the wavelength calibrations of the O & E beams are in agreement. This flexibility is most notably missed when performing calibrations of observations taken using the PG0300 grating<sup>1</sup> due to the very sparse spectral features of the Argon arc lamp used by SALT as well as second order contamination which differs between the O & E beams.

The developed tools work in conjunction with the existing pipeline and provide a method to perform the wavelength calibrations using conventional IRAF [10] methods. Figure 1 shows the typical workflow for data reductions of spectropolarimetric SALT data. Items in blue refer to processing steps completed entirely using POLSALT while items in orange refer to processing steps completed using the developed tools. The single green item refers to the wavelength calibration

---

<sup>1</sup>This grating has been decommissioned and replaced by the PG0700, and is not available for general use as of November 2022.

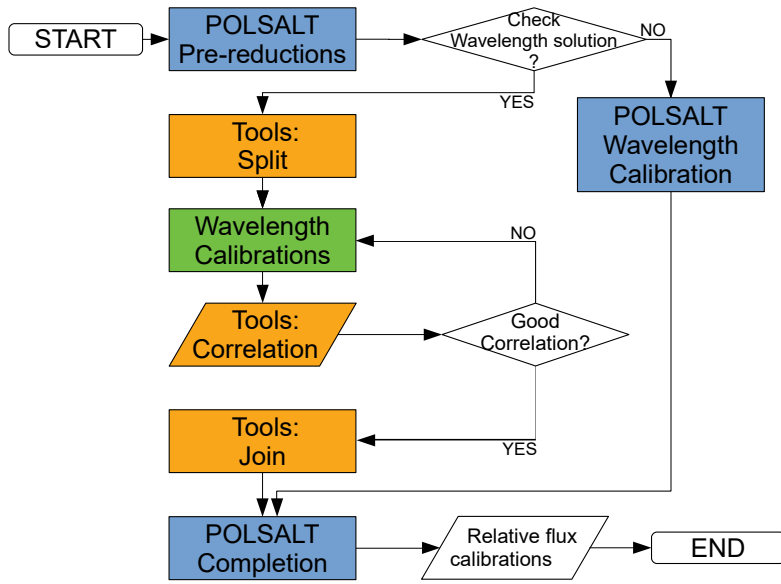


**Figure 1:** A general workflow for data reductions using a combination of **POLSALT** and our developed tools.

| Source      | Observation date | Grating angle<br>(°) | Slit width<br>(") | Exposure time<br>(sec) | Wavelength range<br>(Å) |
|-------------|------------------|----------------------|-------------------|------------------------|-------------------------|
| Hiltner 652 | 2022 June 10     | 12.878               | 2                 | 48.5                   | 3350 - 6440             |
| 3C 279      | 2017 March 28    | 12.5                 | 1.5               | 480.8                  | 3300 - 6300             |
| 3C 279      | 2017 March 28    | 19.625               | 1.5               | 480.8                  | 5800 - 8800             |
| 3C 279      | 2017 March 31    | 12.5                 | 1.5               | 480.8                  | 3300 - 6300             |
| 3C 279      | 2017 March 31    | 19.625               | 1.5               | 480.8                  | 5800 - 8800             |
| 3C 279      | 2017 May 17      | 12.5                 | 1.5               | 720.8                  | 3300 - 6300             |
| 3C 279      | 2017 May 17      | 19.625               | 1.5               | 720.8                  | 5800 - 8800             |

**Table 1:** All spectropolarimetric observations taken with SALT and the RSS and used as part of development and testing of the supplementary tools.

done in **IRAF**. Additional tools to cross-check that the wavelength calibration is consistent across both beams have also been implemented.<sup>2</sup>

### 3. Observations

The spectropolarimetric observations were taken using the RSS mounted on SALT, in **LINEAR** mode. The spectropolarimetric standard, Hiltner 652, was observed in 2022 and the blazar 3C 279, was observed in 2017, as summarized in Table 1. All observations presented here were observed using the PG0900 and were reduced following the reduction workflow as described in Figure 1.

<sup>2</sup>A further, in-depth, discussion of the developed tools can be found at [9].

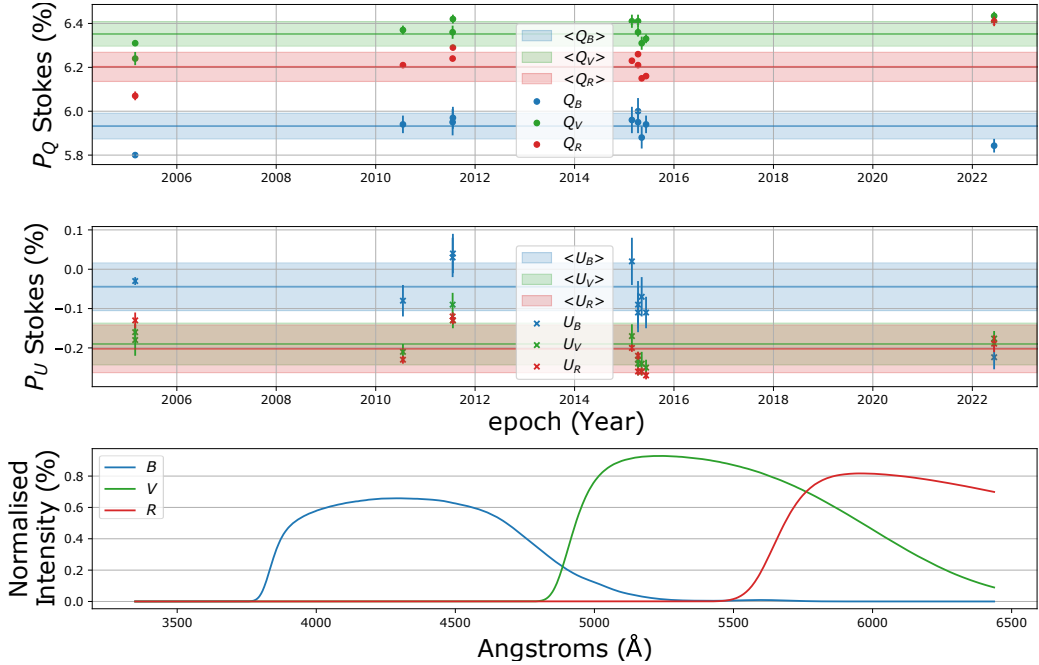


**Figure 2:** The reduced Q and U Stokes parameters for Hiltner 652 obtained with SALT in 2022 (post 2020) calculated by convolving the spectropolarimetry with the Johnson-Cousins filter pass-bands. This is compared to the published FORS1 [11] and FORS2 [12] observation results (top and middle panels). The average of the FORS reduced Stokes parameters as well as their standard deviation are plotted as the horizontal lines and shaded regions, respectively. Hiltner 652 was observed by SALT in 2022, by FORS1 from 1999 to 2006 (shown as average value at March 2005), and by FORS2 from 2010 to 2016. Finally, the Johnson-Cousins filter pass-band's used by POLSALT to calculate the stokes parameters in the different filters are shown in the bottom panel.

#### 4. Results

The linear Stokes parameters,  $Q$  &  $U$ , normalized to the total intensity, referred to henceforth as the reduced Stokes parameters,  $P_Q$  &  $P_U$ , are relative quantities which are used to calculate the polarisation properties, and from which the fraction of linear polarisation may be easily calculated as  $P_L = \sqrt{P_Q^2 + P_U^2}$  [13]. The reduced Stokes parameters of Hiltner 652, convolved against the Johnson-Cousins filter pass-bands, as performed by POLSALT, are shown in Figure 2 and are compared against published filtered reduced Stokes parameters obtained with FORS1 [11] and FORS2 [12]. The bottom panel of Figure 2 also shows the filter band-passes for the wavelength range covered by the SALT spectropolarimetry; note that the full  $R$  band is not covered by the observation setup.

The reduced Stokes parameters of Hiltner 652 fall within or near the  $1\sigma$  level of the previously published reduced Stokes parameters over the course of multiple years. This shows that Hiltner 652 is not only a good standard for spectropolarimetric observations but also that using POLSALT with the supplementary wavelength calibrations correctly calculated the Stokes parameters.

The blazar 3C 279 was observed during periods of enhanced and flaring  $\gamma$ -ray activity for energies of 0.1 – 100 GeV and were sourced from the Fermi Light Curve Repository (Fermi LCR)

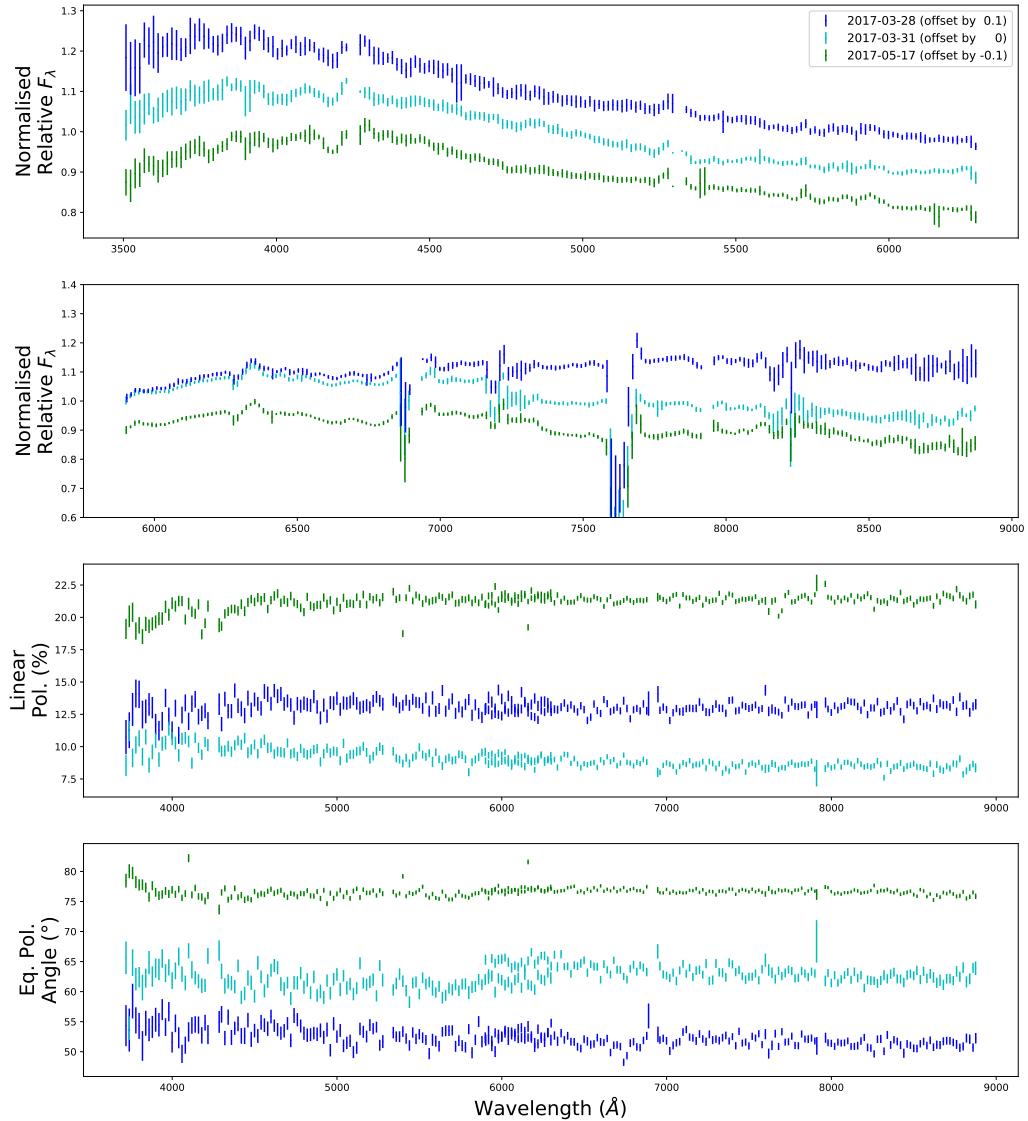


**Figure 3:** Optical spectropolarimetric observations of 3C 279 during two different periods of flaring. The relative flux calibrated spectra for the grating angles  $12.5^\circ$  (top), observed first at each epoch, and  $19.625^\circ$  (second from top), the degree of polarisation (third from top), and the polarisation angle (bottom).

[14]. 3C 279 was observed at fluxes of  $1.58 \times 10^{-6}$ ,  $2.87 \times 10^{-6}$ , and  $2.00 \times 10^{-6}$  ph cm $^{-2}$  s $^{-1}$  as compared to a ‘quiescent’ median flux of  $4.59 \times 10^{-7}$  ph cm $^{-2}$  s $^{-1}$ .

Figure 3 shows the relative flux calibrated spectra normalized to the spectrum’s mean (and offset as indicated), degree of polarisation, and polarisation angle for 3C 279. The relative flux was normalized to better compare how the shape of the spectrum changes during the differing  $\gamma$ -ray states. 3C 279 showed variable flux and polarisation during the three observations, with the polarisation changing by  $\sim 12.23\%$  and the angle changing by  $\sim 24.22^\circ$ . The relative spectral shape remains similar over all three observations, however the second observation (2017-03-31) appears to show a slightly brighter spectrum in the blue. There is also a relatively good agreement

in the polarisation at the wavelength overlap for the different grating angles. The difference of the polarisation and degree of polarisation is on the order of 0.25 % and 1.25°, respectively.

## 5. Discussion and Conclusions

In this paper we have considered the observations of a spectropolarimetric standard, Hiltner 652, and a flaring blazar, 3C 279, to test our supplementary tools used for the reduction of spectropolarimetric data obtained with the RSS. The results serve to confirm that the supplementary tools' wavelength reductions, in combination with POLSALT, produces the correct polarisation behavior. Our results for Hiltner 652 agree well with the historical results obtained using the FOcal Reducer and low dispersion Spectrograph (FORS1 and FORS2) mounted at the Very Large Telescope (VLT).

For 3C 279, there is similarly good agreement between the polarisation for the observations taken at two grating angles where the wavelength ranges overlap. Some disagreement is found which may be due to the inherent nature of flaring blazars which cause the polarisation angle to drastically vary and the two observations at different grating angles are not taken simultaneously. Additionally, the disagreement may be due to a lower Signal-to-Noise Ratio (SNR) at the edges of the RSS, which would introduce a larger systematic error. The lower SNR could originate from either blaze effects, or from the extraction of the trace, which is currently limited to a rectangular aperture in the current POLSALT pipeline.

The results show that our supplementary wavelength calibrations for POLSALT increase the efficiency of the data reduction and produce acceptable results. This reduction procedure has been used for the reduction of a number of blazar observations undertaken as part of a long term monitoring campaign [15].

## Acknowledgments

All observations taken in this study were obtained using the RSS mounted on SALT under the programme ID 2016-2-LSP-001 (PI DAH Buckley).

## References

- [1] C.M. Urry and P. Padovani, *Unified Schemes for Radio-Loud Active Galactic Nuclei*, *Publications of the Astronomical Society of the Pacific* **107** (1995) 803 [[astro-ph/9506063](#)].
- [2] G. Ghisellini, F. Tavecchio, L. Foschini, G. Ghirlanda, L. Maraschi and A. Celotti, *General physical properties of bright Fermi blazars*, *Monthly Notices of the Royal Astronomical Society* **402** (2010) 497 [[0909.0932](#)].
- [3] M. Böttcher, A. Reimer, K. Sweeney and A. Prakash, *Leptonic and hadronic modeling of fermi-detected blazars*, *The Astrophysical Journal* **768** (2013) 54.

- [4] H.M. Schutte, M. Böttcher, J. Barnard, A. Dmytriiev, B. van Soelen, A. Falcone et al., *Modeling the Multi-wavelength Polarization and Spectral Energy Distributions of Blazars*, in *44th COSPAR Scientific Assembly. Held 16-24 July*, vol. 44, p. 1869, July, 2022.
- [5] H.M. Schutte, R.J. Britto, M. Böttcher, B. van Soelen, J.P. Marais, A. Kaur et al., *Modeling the spectral energy distributions and spectropolarimetry of blazars—application to 4C+01.02 in 2016-2017\**, *The Astrophysical Journal* **925** (2022) 139.
- [6] E.B. Burgh, K.H. Nordsieck, H.A. Kobulnicky, T.B. Williams, D. O'Donoghue, M.P. Smith et al., *Prime Focus Imaging Spectrograph for the Southern African Large Telescope: optical design*, in *Instrument Design and Performance for Optical/Infrared Ground-based Telescopes*, M. Iye and A.F.M. Moorwood, eds., vol. 4841 of *Society of Photo-Optical Instrumentation Engineers (SPIE) Conference Series*, pp. 1463–1471, Mar., 2003, DOI.
- [7] H.A. Kobulnicky, K.H. Nordsieck, E.B. Burgh, M.P. Smith, J.W. Percival, T.B. Williams et al., *Prime focus imaging spectrograph for the Southern African large telescope: operational modes*, in *Instrument Design and Performance for Optical/Infrared Ground-based Telescopes*, M. Iye and A.F.M. Moorwood, eds., vol. 4841 of *Society of Photo-Optical Instrumentation Engineers (SPIE) Conference Series*, pp. 1634–1644, Mar., 2003, DOI.
- [8] S. Crawford and K. Nordsieck, “Polsalt.” <https://github.com/saltastro/polsalt>, 2020.
- [9] J. Cooper, B. van Soelen and R. Britto, *Development of tools for SALT/RSS spectropolarimetry reductions: application to the blazar 3C279*, in *High Energy Astrophysics in Southern Africa 2021*, p. 56, May, 2022, DOI.
- [10] D. Tody, *The IRAF Data Reduction and Analysis System*, in *Instrumentation in astronomy VI*, D.L. Crawford, ed., vol. 627 of *Society of Photo-Optical Instrumentation Engineers (SPIE) Conference Series*, p. 733, Jan., 1986, DOI.
- [11] L. Fossati, S. Bagnulo, E. Mason and E. Landi Degl'Innocenti, *Standard Stars for Linear Polarization Observed with FORS1*, in *The Future of Photometric, Spectrophotometric and Polarimetric Standardization*, C. Sterken, ed., vol. 364 of *Astronomical Society of the Pacific Conference Series*, p. 503, Apr., 2007.
- [12] A. Cikota, F. Patat, S. Cikota and T. Faran, *Linear spectropolarimetry of polarimetric standard stars with VLT/FORS2*, *Monthly Notices of the Royal Astronomical Society* **464** (2017) 4146 [1610.00722].
- [13] E. Landi Degl'Innocenti, S. Bagnulo and L. Fossati, *Polarimetric Standardization*, in *The Future of Photometric, Spectrophotometric and Polarimetric Standardization*, C. Sterken, ed., vol. 364 of *Astronomical Society of the Pacific Conference Series*, p. 495, Apr., 2007, DOI [astro-ph/0610262].

- [14] S. Abdollahi, M. Ajello, L. Baldini, J. Ballet, D. Bastieri, J.B. Gonzalez et al., *The fermi-lat light curve repository*, 2023. 10.48550/ARXIV.2301.01607.
- [15] J. Barnard, B. van Soelen, J. Cooper, R. Britto, J.P. Marais, I. van der Westhuizen et al., *Optical Spectropolarimetry Observations of the BL Lac-type object PKS 0537-441 after a period of quiescence*, in *High Energy Astrophysics in Southern Africa 2021*, p. 9, May, 2022, DOI.

# Bibliography

R. R. J. Antonucci and J. S. Miller. Spectropolarimetry and the nature of NGC 1068. *ApJ*, 297:621–632, October 1985. doi: 10.1086/163559.

George B. Arfken and Hans J. Weber. Mathematical methods for physicists, 1999.

Astropy Collaboration, T. P. Robitaille, E. J. Tollerud, P. Greenfield, M. Droettboom, E. Bray, T. Aldcroft, M. Davis, A. Ginsburg, A. M. Price-Whelan, W. E. Kerzendorf, A. Conley, N. Crighton, K. Barbary, D. Muna, H. Ferguson, F. Grollier, M. M. Parikh, P. H. Nair, H. M. Unther, C. Deil, J. Woillez, S. Conseil, R. Kramer, J. E. H. Turner, L. Singer, R. Fox, B. A. Weaver, V. Zabalza, Z. I. Edwards, K. Azalee Bostroem, D. J. Burke, A. R. Casey, S. M. Crawford, N. Dencheva, J. Ely, T. Jenness, K. Labrie, P. L. Lim, F. Pierfederici, A. Pontzen, A. Ptak, B. Refsdal, M. Servillat, and O. Streicher. Astropy: A community Python package for astronomy. *A&A*, 558:A33, October 2013. doi: 10.1051/0004-6361/201322068.

Astropy Collaboration, A. M. Price-Whelan, B. M. Sipőcz, H. M. Günther, P. L. Lim, S. M. Crawford, S. Conseil, D. L. Shupe, M. W. Craig, N. Dencheva, A. Ginsburg, J. T. VanderPlas, L. D. Bradley, D. Pérez-Suárez, M. de Val-Borro, T. L. Aldcroft, K. L. Cruz, T. P. Robitaille, E. J. Tollerud, C. Ardelean, T. Babej, Y. P. Bach, M. Bachetti, A. V. Bakanov, S. P. Bamford, G. Barentsen, P. Barmby, A. Baumbach, K. L. Berry, F. Biscani, M. Boquien, K. A. Bostroem, L. G. Bouma, G. B. Brammer, E. M. Bray, H. Breytenbach, H. Buddelmeijer, D. J. Burke, G. Calderone, J. L. Cano Rodríguez, M. Cara, J. V. M. Cardoso, S. Cheedella, Y. Copin, L. Corrales, D. Crichton, D. D’Avella, C. Deil, É. Depagne, J. P. Dietrich, A. Donath, M. Droettboom, N. Earl, T. Erben, S. Fabbro, L. A. Ferreira, T. Finethy, R. T. Fox, L. H. Garrison, S. L. J. Gibbons, D. A. Goldstein, R. Gommers, J. P. Greco, P. Greenfield, A. M. Groener, F. Grollier, A. Hagen, P. Hirst, D. Homeier, A. J. Horton, G. Hosseinzadeh, L. Hu, J. S. Hunkeler, Ž. Ivezić, A. Jain, T. Jenness, G. Kanarek, S. Kendrew, N. S. Kern, W. E. Kerzendorf, A. Khvalko, J. King, D. Kirkby, A. M. Kulkarni, A. Kumar, A. Lee, D. Lenz, S. P. Littlefair, Z. Ma, D. M. Macleod, M. Mastropietro, C. McCully, S. Montagnac, B. M. Morris, M. Mueller, S. J. Mumford, D. Muna, N. A. Murphy, S. Nelson, G. H. Nguyen, J. P. Ninan, M. Nöthe, S. Ogaz, S. Oh, J. K. Parejko, N. Parley, S. Pasqual, R. Patil, A. A. Patil, A. L. Plunkett, J. X. Prochaska, T. Rastogi, V. Reddy Janga, J. Sabater, P. Sakurikar, M. Seifert, L. E. Sherbert, H. Sherwood-Taylor, A. Y. Shih, J. Sick, M. T. Silbiger, S. Singanamalla, L. P. Singer, P. H. Sladen, K. A. Sooley, S. Sornarajah, O. Streicher, P. Teuben, S. W. Thomas, G. R. Tremblay, J. E. H. Turner, V. Terrón, M. H. van Kerkwijk, A. de la Vega, L. L. Watkins, B. A. Weaver, J. B.

- Whitmore, J. Woillez, V. Zabalza, and Astropy Contributors. The Astropy Project: Building an Open-science Project and Status of the v2.0 Core Package. AJ, 156(3):123, September 2018. doi: 10.3847/1538-3881/aabc4f.
- Astropy Collaboration, Adrian M. Price-Whelan, Pey Lian Lim, Nicholas Earl, Nathaniel Starkman, Larry Bradley, David L. Shupe, Aarya A. Patil, Lia Corrales, C. E. Brasseur, Maximilian N"othe, Axel Donath, Erik Tollerud, Brett M. Morris, Adam Ginsburg, Eero Vaher, Benjamin A. Weaver, James Tocknell, William Jamieson, Marten H. van Kerkwijk, Thomas P. Robitaille, Bruce Merry, Matteo Bachetti, H. Moritz G"unther, Thomas L. Aldcroft, Jaime A. Alvarado-Montes, Anne M. Archibald, Attila B'odi, Shreyas Bapat, Geert Barentsen, Juanjo Baz'an, Manish Biswas, M'ed'eric Boquien, D. J. Burke, Daria Cara, Mihai Cara, Kyle E. Conroy, Simon Conseil, Matthew W. Craig, Robert M. Cross, Kelle L. Cruz, Francesco D'Eugenio, Nadia Dencheva, Hadrien A. R. Devillepoix, J"org P. Dietrich, Arthur Davis Eigenbrot, Thomas Erben, Leonardo Ferreira, Daniel Foreman-Mackey, Ryan Fox, Nabil Freij, Suyog Garg, Robel Geda, Lauren Glattly, Yash Gondhalekar, Karl D. Gordon, David Grant, Perry Greenfield, Austen M. Groener, Steve Guest, Sebastian Gurovich, Rasmus Handberg, Akeem Hart, Zac Hatfield-Dodds, Derek Homeier, Griffin Hosseinzadeh, Tim Jenness, Craig K. Jones, Prajwel Joseph, J. Bryce Kalmbach, Emir Karamehmetoglu, Mikolaj Kaluszy'nski, Michael S. P. Kelley, Nicholas Kern, Wolfgang E. Kerzendorf, Eric W. Koch, Shankar Kulumani, Antony Lee, Chun Ly, Zhiyuan Ma, Conor MacBride, Jakob M. Maljaars, Demitri Muna, N. A. Murphy, Henrik Norman, Richard O'Steen, Kyle A. Oman, Camilla Pacifici, Sergio Pascual, J. Pascual-Granado, Rohit R. Patil, Gabriel I. Perren, Timothy E. Pickering, Tanuj Rastogi, Benjamin R. Roulston, Daniel F. Ryan, Eli S. Rykoff, Jose Sabater, Parikshit Sakurikar, Jes'us Salgado, Aniket Sanghi, Nicholas Saunders, Volodymyr Savchenko, Ludwig Schwardt, Michael Seifert-Eckert, Albert Y. Shih, Anany Shrey Jain, Gyanendra Shukla, Jonathan Sick, Chris Simpson, Sudheesh Singanamalla, Leo P. Singer, Jaladh Singhal, Manodeep Sinha, Brigitta M. SipHocz, Lee R. Spitler, David Stansby, Ole Streicher, Jani Sumak, John D. Swinbank, Dan S. Taranu, Nikita Tewary, Grant R. Tremblay, Miguel de Val-Borro, Samuel J. Van Kooten, Zlatan Vasovi'c, Shresth Verma, Jos'e Vin'icius de Miranda Cardoso, Peter K. G. Williams, Tom J. Wilson, Benjamin Winkel, W. M. Wood-Vasey, Rui Xue, Peter Yoachim, Chen Zhang, Andrea Zonca, and Astropy Project Contributors. The Astropy Project: Sustaining and Growing a Community-oriented Open-source Project and the Latest Major Release (v5.0) of the Core Package. ApJ, 935(2):167, August 2022. doi: 10.3847/1538-4357/ac7c74.
- S. Bagnulo, M. Landolfi, J. D. Landstreet, E. Landi Degl'Innocenti, L. Fossati, and M. Sterzik. Stellar spectropolarimetry with retarder waveplate and beam splitter devices. Publications of the Astronomical Society of the Pacific, 121(883):993, aug 2009. doi: 10.1086/605654. URL <https://dx.doi.org/10.1086/605654>.
- Erasmus Bartholinus. Experimenta crystalli islandici dis-diaclastici, quibus mira et insolita refractio detegitur (copenhagen, 1670). Edinburgh Philosophical Journal, 1:271, 1670.

D. Scott Birney, Guillermo Gonzalez, and David Oesper.

- Observational Astronomy - 2nd Edition. Cambridge University Press, 2006. doi: 10.2277/0521853702.
- Janus D. Brink, Moses K. Mogotsi, Melanie Saayman, Nicolaas M. Van der Merwe, Jonathan Love, and Alrin Christians. Preparing the SALT for near-infrared observations. In Heather K. Marshall, Jason Spyromilio, and Tomonori Usuda, editors, Ground-based and Airborne Telescopes IX, volume 12182 of Society of Photo-Optical Instrumentation Engineers (SPIE) Conference Series, page 121822E, August 2022. doi: 10.1117/12.2627328.
- D. A. H. Buckley, J. Brink, N. S. Loaring, A. Swat, and H. L. Worters. The Southern African Large Telescope (SALT) calibration system. In Ian S. McLean and Mark M. Casali, editors, Ground-based and Airborne Instrumentation for Astronomy II, volume 7014, page 70146H. International Society for Optics and Photonics, SPIE, 2008. doi: 10.1117/12.790385. URL <https://doi.org/10.1117/12.790385>.
- David A. H. Buckley, Gerhard P. Swart, and Jacobus G. Meiring. Completion and commissioning of the Southern African Large Telescope. In Larry M. Stepp, editor, Society of Photo-Optical Instrumentation Engineers (SPIE) Conference Series, volume 6267 of Society of Photo-Optical Instrumentation Engineers (SPIE) Conference Series, page 62670Z, June 2006. doi: 10.1117/12.673750.
- Christian Buil. CCD astronomy : construction and use of an astronomical CCD camera / Christian Buil ; translated and adapted from the French by Emmanuel and Barbara Davoust. Willmann-Bell, Richmond, Va, 1st english ed. edition, 1991. ISBN 0943396298.
- Eric B. Burgh, Kenneth H. Nordsieck, Henry A. Kobulnicky, Ted B. Williams, Daragh O'Donoghue, Michael P. Smith, and Jeffrey W. Percival. Prime Focus Imaging Spectrograph for the Southern African Large Telescope: optical design. In Masanori Iye and Alan F. M. Moorwood, editors, Instrument Design and Performance for Optical/Infrared Ground-based Telescopes, volume 4841 of Society of Photo-Optical Instrumentation Engineers (SPIE) Conference Series, pages 1463–1471, March 2003. doi: 10.1117/12.460312.
- Subrahmanyan Chandrasekhar. Radiative transfer, 1950.
- Marshall H. Cohen. Genesis of the 1000-foot Arecibo dish. Journal of Astronomical History and Heritage, 12(2):141–152, July 2009.
- E. Collett. Field Guide to Polarization. Field Guides. SPIE Press, 2005. ISBN 9780819458681. URL <https://books.google.co.za/books?id=51JwcCsLbLsC>.
- J. Cooper and B. van Soelen. SALT Spectropolarimetric Pipeline Comparisons. In High Energy Astrophysics in Southern Africa 2022, page 56, December 2023.
- J. Cooper, B. van Soelen, and R. Britto. Development of tools for SALT/RSS spectropo-

- lariometry reductions: application to the blazar 3C279. In High Energy Astrophysics in Southern Africa 2021, page 56, May 2022. doi: 10.22323/1.401.0056.
- M. Craig, S. Crawford, M. Seifert, T. Robitaille, B. Sipőcz, J. Walawender, Z. Vinícius, J. P. Ninan, M. Droettboom, J. Youn, E. Tollerud, E. Bray, N. Walker, Janga V. R., C. Stotts, H. M. Günther, E. Rol, Yoonsoo P. Bach, L. Bradley, C. Deil, A. Price-Whelan, K. Barbary, A. Horton, W. Schoenell, N. Heidt, F. Gasdia, S. Nelson, and O. Streicher. astropy/ccdproc: v1.3.0.post1, December 2017. URL <https://doi.org/10.5281/zenodo.1069648>.
- G. Dahlquist and Å. Björck. Numerical Methods. Dover Books on Mathematics. Dover Publications, 2003. ISBN 9780486428079. URL <https://books.google.co.ls/books?id=armfeHpJIwAC>.
- E. Landi Degl’Innocenti, S. Bagnulo, and L. Fossati. Polarimetric standardization, 2006.
- Egidio Landi Degl’Innocenti. The physics of polarization. Proceedings of the International Astronomical Union, 10(S305):1–1, 2014.
- Egidio Landi Degl’Innocenti and M. Landolfi. Polarization in Spectral Lines, volume 307. Springer Dordrecht, 2004. doi: 10.1007/978-1-4020-2415-3.
- Königlich Bayerische Akademie der Wissenschaften. Denkschriften der Königlichen Akademie der Wissenschaften zu München für das Jahre 1820 und 1821, volume 8. Die Akademie, 1824. URL <https://books.google.co.za/books?id=k-EAAAAYAAJ>.
- J. F. Donati, M. Semel, B. D. Carter, D. E. Rees, and A. Collier Cameron. Spectropolarimetric observations of active stars. MNRAS, 291(4):658–682, November 1997. doi: 10.1093/mnras/291.4.658.
- I. V. Florinsky and A. N. Pankratov. Digital terrain modeling with the chebyshev polynomials. Machine Learning and Data Analysis, 1(12):1647 – 1659, 2015. doi: 10.48550/ARXIV.1507.03960. URL <https://arxiv.org/abs/1507.03960>.
- Augustin Fresnel. Oeuvres completes d’Augustin Fresnel: 3. Imprimerie impériale, 1870.
- L. M. Freyhammer, M. I. Andersen, T. Arentoft, C. Sterken, and P. Nørregaard. On Cross-talk Correction of Images from Multiple-port CCDs. Experimental Astronomy, 12(3):147–162, January 2001. doi: 10.1023/A:1021820418263.
- David J Griffiths. Introduction to electrodynamics, 2005.
- George E. Hale. The Zeeman Effect in the Sun. PASP, 20(123):287, December 1908. doi: 10.1086/121847.
- George E. Hale. 16. On the Probable Existence of a Magnetic Field in Sun-Spots, pages 96–105. Harvard University Press, Cambridge, MA and London, England, 1979. ISBN

9780674366688. doi: doi:10.4159/harvard.9780674366688.c19. URL <https://doi.org/10.4159/harvard.9780674366688.c19>.
- P. D. Hale and G. W. Day. Stability of birefringent linear retarders(waveplates). *Appl. Opt.*, 27(24):5146–5153, Dec 1988. doi: 10.1364/AO.27.005146. URL <https://opg.optica.org/ao/abstract.cfm?URI=ao-27-24-5146>.
- C. R. Harris, K. J. Millman, S. J. van der Walt, R. Gommers, P. Virtanen, D. Cournapeau, E. Wieser, J. Taylor, S. Berg, N. J. Smith, R. Kern, M. Picus, S. Hoyer, M. H. van Kerkwijk, M. Brett, A. Haldane, J. F. del Río, M. Wiebe, P. Peterson, P. Gérard-Marchant, K. Sheppard, T. Reddy, W. Weckesser, H. Abbasi, C. Gohlke, and T. E. Oliphant. Array programming with NumPy. *Nature*, 585(7825):357–362, September 2020. doi: 10.1038/s41586-020-2649-2. URL <https://doi.org/10.1038/s41586-020-2649-2>.
- E. Hecht. *Optics*. Pearson Education, Incorporated, 2017. ISBN 9780133977226. URL <https://books.google.co.za/books?id=ZarLoQEACAAJ>.
- Steve B. Howell. *Handbook of CCD Astronomy*, volume 5. Cambridge University Press, 2006.
- J. D. Hunter. Matplotlib: A 2d graphics environment. *Computing in Science & Engineering*, 9(3):90–95, 2007. doi: 10.1109/MCSE.2007.55.
- Christian Huygens. Treatise on light, 1690. translated by Thompson, s. p., 1690. URL <https://www.gutenberg.org/files/14725/14725-h/14725-h.htm>.
- Mourad E. H. Ismail. *Classical and Quantum Orthogonal Polynomials in One Variable*. Encyclopedia of Mathematics and its Applications. Cambridge University Press, 2005. doi: 10.1017/CBO9781107325982.
- James Janesick, James T. Andrews, and Tom Elliott. Fundamental performance differences between CMOS and CCD imagers: Part 1. In David A. Dorn and Andrew D. Holland, editors, *Society of Photo-Optical Instrumentation Engineers (SPIE) Conference Series*, volume 6276 of *Society of Photo-Optical Instrumentation Engineers (SPIE) Conference Series*, page 62760M, June 2006. doi: 10.1117/12.678867.
- F.A. Jenkins and H.E. White. *Fundamentals of Optics*. International student edition. McGraw-Hill, 1976. ISBN 9780070323308. URL <https://books.google.co.za/books?id=dCdRAAAAMAAJ>.
- Christoph U. Keller. Instrumentation for astrophysical spectropolarimetry. *Astrophysical Spectropolarimetry*, 1:303–354, 2002.
- G. Kirchhoff and R. Bunsen. Chemische Analyse durch Spectralbeobachtungen. *Annalen der Physik*, 189(7):337–381, January 1861. doi: 10.1002/andp.18611890702.
- Henry A. Kobulnicky, Kenneth H. Nordsieck, Eric B. Burgh, Michael P. Smith, Jeffrey W. Percival, Ted B. Williams, and Darragh O'Donoghue. Prime focus imaging spectrograph

for the Southern African large telescope: operational modes. In Masanori Iye and Alan F. M. Moorwood, editors, *Instrument Design and Performance for Optical/Infrared Ground-based Telescopes*, volume 4841 of *Society of Photo-Optical Instrumentation Engineers (SPIE) Conference Series*, pages 1634–1644, March 2003. doi: 10.1117/12.460315.

Gerard Leng. Compression of aircraft aerodynamic database using multivariable cheby-shev polynomials. *Advances in Engineering Software*, 28(2):133–141, 1997. ISSN 0965-9978. doi: [https://doi.org/10.1016/S0965-9978\(96\)00043-9](https://doi.org/10.1016/S0965-9978(96)00043-9). URL <https://www.sciencedirect.com/science/article/pii/S0965997896000439>.

Dave Litwiller. Ccd vs. cmos. *Photonics spectra*, 35(1):154–158, 2001.

Dongyue Liu and Bryan M. Hennelly. Improved wavelength calibration by modeling the spectrometer. *Applied Spectroscopy*, 76(11):1283–1299, 2022. doi: 10.1177/00037028221111796. URL <https://doi.org/10.1177/00037028221111796>. PMID: 35726593.

Etienne L. Malus. Sur une propriété de la lumière réfléchie. *Mém. Phys. Chim. Soc. d'Arcueil*, 2:143–158, 1809.

Curtis McCully, Steve Crawford, Gabor Kovacs, Erik Tollerud, Edward Betts, Larry Bradley, Matt Craig, James Turner, Ole Streicher, Brigitta Sipocz, Thomas Robitaille, and Christoph Deil. astropy/astroscrappy: v1.0.5 zenodo release, November 2018. URL <https://doi.org/10.5281/zenodo.1482019>.

I. Newton and W. Innys. *Opticks:: Or, A Treatise of the Reflections, Refractions, Inflections and Colours of Light*. Opticks:: Or, A Treatise of the Reflections, Refractions, Inflections and Colours of Light. William Innys at the West-End of St. Paul's., 1730. URL <https://books.google.co.za/books?id=GnAFAAAAQAAJ>.

Kenneth H. Nordsieck, Kurt P. Jaehnig, Eric B. Burgh, Henry A. Kobulnicky, Jeffrey W. Percival, and Michael P. Smith. Instrumentation for high-resolution spectropolarimetry in the visible and far-ultraviolet. In Silvano Fineschi, editor, *Polarimetry in Astronomy*, volume 4843 of *Society of Photo-Optical Instrumentation Engineers (SPIE) Conference Series*, pages 170–179, February 2003. doi: 10.1117/12.459288.

D. O'Donoghue, D. A. H. Buckley, L. A. Balona, D. Bester, L. Botha, J. Brink, D. B. Carter, P. A. Charles, A. Christians, F. Ebrahim, R. Emmerich, W. Esterhuyse, G. P. Evans, C. Fourie, P. Fourie, H. Gajjar, M. Gordon, C. Gumede, M. de Kock, A. Koeslag, W. P. Koorts, H. Kriel, F. Marang, J. G. Meiring, J. W. Menzies, P. Menzies, D. Metcalfe, B. Meyer, L. Nel, J. O'Connor, F. Osman, C. Du Plessis, H. Rall, A. Riddick, E. Romero-Colmenero, S. B. Potter, C. Sass, H. Schalekamp, N. Sessions, S. Siyengo, V. Sopela, H. Steyn, J. Stoffels, J. Scholtz, G. Swart, A. Swat, J. Swiegers, T. Tiheli, P. Vaisanen, W. Whittaker, and F. van Wyk. First science with the Southern African Large Telescope: peering at the accreting polar caps of the eclipsing polar SDSS J015543.40+002807.2. *MNRAS*, 372(1):151–162, October 2006. doi: 10.1111/j.1365-2966.2006.10834.x.

- Darragh O'Donoghue. Correction of spherical aberration in the Southern African Large Telescope (SALT). In Philippe Dierickx, editor, Optical Design, Materials, Fabrication, and Maintenance, volume 4003 of Society of Photo-Optical Instrumentation Engineers (SPIE) Conference Series, pages 363–372, July 2000. doi: 10.1117/12.391526.
- Darragh O'Donoghue. Atmospheric dispersion corrector for the Southern African Large Telescope (SALT). In Richard G. Bingham and David D. Walker, editors, Large Lenses and Prisms, volume 4411 of Society of Photo-Optical Instrumentation Engineers (SPIE) Conference Series, pages 79–84, February 2002. doi: 10.1117/12.454874.
- Ferdinando Patat and Martino Romaniello. Error Analysis for Dual-Beam Optical Linear Polarimetry. PASP, 118(839):146–161, January 2006. doi: 10.1086/497581.
- Alba Peinado, Angel Lizana, Josep Vidal, Claudio Iemmi, and Juan Campos. Optimization and performance criteria of a stokes polarimeter based on two variable retarders. Opt. Express, 18(10):9815–9830, May 2010. doi: 10.1364/OE.18.009815. URL <https://opg.optica.org/oe/abstract.cfm?URI=oe-18-10-9815>.
- W. H. Press, S. A. Teukolsky, W. T. Vetterling, and B. P. Flannery. Numerical Recipes 3rd Edition: The Art of Scientific Computing. Cambridge University Press, 2007. ISBN 9780521880688. URL <https://books.google.co.za/books?id=1aA0dzK3FegC>.
- J. R. Priebe. Operational form of the mueller matrices. J. Opt. Soc. Am., 59(2):176–180, Feb 1969. doi: 10.1364/JOSA.59.000176. URL <https://opg.optica.org/abstract.cfm?URI=josa-59-2-176>.
- Lawrence W. Ramsey, M. T. Adams, Thomas G. Barnes, John A. Booth, Mark E. Cornell, James R. Fowler, Niall I. Gaffney, John W. Glaspey, John M. Good, Gary J. Hill, Philip W. Kelton, Victor L. Krabbendam, L. Long, Phillip J. MacQueen, Frank B. Ray, Randall L. Ricklefs, J. Sage, Thomas A. Sebring, W. J. Spiesman, and M. Steiner. Early performance and present status of the Hobby-Eberly Telescope. In Larry M. Stepp, editor, Advanced Technology Optical/IR Telescopes VI, volume 3352 of Society of Photo-Optical Instrumentation Engineers (SPIE) Conference Series, pages 34–42, August 1998. doi: 10.1117/12.319287.
- Maria C. Simon. Wollaston prism with large split angle. Appl. Opt., 25(3):369–376, Feb 1986. doi: 10.1364/AO.25.000369. URL <https://opg.optica.org/ao/abstract.cfm?URI=ao-25-3-369>.
- G. G. Stokes. On the Composition and Resolution of Streams of Polarized Light from different Sources. Transactions of the Cambridge Philosophical Society, 9:399, January 1852.
- Doug Tody. The IRAF Data Reduction and Analysis System. In David L. Crawford, editor, Instrumentation in astronomy VI, volume 627 of Society of Photo-Optical Instrumentation Engineers (SPIE) Conference Series, page 733, January 1986. doi: 10.1117/12.968154.

Doug Tody. IRAF in the Nineties. In R. J. Hanisch, R. J. V. Brissenden, and J. Barnes, editors, *Astronomical Data Analysis Software and Systems II*, volume 52 of *Astronomical Society of the Pacific Conference Series*, page 173, January 1993.

Stephen F. Tonkin. *Practical Amateur Spectroscopy*. The Patrick Moore Practical Astronomy Series. Springer London, 2013. ISBN 9781447101277. URL <https://books.google.fr/books?id=b2fgBwAAQBAJ>.

Pieter G. van Dokkum. Cosmic-Ray Rejection by Laplacian Edge Detection. *PASP*, 113(789):1420–1427, November 2001. doi: 10.1086/323894.

Pauli Virtanen, Ralf Gommers, Travis E. Oliphant, Matt Haberland, Tyler Reddy, David Cournapeau, Evgeni Burovski, Pearu Peterson, Warren Weckesser, Jonathan Bright, Stéfan J. van der Walt, Matthew Brett, Joshua Wilson, K. Jarrod Millman, Nikolay Mayorov, Andrew R. J. Nelson, Eric Jones, Robert Kern, Eric Larson, C J Carey, İlhan Polat, Yu Feng, Eric W. Moore, Jake VanderPlas, Denis Laxalde, Josef Perktold, Robert Cimrman, Ian Henriksen, E. A. Quintero, Charles R. Harris, Anne M. Archibald, Antônio H. Ribeiro, Fabian Pedregosa, Paul van Mulbregt, and SciPy 1.0 Contributors. SciPy 1.0: Fundamental Algorithms for Scientific Computing in Python. *Nature Methods*, 17:261–272, 2020. doi: 10.1038/s41592-019-0686-2.

L. Wang and J. C. Wheeler. Spectropolarimetry of supernovae. *ARA&A*, 46:433–474, September 2008. doi: 10.1146/annurev.astro.46.060407.145139.

Marsha J. Wolf, Matthew A. Bershady, Michael P. Smith, Kurt P. Jaehnig, Jeffrey W. Percival, Joshua E. Oppor, Mark P. Mulligan, and Ron J. Koch. Laboratory performance and commissioning status of the SALT NIR integral field spectrograph. In Christopher J. Evans, Julia J. Bryant, and Kentaro Motohara, editors, *Ground-based and Airborne Instrumentation for Astronomy IX*, volume 12184 of *Society of Photo-Optical Instrumentation Engineers (SPIE) Conference Series*, page 1218407, August 2022. doi: 10.1117/12.2630242.

William H. Wollaston. XII. A Method of Examining Refractive and Dispersive Powers, by Prismatic Reflection. *Philosophical Transactions of the Royal Society of London Series I*, 92:365–380, January 1802. doi: 10.1098/rstl.1802.0013.

# Glossary

**FITS extensions** Extensions used in FITS files to store different types of data.

‘**BPM**’ The Bad Pixel Map extension in a FITS file.

‘**Primary**’ The Primary extension of a FITS file which contains the file Header.

‘**SCI**’ The Science data extension in a FITS file.

‘**VAR**’ The Variance data extension in a FITS file.

‘**WAV**’ The Wavelength extension in a FITS file.

**Johnson-Cousins photometric system** A widely-used system of broad-band photometry that uses a set of standard filters to measure the magnitudes of stars and other astronomical objects.

*U* The ultraviolet filter, typically centered around 3640 Å.

*B* The blue filter, typically centered around 4420 Å.

*V* The visual filter, designed to approximate human visual sensitivity and typically centered around 5400 Å.

*R* The red filter, typically centered around 6580 Å.

*I* The infrared filter, typically centered around 8060 Å.